

**The importance of charged amino acids in the human  
Organic Anion Transporter 1**

Dissertation  
zur Erlangung des Doktorgrades  
der Mathematisch-Naturwissenschaftlichen Fakultäte  
der Georg-August-Universität zu Göttingen

vorgelegt von  
Ahsan Naqi Rizwan  
aus Lucknow, India

Göttingen 2006

D7

Referent:	Prof. Dr. R. Hardeland
Korreferent:	Prof. Dr. D. Doenecke
Tag der mündlichen Prüfung:	16. Januar 2007

---

<b>ABBREVIATIONS.....</b>	<b>1</b>
<b>ABSTRACT .....</b>	<b>3</b>
<b>1. INTRODUCTION .....</b>	<b>4</b>
1.1 The organic anion transporter (OAT) family .....	4
1.2 Cloning and tissue expression of OAT1.....	7
1.3 Biopharmaceutical, physiological, and pathological roles of OAT1 .....	8
1.3.1 Substrates of OATs.....	8
1.3.2 Involvement of OATs in toxicity .....	11
1.3.3 OATs in pathophysiological states.....	13
1.3.3.1 Altered expression of OATs in diseased states .....	14
1.3.3.2 Drug-drug interactions.....	15
1.3.3.3 Single nucleotide polymorphisms (SNPs).....	16
1.4 Current knowledge about the structure and regulation of OATs .....	17
1.4.1 Structure-function relations .....	17
1.4.1.1 Mutagenesis studies.....	18
1.4.1.2 Molecular modeling of hOAT1 .....	21
1.4.2 Regulation.....	23
1.4.2.1. Phosphorylation.....	23
1.4.2.2. Glycosylation.....	24
1.4.2.3 Gender differences.....	25
1.4.2.4 Oligomerization.....	25
1.5 Aims of the present study .....	25
<b>2. MATERIALS.....</b>	<b>27</b>
2.1 Oligonucleotide Primers.....	27
2.2 Enzymes .....	28
2.3 Chemicals and radiochemicals .....	28
2.4 Cell lines.....	28
2.5 Buffers .....	29
2.6 Cell culture media and supplements.....	29
2.7 Plasmid vectors.....	30
2.8 Bacteria.....	31

---

2.9	Kits .....	32
2.10	Software.....	32
2.11	Equipment.....	33
<b>3.</b>	<b>METHODS.....</b>	<b>35</b>
3.1.	Molecular biological methods .....	35
3.1.1	Site-Directed Mutagenesis.....	35
3.1.2	cRNA synthesis .....	37
3.1.3	Restriction digestion.....	38
3.1.4	DNA isolation and purification .....	39
3.1.4.1	Agarose gel electrophoresis.....	39
3.1.4.2	Isolation of plasmid DNA .....	39
3.1.4.3	Ethanol precipitation .....	40
3.1.5	DNA sequencing and analysis.....	40
3.2	Cell biological methods.....	42
3.2.1	Expression of hOAT1 in <i>Xenopus laevis</i> oocytes .....	42
3.2.1.1	Preparation of oocytes .....	42
3.2.1.2	Oocyte injection.....	44
3.2.1.3	Transport experiments .....	44
3.2.1.4	Transport under chloride free conditions .....	44
3.2.1.5	<i>Cis</i> -inhibition experiments .....	45
3.2.1.6	<i>Trans</i> -stimulation experiments.....	45
3.2.1.7	Kinetics.....	45
3.2.2	Expression of hOAT1 in HEK293 cells .....	46
3.2.2.1	Cultivation of HEK-293 cells stably transfected with hOAT1 .....	46
3.2.2.2	Uptake of radiolabeled substances in HEK-293 cells .....	47
3.2.2.3	Uptake of 6-CF in HEK-293 cells .....	49
3.3	Immunocytochemistry .....	49
3.3.1	Immunocytochemical detection of mutant and wild-type transporters .....	50
3.3.2	Fluorescence microscopy .....	50
3.4	Statistical analyses.....	51
<b>4.</b>	<b>RESULTS.....</b>	<b>52</b>
4.1.	Use of a fluorescent organic anion to characterize hOAT1-mediated transport in a cell line stably expressing hOAT1.....	52
4.1.1	Transport of 6-carboxy fluorescein (6-CF) in HEK-293 cells stably expressing hOAT1 .....	52
4.1.1.1	Time course of 6-carboxy fluorescein uptake .....	53
4.1.1.2	Determination of $K_m$ of hOAT1 for 6-CF.....	55

---

4.2	Interaction of hOAT1 with intermediates of Krebs cycle .....	55
4.2.1	<i>Cis</i> -inhibition by Krebs cycle intermediates .....	56
4.2.2	IC <sub>50</sub> determination of Krebs cycle intermediates .....	58
4.3	The influence of pH and chloride on hOAT1, characterized in stably transfected HEK-293 cells .....	60
4.3.1	Stimulation of hOAT1-mediated transport by acidic pH .....	61
4.3.2	Stimulation of hOAT1-mediated transport by chloride.....	62
4.3.3	Combined effects of pH and chloride replacement upon hOAT1-mediated transport.....	63
4.3.4	Effect of increasing chloride concentration on PAH uptake by HEK-293 cells stably transfected with hOAT1 .....	65
4.4	Mutational analysis of hOAT1 .....	67
4.4.1	Alignments and sequence characteristics of OATs: identifying important amino acid residues .....	68
4.4.2	Generation of R466 mutants.....	70
4.4.3	Functional characterization of R466 mutants.....	71
4.4.3.1	PAH transport by R466 mutants.....	71
4.4.3.2	<i>Trans</i> -stimulation of PAH transport by mutations of arginine 466.....	72
4.4.3.3	Membrane trafficking of the R466 mutants .....	73
4.4.4	Characterization of the R466K mutant.....	74
4.4.4.1	PAH transport by the R466K mutant .....	74
4.4.4.2	<i>Trans</i> -stimulation by glutarate .....	75
4.4.4.3	<i>Cis</i> -inhibition.....	76
4.4.4.4	The effect of chloride upon wt- or mutant R466K-hOAT1 mediated transport.....	77
4.4.4.5	The effect of chloride upon wt- or mutant R466K-hOAT1 mediated transport of other substrates.....	79
4.5	Kinetic analyses of wt and R466K-hOAT1.....	80
4.5.1	Determinations of K <sub>m</sub> of mutant R466K and wild type hOAT1 for PAH, .... in the presence and absence of chloride .....	81
4.6	Mutations of other charged residues in hOAT1 .....	84
4.6.1	Generation and functional testing of K382 mutants.....	85
4.6.2	Generation and functional testing of R466K+K382R double mutant.....	86
4.6.3	Generation and functional testing of mutations in other charged residues.....	87
	.....	87
<b>5.</b>	<b>DISCUSSION.....</b>	<b>89</b>
5.1	Characterizing hOAT1-mediated transport in stably transfected HEK-293 cells ..	89
5.1.1	Use of 6-carboxyfluorescein as a substrate for hOAT1-mediated ..... transport studies.....	89

---

---

5.1.2	Interaction of hOAT1 with intermediates of Krebs cycle .....	90
5.1.3	The influence of chloride substitution on hOAT1 mediated transport.....	91
5.2	Mutational analysis of hOAT1 .....	92
5.2.1	Mutation of charged residues in hOAT1 .....	92
5.2.2	Characterization of mutations produced in arginine at position 466.....	93
5.3	Outlook.....	96
<b>6.</b>	<b>REFERENCES .....</b>	<b>97</b>
	<b>ACKNOWLEDGEMENTS .....</b>	<b>108</b>
	<b>PUBLICATIONS.....</b>	<b>109</b>
	<b>CONFERENCES.....</b>	<b>110</b>
	<b>BIOGRAPHY .....</b>	<b>111</b>

## ABBREVIATIONS

Å	Angstrom
ATP	adenosine triphosphate
BSA	bovine serum albumin
°C	degrees Celsius
cAMP	cyclic adenosine monophosphate
6-CF	6-carboxyflorescein
C-terminus	carboxy-terminus
cDNA	complementary DNA
CKII	casein kinase II
cRNA	complementary RNA
Da	Dalton
DMSO	dimethyl sulfoxid
dNTP	deoxyribonucleotide phosphate
Fig.	figure
NaDC-3	sodium/dicarboxylate cotransporter 3
h	hour
HEK-293	human embryonic kidney cell line
hNLT	human novel liver transporter
hOAT	human organic anion transporter
IC <sub>50</sub>	half maximal inhibitory concentration
k	kilo
K <sub>m</sub>	Michaelis Menten constant
LB	Luria Bertani broth
M	molar (moles per litre)
µM	micromolar
MAPK	mitogen-associated protein kinase
ml	millilitre
mRNA	messenger RNA
MRP2	multiple drug resistance-associated protein 2
N-terminus	amino-terminus
NKT	novel kidney transporter
NLT	novel liver transporter
NPT1	sodium phosphate transporter 1
NSAIDs	non-steroidal anti-inflammatory drugs
OAT	organic anion transporter
OCT	organic cation transporter
ORI	oocyte Ringer's solution
OTA	ochratoxin A
PAH	<i>para</i> -aminohippurate
PBS	phosphate-buffered saline
PCR	polymerase chain reaction
PI3K	phosphatidyl inositol-3-kinase
PKA	cAMP-associated protein kinase
PKC	protein kinase C

pmol	picomole
RNA	ribonucleic acid
RNase	ribonuclease
NaDC-1	sodium/dicarboxylate cotransporter
rpm	revolutions per minute
RST	renal specific transporter
SEM	standard error of the mean
TAE	tris-acetate-EDTA
TBE	tris-borate-EDTA
TK	tyrosine kinase
TLC	tauroithocholate
TLC-S	sulfated tauroithocholate
Tris	tris-(hydroxymethyl)-aminomethane
U	unit
UTR	untranslated region
UV	ultraviolet
V	volts
V <sub>max</sub>	maximum transport rate

**Single letter codes used for denoting amino acids**

Alanine	A
Arginine	R
Asparagine	N
Aspartic acid	D
Cysteine	C
Glutamine	Q
Glutamic acid	E
Glycine	G
Histidine	H
Isoleucine	I
Leucine	L
Lysine	K
Methionine	M
Phenylalanine	F
Proline	P
Serine	S
Threonine	T
Tryptophan	W
Tyrosine	Y
Valine	V



**ABSTRACT**

The organic anion transporter 1 (OAT1) is key for the secretion of organic anions in renal proximal tubules. However, not much is currently known about structure-activity relationships or substrate-binding and translocation. In this study we investigated the role of conserved charged residues possibly important for substrate binding and turnover of the transporter. Another part of the study sought to characterize the effect of pH, interaction with Krebs cycle intermediates and investigation of the chloride-mediated stimulation of hOAT1. In HEK293 cells stably expressing hOAT1 the relative degree of competitive inhibition of carboxyfluorescein uptake was as follows:  $\alpha$ -ketoglutarate > succinate > citrate > malate. Removal of chloride markedly slowed down the transporter. Lowering pH from 7.4 to 6.0 during transport experiments increased uptake of PAH and glutarate significantly. Numerous charge conservative and non-conservative replacements were made in cationic residues though site-directed mutagenesis and characterized. Though all mutations resulted in markedly reduced transport function, a conserved, positively charged arginine residue R466 in the 11<sup>th</sup> transmembrane helix was interesting. The replacement of arginine by the positively charged lysine (R466K) did not impair expression of hOAT1 at the plasma membrane of *Xenopus laevis* oocytes, but decreased the transport of *p*-aminohippurate (PAH) considerably. Extracellular glutarate inhibited, and intracellular glutarate *trans*-stimulated, wild type and mutated OAT1, suggesting, for the mutant R466K, an unimpaired interaction with dicarboxylates. However, when R466 was replaced by the negatively charged aspartate (R466D), glutarate no longer interacted with the mutant. PAH uptake by wild type hOAT1 was strongly stimulated in the presence of chloride, whereas the R466K mutant was chloride-insensitive. Likewise, the uptake of labelled glutarate or ochratoxin A was chloride-dependent in the wild type, but not in the mutant R466K. Kinetic experiments revealed that chloride did not alter the apparent  $K_m$  for PAH, but influenced  $V_{max}$  in wild type OAT1-expressing oocytes. In R466K mutants, the apparent  $K_m$  for PAH was similar to that of the wild type, but  $V_{max}$  was changed. We conclude that R466 influences the binding of glutarate, but not interaction with PAH, and R466 interacts with chloride which is a major determinant in substrate movements through the transporter.

## 1. INTRODUCTION

A variety of endogenous and exogenous compounds our bodies are exposed to can be classified as organic anions. Their elimination is essential for the maintenance of homeostasis. Organs such as the kidneys, liver, and intestine defend the body against potentially harmful effects of these compounds by biotransformation into less active metabolites and by the excretory transport process (Schwenk, 1987; van Montfoort et al., 2003). Following the first observations almost 70 years ago that the anionic dye phenolsulphophthalein was highly concentrated in renal convoluted tubules (Marshall EK Jr and Vickers JL, 1923), research in the field of tubular secretion has made tremendous progress. It has been established that the process of secreting organic anions and cations through proximal tubular cells is achieved via transporters, involving the uptake of organic ions into the cells from the blood across the basolateral membrane followed by extrusion across the brush-border membrane into the proximal tubular fluid (Burckhardt et al., 2001).

### 1.1 The organic anion transporter (OAT) family

The organic anion transporters (OATs) of the SLC22 gene family are characterized by remarkably broad substrate specificity: they handle small, amphiphilic organic anions of diverse chemical structures, uncharged molecules, and even some organic cations (Burckhardt and Burckhardt, 2003; Koepsell and Endou, 2004). Present, functionally characterized transporters of the OAT family are enlisted in table 1.1. Given the broad specificity, it is of no surprise that organic anion transporters interact with many commonly used anionic drugs such as  $\beta$ -lactam antibiotics, antivirals, ACE inhibitors, diuretics, NSAIDs etc. (Burckhardt and Burckhardt, 2003). Since OATs are typically found at boundary epithelia, these transporters play an important role in distribution and excretion of drugs. Moreover, OATs can be the site of drug-drug interactions during competition of two or more drugs for the same transporter, and mediate cell damage by transporting cytotoxic compounds.

OATs do not directly utilize ATP hydrolysis for energetization of substrate translocation. Most, if not all, members of the OAT family operate as anion exchangers, i. e. they couple the uptake of an organic anion into the cell to the release of another organic anion from the cell. Thereby, OATs utilize existing intracellular > extracellular gradients of anions, e. g.  $\alpha$ -ketoglutarate, lactate and nicotinate, to drive uphill uptake of organic anions against the inside negative membrane potential. In kidney proximal tubules, OATs are functionally coupled to  $\text{Na}^+$ -driven mono- and dicarboxylate transporters that establish and maintain the intracellular > extracellular gradients of lactate, nicotinate, and  $\alpha$ -ketoglutarate (Fig. 1.1) (Rizwan and Burckhardt, 2006).

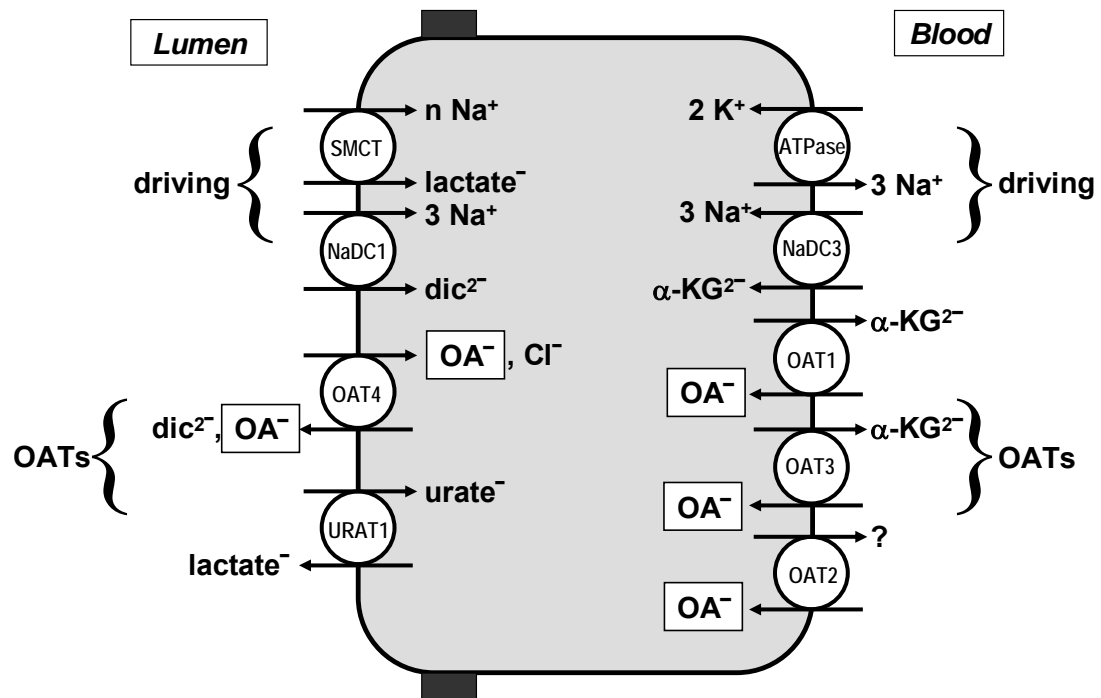


**Figure 1.1 Schematic representation of transport processes associated with the secretion/reabsorption of organic anions in a human renal proximal tubule cell.** The upper transporters SMCT and NaDC1 in the apical, and  $\text{Na}^+$ ,  $\text{K}^+$ -ATPase and NaDC3 in the basolateral membrane are collectively driving the organic anion transporters OAT4 and URAT1 in the apical, and OAT1 and OAT3 in the basolateral membrane. The driving ion for OAT2 is unknown. Abbreviations:  $\alpha$ - $\text{KG}^{2-}$ ,  $\alpha$ -ketoglutarate;  $\text{dic}^{2-}$ , dicarboxylate (succinate,  $\alpha$ -ketoglutarate); NaDC, sodium dicarboxylate cotransporter;  $\text{OA}^-$ , organic anion/anionic drug; OAT, organic anion transporter; SMCT, sodium monocarboxylate cotransporter; URAT, urate transporter

**Table 1.1 Organic anion transporter (OAT) family**

Gene name	Protein name	Tissue distribution	Predominant substrates
SLC22A6	OAT1	Kidney, brain	PAH, PGE <sub>2</sub> , urate, NSAIDs, antiviral agents, MTX, OTA, β-lactam antibiotics, ACE inhibitors, uremic toxins
SLC22A7	OAT2	Liver, kidney	PGE <sub>2</sub> , PGF <sub>2α</sub> , tetracycline
SLC22A8	OAT3	kidney, brain	ES, cAMP, cGMP, E217βG, DHEAS, PGE <sub>2</sub> , PGF <sub>2α</sub> , OTA, MTX, cimetidine, tetracycline, uremic toxins
SLC22A11	OAT4	kidney, placenta	ES, DHEAS, PGE <sub>2</sub> , PGF <sub>2α</sub> , tetracycline, MTX, OTA
SLC22A12	URAT1	kidney	urate
Slc22a19	OAT5	kidney	ES, DHEAS, OTA

PAH: p-aminohippurate; PG: prostaglandin; NSAIDs: nonsteroidal inflammatory drugs; MTX: methotrexate; OTA: ochratoxin A; ACE: angiotensin-converting enzyme; ES: estrone sulfate; E217βG: estradiol 17β-D-glucuronide; DHEAS, dehydroepiandrosterone sulfate.

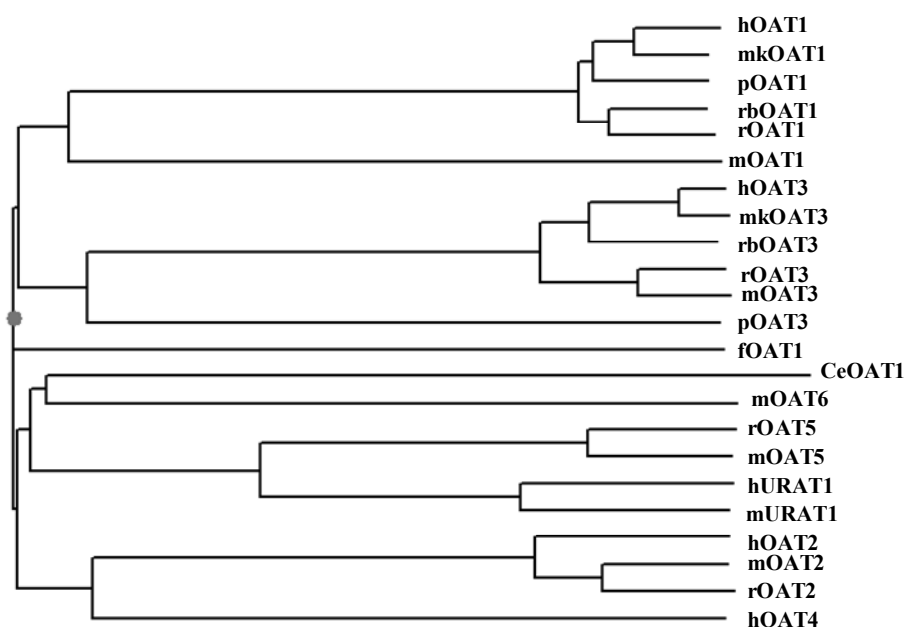


**Figure 1.2 Phylogenetic relations of cloned and functionally characterized organic anion transporters.** The dendrogram was constructed using PhyloDraw software (<http://pearl.cs.pusan.ac.kr/phylo draw>)

Figure 1.2 shows a dendrogram of all functionally characterized Organic Anion Transporters that belong to the solute carrier family SLC22. Members of multispecific organic anion transporter family SLC22 that have been identified by molecular cloning are enlisted in Table 1.1. Also given are their tissue distribution and predominant substrates.

## 1.2 Cloning and tissue expression of OAT1

The Organic Anion Transporter 1 (OAT1) was the first organic anion transporter to be cloned from rat (Sekine et al., 1997; Sweet et al., 1997), mouse (Lopez-Nieto et al., 1997), and flounder kidneys (Wolff et al., 1997). The human orthologue, hROAT1 was first cloned in 1998 (Reid et al., 1998), later also by other laboratories as hOAT1 (Hosoyamada et al., 1999); (Race et al., 1999) and as PAHT (Lu et al., 1999). Later on, the orthologues from, monkey (Tahara et al., 2005), pig (Hagos et al., 2002), rabbit (Bahn et al., 2002), and *C. elegans* (George et al., 1999) were cloned. The organic anion transporter from flounder kidney turned out to be functionally an intermediate between, or a precursor of, OAT1 and OAT3 (Aslamkhan et al., 2006). Likewise, it is not clear whether the *C. elegans* "OAT1" is an orthologue of the mammalian OAT1. Figure 1.2 would rather suggest a distant relation to mOAT6.

The gene for hOAT1, SLC22A6, is located on chromosome 11q12.3 (Bahn et al., 2000), being paired with the gene for OAT3 (Eraly et al., 2003). The mammalian OAT1s consist of 545-551 amino acids, and secondary structure algorithms predict 12 transmembrane helices with the N- and C-termini located at the cytosolic side of the plasma membrane (Fig. 1.3). In man, a longer splice variant with 563 amino acids and two shorter, non-functional splice variants were found (Bahn et al., 2004a; Hosoyamada et al., 1999).

Immunohistological studies have revealed the expression of OAT1 at the basolateral membrane of proximal tubule cells in human (Hosoyamada et al., 1999; Motohashi et al., 2002), rat (Kojima et al., 2002; Ljubojevic et al., 2004), and mouse (Bahn et al.,

2005) kidneys. Besides kidneys, human OAT1 has been shown to be located at the choroid plexus (Alebouyeh et al., 2003), and recent studies on mouse brain revealed mOAT1 expression in neurones of cortex and hippocampus (Bahn et al., 2005).

### **1.3 Biopharmaceutical, physiological, and pathological roles of OAT1**

Characterization of the OAT family members has brought us a step further in the elucidation of molecular mechanisms for drug elimination and distribution. The fact that OATs interact with numerous endogenous and xenobiotic compounds means that they play an important role not only in drug elimination, pharmacokinetics and toxicity but also in pathological conditions.

#### **1.3.1 Substrates of OATs**

Substrates for the renal organic anion transport system include a number of chemically heterogeneous weak acids with a carbon backbone and a net negative charge at physiological pH ( $pK_a < 7$ ). Their structures may be aromatic or aliphatic. The classical organic anions, monovalent hydrophobic anions with a negative or partial negative charge, interact best with the transporter. These compounds require a hydrophobic moiety of at least 4 Å in length. The system also interacts with divalent anions, including some zwitterions, for which optimal interaction with the transporter requires a charge separation of 6-7 Å. In addition, these compounds may contain a hydrophobic moiety of up to 10 Å in length. The affinity of the transporter for both mono- and divalent anions increases with hydrophobicity and charge strength. Finally, non-ionizable hydrophobic compounds also interact with the transporter (Ullrich, 1997). Historically, *p*-aminohippurate (PAH) has been used as a prototypical substrate for the renal organic anion transport system. PAH is a high-affinity substrate and is almost completely extracted by the renal organic anion transport system during a single pass through the kidney when its serum concentration is low, which indicates active transport. Thus, PAH is a high affinity and OAT1 specific  $OA^-$  and is the substrate of choice for studies on hOAT1.

A prominent feature of OAT1 is that it interacts with and transports a variety of organic anions with unrelated chemical structures. Various endogenous organic anions, uremic substances, drugs, and environmental compounds have been shown to be substrates of OAT1. Therefore, multispecificity of the OAT1 is suitable for elimination of a variety of endogenous metabolites and xenobiotics.

*Endogenous compounds* - OAT1, together with OAT3, is responsible for the first step of renal organic anion secretion, the uptake of organic anions from the blood across the basolateral membrane into proximal tubule cells. The uptake occurs in exchange for intracellular  $\alpha$ -ketoglutarate (see also Figure 1.1). The transport of the following radioactively labelled, endogenous compounds has been demonstrated for OAT1: the metabolic intermediate  $\alpha$ -ketoglutarate (Lu et al., 1999; Sekine et al., 1997), the local hormones prostaglandin E<sub>2</sub> and F<sub>2 $\alpha$</sub>  (Kimura et al., 2002; Sekine et al., 1997), the second messengers cAMP and cGMP (Sekine et al., 1997), the vitamin folate (Uwai et al., 1998), and the purine breakdown product urate (Ichida et al., 2003; Sekine et al., 1997). Several other endogenous compounds inhibit OAT1, *e.g.* the hormones corticosterone and dehydroepiandrosterone sulfate (Beery et al., 2003; Hasegawa et al., 2003), the vitamin nicotinate (Sugawara et al., 2005), the purine metabolites xanthine and hypoxanthine (Sugawara et al., 2005), and acidic metabolites of the neurotransmitters norepinephrine (vanillinemandelate), dopamine (3,4-dihydroxyphenyl acetate, homovanillate), 5-hydroxytryptamine (5-hydroxyindoleacetate), and of cerebral tryptophan metabolism (quinolinate, kynurenate) (Alebouyeh et al., 2003; Bahn et al., 2005). The interaction of OAT1 with neurotransmitter metabolites strongly suggests that OAT1 is responsible for both removal of these metabolites from the brain and for renal excretion.

Recently, an OAT1 knockout mouse has been generated (Eraly et al., 2006). The mice were normal and fertile. The kidneys were histologically unchanged, had a normal GFR, salt and water excretion. PAH clearance and the excretion of 3-hydroxybutyrate, 3-hydroxyisobutyrate, 3-hydroxypropionate, benzoate, 4-hydroxyphenylpyruvate, 4-hydroxyphenyllactate, 4-hydroxyphenylacetate and N-acetylaspartate were decreased, indicating that these substances occur endogenously as metabolites and are secreted

through OAT1. For some of these substances,  $K_i$  values were determined: 4-hydroxyphenylpyruvate (56  $\mu\text{M}$ ), benzoate (253  $\mu\text{M}$ ), 4-hydroxyphenyllactate (390  $\mu\text{M}$ ), N-acetylaspartate (841  $\mu\text{M}$ ), 3-hydroxybutyrate (3.3 mM) (Eraly et al., 2006). Thus, OAT1 contributes to renal excretion of various metabolites, but normal life in mice is possible without this transporter, probably because OAT3 can take over the task.

*Exogenous compounds* - Numerous drugs have been tested as possible substrates of OAT1. Either transport of radiolabeled drugs was demonstrated or inhibition of uptake of the prototypical labelled substrate, PAH, by unlabelled drugs was shown. Table 1 gives some examples of drugs that have been found to interact with human OAT1 (Rizwan and Burckhardt, 2006).

**Table 1.1 Examples of drugs interacting with human OAT1**

<b>Class</b>	<b>Tested compounds</b>
Antibiotics	benzylpenicillin, cefadroxil, cefamandole, cefazolin, cefoperazone, cefotaxime, ceftriaxone, cephaloridine, cephalotin, cephradine, cinoxacin, doxycyclin, minocycline, nalidixate, oxytetracycline, tetracycline*
Antivirals	acyclovir*, adefovir*, cidofovir*, ganciclovir*, PMEDAP <sup>1</sup> *, PMEG <sup>1</sup> *, tenofovir*, zalcitabine*, zidovudine*
H <sub>2</sub> antagonists	cimetidine*, ranitidine*
Antihypertensives	captopril, losartan
Cytostatic	methotrexate*
Diuretics	acetazolamide, bumetanide*, chlorothiazide, cyclothiazide, ethacrynate, furosemide*, hydrochlorothiazide, methazolamide, trichlormethiazide
NSAIDs <sup>1</sup>	acetaminophen, acetylsalicylate, diclofenac, diflusal, etodolac, flufenamate, flurbiprofen, ibuprofen*, indomethacin*, ketoprofen*, loxoprofen, mefenamate, naproxen, phenacetin, phenylbutazon, piroxicam, salicylate, sulindac



---

Statins	fluvastatin, pravastatin, simvastatin
Uricosurics; purine metabolism	allopurinol, benzbromarone, probenecid

---

<sup>1</sup> abbreviations: NSAID, non-steroidal anti-inflammatory drug; PMEDAP, 9-(2-phosphonyl-methoxyethyl)-diaminopurine; PMEG, 9-(2-phosphonyl-methoxyethyl)-guanidine; \* transport has been demonstrated

### 1.3.2 Involvement of OATs in toxicity

Since OATs are capable of handling an enormous variety of structurally diverse organic anions as substrates they may be intimately involved in the distribution and elimination of many potentially toxic endogenous and exogenous organic anions. Indeed, the nature of these substrates suggests that proper OAT function is essential to maintaining total body homeostasis and that altered OAT function (and/or expression) may be a key factor in the progression of certain disease states.

*Nephrotoxic drugs* - It is highly likely that OAT1 and OAT3 contribute significantly to nephrotoxicity by taking up cephaloridine and antiviral drugs from the blood into the cells. Particularly, proximal tubule cells are exposed to cytotoxic drugs because they express OAT1 and OAT3.  $\beta$ -Lactam antibiotics are in addition taken up from the apical cell side by the H<sup>+</sup>-peptide cotransporter PEPT2 (Boll et al., 1996) and thus a high intracellular concentration can be achieved. Strategies to prevent the nephrotoxicity of antibiotics involve the use of inhibitors of OATs such as cilastatin and betamipron (Tune, 1997). The use of NSAIDs (Mulato et al., 2000) and probenecid (Lacy et al., 1998; Yarchoan et al., 1989) can reduce renal excretion of antiviral drugs and nephrotoxicity. Thereby, intentional drug-drug interaction provides a means to prevent organ damage. As pointed out by (Sweet, 2005), inhibition of OATs has not only an impact on the kidneys, but also on liver and brain. Inhibition of OATs in the liver could impair drug metabolism, and inhibition of OATs in choroid plexus and the blood brain barrier could prevent the removal of drugs from the brain and cause cerebral symptoms.

*Uremic toxins* - During renal failure, several organic anions are accumulated in the plasma and cause side effects. These compounds called uremic toxins include indoxyl

sulfate (IS), indole acetate (IA), hippurate (HA), and 3-carboxy-4-methyl-5-propyl-2-furanpropionate (CMPF) (Sun et al., 2006). IS and CMPF themselves cause renal failure and aggravate the situation. HA and CMPF are made responsible for neurological disorders accompanying the renal failure, HA interferes with the glucose utilization in skeletal muscle, and CMPF inhibits the binding of drugs to albumin (Sun et al., 2006). All these uremic toxins are substrates of hOAT1. Indoxyl sulfate was transported with a  $K_m$  of 20.5  $\mu\text{M}$ , and inhibited OAT1-mediated transport with  $\text{IC}_{50}$  values between 13.2 and 83  $\mu\text{M}$  (Enomoto et al., 2003; Motojima et al., 2002). Indole acetate was taken up by hOAT1 with a  $K_m$  of 14  $\mu\text{M}$ , and inhibited transport with  $\text{IC}_{50}$  values 21 and 83  $\mu\text{M}$  (Deguchi et al., 2004; Motojima et al., 2002). Hippurate uptake occurred with a  $K_m$  of 23.5  $\mu\text{M}$ , and inhibition of hOAT1 with an  $\text{IC}_{50}$  of 18.8  $\mu\text{M}$ ; the respective numbers for CMPF are 141  $\mu\text{M}$  for  $K_m$  and 247  $\mu\text{M}$  for  $\text{IC}_{50}$  (Deguchi et al., 2004). IS and IA uptake increased the production of oxygen radicals, and probenecid inhibited this effect (Motojima et al., 2003). Indoxyl sulfate interacted also with OAT3 [ $K_m$  263  $\mu\text{M}$ ;  $K_i$  169  $\mu\text{M}$  (Deguchi et al., 2004; Enomoto et al., 2003)] and OAT4 [ $K_i$  181  $\mu\text{M}$  (Enomoto et al., 2003)], indole acetate (no transport, but inhibition with  $\text{IC}_{50}$  491  $\mu\text{M}$ ), hippurate (no transport, but inhibition with  $\text{IC}_{50}$  of 30.8  $\mu\text{M}$ ), and CMPF with OAT3 [ $K_m$  for uptake 26.5  $\mu\text{M}$ ;  $\text{IC}_{50}$  27.9  $\mu\text{M}$  (Deguchi et al., 2004)]. Thus, OAT1 and OAT3 are involved in the uptake of uremic toxins and their excretion. In renal failure, however, the capacity to excrete uremic toxins is decreased. Accumulation of the toxins inhibits the remaining OAT1 and OAT3 progressively, which could cause severe problems with the excretion of antibiotics, methotrexate, antivirals, etc.

*Environmental toxins* - The herbicide 2,4-dichlorophenoxyacetate (2,4-D) is a substrate of hOAT1 [(Aslamkhan et al., 2006; Cihlar et al., 1999);  $K_m$  for uptake 5.77  $\mu\text{M}$  (Tahara et al., 2005)] and hOAT3 [weak transport (Aslamkhan et al., 2006)]. N-acetyl-L-cysteine S-conjugates resulting from glutathione conjugation of toxic compounds are substrates of rOAT1 (Pombrio et al., 2001) and probably also of human OAT1. The cysteine conjugates S-benzothiazolcysteine, S-chlorotrifluoroethylcysteine, and S-dichlorovinylcysteine inhibited hOAT1 with  $\text{IC}_{50}$  values of 9.9  $\mu\text{M}$ , 177  $\mu\text{M}$ , and 208  $\mu\text{M}$ , respectively (Groves et al., 2003). Complexes between mercury and N-acetyl-L-

cysteine [NAC-Hg,  $K_m$  44  $\mu\text{M}$  (Aslamkhan et al., 2003); NAC-Hg-CH<sub>3</sub> (Koh et al., 2002),  $K_m$  79.5  $\mu\text{M}$ ; NAC-Hg-NAC,  $K_m$  144  $\mu\text{M}$  (Zalups and Ahmad, 2005)], L-cysteine [Cys-Hg (144); Cys-Hg-Cys,  $K_m$  91  $\mu\text{M}$ ], and homocysteine (Hcy) [CH<sub>3</sub>-Hg-Hcy,  $K_m$  39  $\mu\text{M}$  (148); Hcy-Hg-Hcy (Zalups et al., 2004)] are transported by hOAT1, and NAC-Hg by hOAT3 (Aslamkhan et al., 2006). Cell toxicity of Hcy-Hg complexes was higher in OAT1-expressing cells than in mock. These findings explain why mercury is accumulated particularly in proximal tubule cells. Fortunately, the same transporters, OAT1 and OAT3 can be used to direct an antidote, 2,3-dimercaptopropane-1-sulfonate (DMPS), into proximal tubule cells to chelate the mercury, greatly facilitating its excretion. Another heavy metal chelator, 2,3-dimercaptosuccinate (DMSA, succimer), is transported by NaDC3 (Burckhardt et al., 2002) that is also located in the basolateral membrane.

*Carcinogens* - Carcinogenic compounds are also transported by OATs. A prominent example is ochratoxin A that is translocated by hOAT1 [ $K_m$  0.42  $\mu\text{M}$  (Jung et al., 2001)], hOAT3 [ $K_m$  0.75  $\mu\text{M}$  (Jung et al., 2001)], and hOAT4 [ $K_m$  22.9  $\mu\text{M}$  (Babu et al., 2002)]. Recently, it has been shown that sulfoxymethyl pyrenes (SMP) are substrates of hOAT1 and hOAT3 (Bakhiya et al., 2006). At hOAT1, 2- and 4-sulfomethoxypyrenes showed  $K_i$  values of 4.4  $\mu\text{M}$  and 5.1  $\mu\text{M}$ , respectively; at OAT3, the respective  $K_i$  values were 1.9  $\mu\text{M}$  and 2.1  $\mu\text{M}$ . The expression of OAT1 and OAT3 increased the number of SMP-DNA adducts, and probenecid completely prevented this effect. Thus it appears that at least OAT1 and OAT3 can be involved in renal carcinogenesis by taking up ochratoxin A and SMPs from the blood into proximal tubule cells.

### **1.3.3 OATs in pathophysiological states**

Recent studies have indicated that the expressions of OATs are affected in pathophysiological states. As mentioned in the previous section, during the progression of renal insufficiency, various uremic toxins derived from dietary proteins accumulate in plasma. Many uremic toxins are organic anions; their accumulation in the kidney is a result of renal dysfunction, and this also accelerates underlying renal diseases. The

enhanced expression of OATs in uremic circumstances indicates compensatory effects for elimination of uremic substances and leads to progress of the underlying diseases by accumulation of harmful toxins in proximal tubular cells.

### **1.3.3.1 Altered expression of OATs in diseased states**

The expressions of OATs are affected by several renal dysfunction models. In the kidneys, both down- and up-regulation of OATs was observed under various conditions. Acute arterial calcinosis induced by bolus injection of vitamin D3 increased the OAT1 expression level (Quaglia et al., 2003). OAT expression in various human kidney diseases was analyzed using a real-time PCR method (Sakurai et al., 2005). The data indicate that OAT3 expression is decreased in patients with renal diseases. A bilateral ureteral obstruction for 24 hrs decreased renal p-aminohippurate excretion, but increased the amount of OAT1 protein in Western blots (Villar et al., 2005).

OAT expression is influenced not only by renal diseases but also by hepatic diseases. A biliary obstruction for three days (Brandoni et al., 2006) did not change the abundance of total OAT1 protein in rat kidneys, but decreased the amount of OAT1 located in the basolateral membrane. Possibly, OAT1 was partially cleared from the basolateral membrane by endocytosis, and protein kinase C activation may have played a role in this process. OAT3 abundance was increased both, in the total kidney and in the basolateral membrane (Brandoni et al., 2006). Chronic renal failure induced by 5/6 nephrectomy decreased OAT1, but not OAT3, in the basolateral membrane (Monica Torres et al., 2005). Finally, prostaglandin E<sub>2</sub> dose- and time-dependently reduced mRNA and protein of OAT1 and OAT3 in rat kidneys (Sauvant et al., 2006). At an exposure time of 48 hrs, a half-maximal effect on the decrease of OAT1 and OAT3 protein was observed at 23 and 27 nM PGE<sub>2</sub>, respectively. Thus, PGE<sub>2</sub> has two opposing functions: at short exposure times it increases, and at long times it decreases the function of OATs.

Some drugs and toxins were reported to down-regulate the expression of OATs in liver. The activation of "drug-sensing receptors" AhR, CAR, PXR, and Nrf2 by their respective ligands changed the expression of a number of transporters in the hepatocyte (Jigorel et al., 2006). Whereas MDR1, MRP2, MRP3, BCRP and OATP-C were upregulated, a decreased expression was found for MRP6, BSEP, OCT1, OATP-B, OATP8, NTCP, and OAT2. Particularly phenobarbital (acting through CAR) effectively decreased OAT2 expression, whereas the activation of other receptors had smaller effects (Jigorel et al., 2006). Hepatic mRNAs for OCT1 and OAT3, but not for OAT2, were decreased in rats treated with lipopolysaccharide (LPS) (Cherrington et al., 2004).

### **1.3.3.2 Drug-drug interactions**

OATs can be the site of drug-drug interactions during competition of two or more drugs for the same transporter. Drugs present in plasma could affect the transport of the drugs individually and could mutually influence the pharmacokinetics of the drugs. A notable example is the concomitant use of probenecid and penicillin G; the half-life of penicillin G is significantly prolonged when combined with probenecid compared with when it is administered alone (Somogyi, 1996).

It has also been reported that the administration of methotrexate (MTX) with acidic drugs, such as NSAIDs, and  $\beta$ -lactam antibiotics can result in drug-drug interaction that causes severe suppression of bone marrow. An interaction between NSAIDs and methotrexate has been implicated as a cause of severe side effects. Methotrexate is transported by human OAT1 [ $K_m$  724  $\mu$ M (Uwai et al., 2004)], OAT2 [no  $K_m$  available (Sun et al., 2001)], OAT3 [ $K_m$  10.9  $\mu$ M (Cha et al., 2001)], and OAT4 [ $K_m$  17.8  $\mu$ M (Takeda et al., 2002)]. Since all OATs are inhibited by NSAIDs, drug-drug interaction could occur at any of these transporters. If the free plasma concentrations are taken into account, salicylate ( $K_i$  at hOAT3 1,020  $\mu$ M, free conc. 431  $\mu$ M); phenylbutazone (34.7  $\mu$ M / 12.5  $\mu$ M); indomethacin (6.0  $\mu$ M / 8.4  $\mu$ M); and loxoprofen (8.7  $\mu$ M / 20  $\mu$ M) could substantially inhibit OAT3-mediated methotrexate transport and, hence, uptake from the blood into proximal tubule cells. Salicylate [ $IC_{50}$  values at OAT1 between 280

$\mu\text{M}$  and 1.57 mM], phenylbutazone [ $\text{IC}_{50}$  47.9  $\mu\text{M}$ ], indomethacin [ $\text{IC}_{50}$  between 3.0 and 3.8  $\mu\text{M}$ ] and loxoprofen [ $\text{IC}_{50}$  27.1  $\mu\text{M}$ ] should also substantially inhibit hOAT1, decreasing cellular uptake of methotrexate further. The  $\text{IC}_{50}$  values for hOAT2 [salicylate, >2 mM; indomethacin, 64.1  $\mu\text{M}$ ] and OAT4 [salicylate, >2 mM; indomethacin, 10.1  $\mu\text{M}$  (62)] suggest that only indomethacin could substantially inhibit OAT4 *in vivo* (Khamdang et al., 2002). Taken together, salicylate, phenylbutazone, indomethacin, and loxoprofen could be responsible for methotrexate-NSAID interaction at OAT1 and OAT3, and indomethacin also at OAT4. As a consequence, unwanted side-effects, such as bone marrow suppression, could occur as a result of the increase in plasma MTX levels (Asif et al., 2005; Sweet et al., 2003).

More importantly, antiviral drugs are nephrotoxic, and the expression of OAT1 renders cells sensitive to these compounds (Ho et al., 2000). The coadministration of probenecid or NSAIDs, i.e. intended drug-drug interaction, reduced the cytotoxicity of antiviral drugs (Mulato et al., 2000). Therefore, intentional drug-drug interaction provides a means to prevent organ damage. Strategies to prevent the nephrotoxicity of antibiotics involve the use of inhibitors of OATs such as cilastatin and betamipron (Takeda et al., 2001; Tune, 1997). The use of NSAIDs (Mulato et al., 2000) and probenecid (Choudhury and Ahmed, 2006) can reduce renal excretion of antiviral drugs and of nephrotoxicity. Inhibition of OATs has not only an impact on the kidneys, but also on liver and brain. Inhibition of OATs in the liver could impair drug metabolism, and inhibition of OATs in choroid plexus and the blood brain barrier could prevent the removal of drugs from the brain and cause cerebral symptoms (Sweet, 2005).

### **1.3.3.3 Single nucleotide polymorphisms (SNPs)**

In addition to drug-metabolizing enzymes, drug transporters play important roles in determining the pharmacokinetic profiles of drugs and their pharmacological effects. Recent wide-scale sequencing analysis of the human genome has led to identification of the single nucleotide polymorphisms (SNPs) of drug transporters. It has been suggested that drug transporter SNPs are responsible for the interindividual variation in

drug elimination from the body (Ishikawa et al., 2004). With regard to OATs, there are several reports on the occurrence of SNPs both in coding and non-coding (promoter, introns) regions. Recently, two groups reported results of functional analysis of non-synonymous variants of hOAT1 genes (Bleasby et al., 2005; Fujita et al., 2005). For hOAT1, the following amino acid exchanges were reported: L7P (Xu et al., 2005); R50H; P104L; F160L; I226T; A256V; P283L; R287G; A256W; P341L; R454Q; K525I. The SNP R50H (located in the large extracellular loop between TM1 and TM2) was observed in African-Americans and Mexican-Americans with allele frequencies of 0.032 and 0.01 (Fujita et al., 2005). In another study, the SNPs R50H and K525I showed frequencies of 0.04 and 0.005, respectively (Bleasby et al., 2005). When introduced into OAT1 and expressed in *Xenopus laevis* oocytes, the mutant K454Q (located at the cytoplasmic beginning of TM11) was non-functional. All other mutants showed probenecid-inhibitable uptake of p-aminohippurate, ochratoxin A and methotrexate (Fujita et al., 2005). The  $K_m$  values for PAH and ochratoxin A were unchanged. When the  $K_m$  values for adefovir, cidofovir and tenofovir were determined, R50H, showed a significantly increased affinity towards these antiviral nucleoside phosphonates. Therefore, patients carrying the R50H mutation may be more susceptible to renal damage because of a more effective uptake of nephrotoxic antiviral drugs.

#### **1.4 Current knowledge about the structure and regulation of OATs**

Structural knowledge about the OATs is steadily increasing. This section delineates the mutagenesis studies that have been reported in literature so far describing important amino acids for structure/function (through cysteine and alanine scanning), regulation (through glycosylation and phosphorylation) and molecular modeling.

##### **1.4.1 Structure-function relations**

Several structurally related features of OATs are apparent upon sequence analysis. The rat OAT1 shares 96% of similar amino acids with the mouse OAT, and 91% with the human homologue, hOAT1. More distantly related is the flounder OAT1, which shares 57-58% of similar amino acids with rat, mouse, and human OAT1. The hOAT3 shows

51-52%, and rat OAT2 45-46%, similarities, respectively, with the OAT1 proteins. Algorithms predict 12 transmembrane domains (TMD) hOAT1 and this has also been experimentally verified (Xu et al., 2006a; Zhou et al., 2006). Between the first and second predicted TMDs, a long hydrophilic loop is found in all OATs (and in all OCTs). The large extracellular loop between transmembrane helix (TM) 1 and TM2 carries several glycosylation sites, and the intracellular loop between TM6 and TM7 and the C-terminus harbour several consensus sequences for phosphorylation by protein kinases (Fig. 1.3) (Burckhardt and Wolff, 2000). The glycosylation of human and mouse OAT1 is important for proper shuttling of newly synthesized transporters to the cell membrane (Tanaka et al., 2004b). The role of phosphorylation sites is unclear: canonical protein kinase C consensus sites were not involved in the down-regulation of human and mouse OAT1 (Wolff et al., 2003; You et al., 2000), and the sites for casein kinase II, protein kinase A and tyrosine kinases have not been studied so far.

#### **1.4.1.1 Mutagenesis studies**

Amino acid residues important for transport function have been analyzed by site-directed mutagenesis. So far the amino acid residues that are involved in substrate binding or translocation mechanisms of hOAT1 exclusively have not been investigated. In flounder OAT, the cationic amino acid residues lysine (K) at position 394 (TMD 8) and arginine (R) at position 478 (TMD 11) are involved in binding and translocation of dicarboxylates (Wolff et al., 2001). In hOAT1, the arginine at position 466 (TM11) appears to be involved in the interaction with dicarboxylates and with chloride which activates this transporter (Rizwan AN *et. al.*, unpublished). Recently, information regarding functionally critical amino acid residues has been increasing.



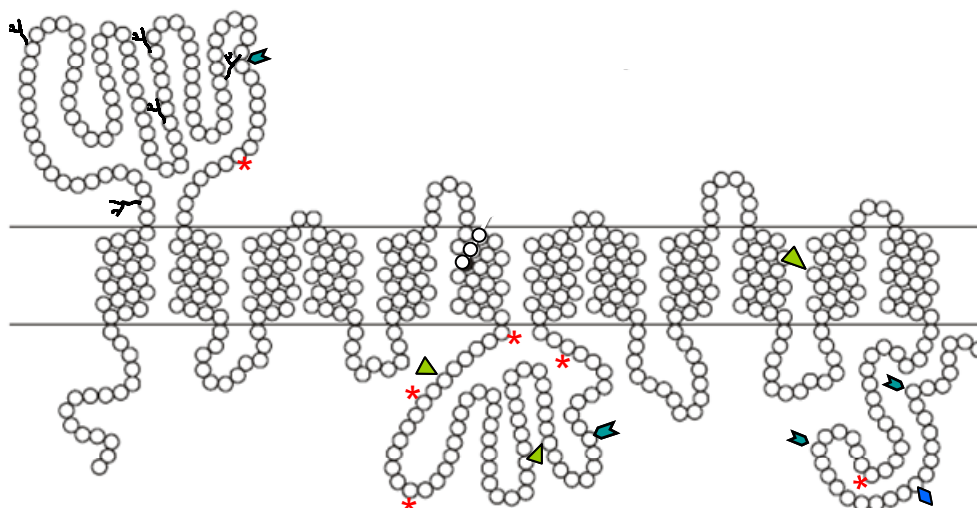


**Figure 1.3 Model of the predicted secondary structure of hROAT1.** This model represents the topology of the hROAT1 as predicted by TopPred 2 and confirmed experimentally (Hong et al., 2006). The consensus sites for enzymatic modification are also shown:  $\text{N}$  = N-glycosylation, \* = protein kinase C,  $\blacktriangle$  = protein kinase A,  $\blacktriangleright$  = casein kinase II,  $\blacklozenge$  = tyrosine kinase.

Site-directed mutagenesis studies revealed that the following residues are important for substrate recognition: Histidine (H) 34, K394, and R478 in flounder OAT1 (Wolff et al., 2001) and K370 and R454 in rOAT3 (Feng et al., 2001). In the flounder OAT1, it was shown that two non-conservative amino acid mutations K394A and R478D resulted in loss of interaction with dicarboxylates but not PAH, suggesting that these cationic residues are important for dicarboxylate but not PAH binding. In the study by Feng *et al.*, the same corresponding amino acids in mouse OAT3 were mutated. Neutral and opposite charge replacements were made as K370A, R454D and R454N. All mutants showed considerably reduced transport of the charged substrates PAH, estrone sulfate (ES) and ochratoxin A (OTA); no transport of the organic cation 1-methyl-4-phenylpyridinium (MPP); but uptake of cimetidine similar to that of wild type. Interaction with the counter-ion  $\alpha$ -ketoglutarate was not tested. Interestingly, although the R454D mutant could not transport MPP, the double mutant R454D/K370A did so in preference to the anion, PAH.

In hOAT1, an alanine scanning mutagenesis study revealed that residues leucine (L) 30 and threonine (T) 36 are important for OAT1 transport activities (Hong et al., 2004).

Progressively smaller side chains at position 30 increasingly impaired hOAT1 function mainly because of the impaired surface expression of the transporter. Substitution of T 36 by serine and cysteine (C) at this position abolished transport activity without affecting the surface expression of the transporter. These results indicate that both the methyl group and the hydroxyl group of T36 could be critical for hOAT1 activity. Recently it was shown that the C-terminus of hOAT1 has two critically important amino acids: the anionic aspartate (D) 506 and L512 (Xu et al., 2006b). D506 was reported to be important because it may maintain structural integrity through the formation of salt bridges with cationic amino acids elsewhere in the transporter. Since the mutant L512V showed similar  $K_m$  but reduced  $V_{max}$  compared to the wild type (wt), it was said to critically affect the turnover of hOAT1. Based on clues from a molecular model of hOAT1, alanine scanning illustrated that two residues, K431 and phenylalanine (F) 438 (TMD 10) result in significant functional losses independent of membrane protein expression differences in a *Xenopus* oocyte expression system. Effects of these residues on *p*-aminohippurate (PAH) and cidofovir transport were assessed by point mutations in a *Xenopus* oocyte expression system. Membrane protein expression was severely limited for the tyrosine (Y) 230A mutant. For the K431A and F438A mutants, [<sup>3</sup>H]-PAH uptake was less than 30% of wild-type hOAT1 uptake after protein expression correction. Reduced  $V_{max}$  values for the F438A mutant confirmed lower protein expression. In addition, the F438A mutant exhibited an increased affinity for cidofovir but was not significantly different for PAH. Differences in handling of PAH and cidofovir were also observed for the Y230F mutant. Little uptake was determined for cidofovir, while PAH uptake was similar to wild-type hOAT1 (Perry et al., 2006).

The cysteine-modifying reagent *p*-chloromercuribenzenesulphonate (PCMBS) inhibits mOAT1-mediated PAH transport in HeLa cells (Tanaka et al., 2004b). Site-directed mutagenesis studies revealed that single replacement of cysteine (C) residues had no significant effect on mOAT1-mediated PAH transport but that multiple replacements in the C-terminal region (C335 /379/427/434A) resulted in a substantial decrease in transport activity. A simultaneous replacement of all 13 cysteine residues (C-less) led to

a complete loss of transport function. The decrease in or lack of transport activity of the mutants C335 /379/427/434A and C-less was due to the impaired trafficking of the mutant transporters to the cell surface. These results suggest that although cysteine residues are not required for function in mOAT1, their presence appears to be important for targeting of the transporter to the plasma membrane. Since C49A was less sensitive than the wild-type mOAT1, the modification of C49 may play a role in the inhibition of mOAT1 by PCMBs (Tanaka et al., 2004b).

The counterparts of R466 in hOAT1 have been investigated in the organic cation transporters as well, namely - rOCT1 (Gorboulev et al., 1999) and rOCT2 (Bahn et al., 2004b). The effect of a charge conservative mutation and  $K_m$  determination was also made in rOCT1. It was found that  $K_m$  values remained same (MPP for OCT1) or were decreased (choline, TEA, N'-methylnicotinamide for OCT1) whereas maximal transport rate ( $V_{max}$ ) went down severely.

#### **1.4.1.2 Molecular modeling of hOAT1**

Membrane proteins are encoded by almost 30% of gene sequences, but only 89 unique crystal structures exist for these proteins (Perry et al., 2006). Like other membrane proteins, the lack of structural information on OATs prompted the need for a molecular level structural model of OAT1. A structural model of hOAT1 would offer the ability to perform hypothesis driven research, testing substrate/protein interactions experimentally with point mutations and refining the model by experimental outcomes. It also helps, as in the present study, to validate previous/ongoing research on the transporter.

Very recently, a fold-recognition model of hOAT1 based on the structure of the GlpT has been proposed and some residues that align a putative active cavity and may have potential interactions with hOAT1 substrates have been identified (Fig. 1.4) (Perry et al., 2006).

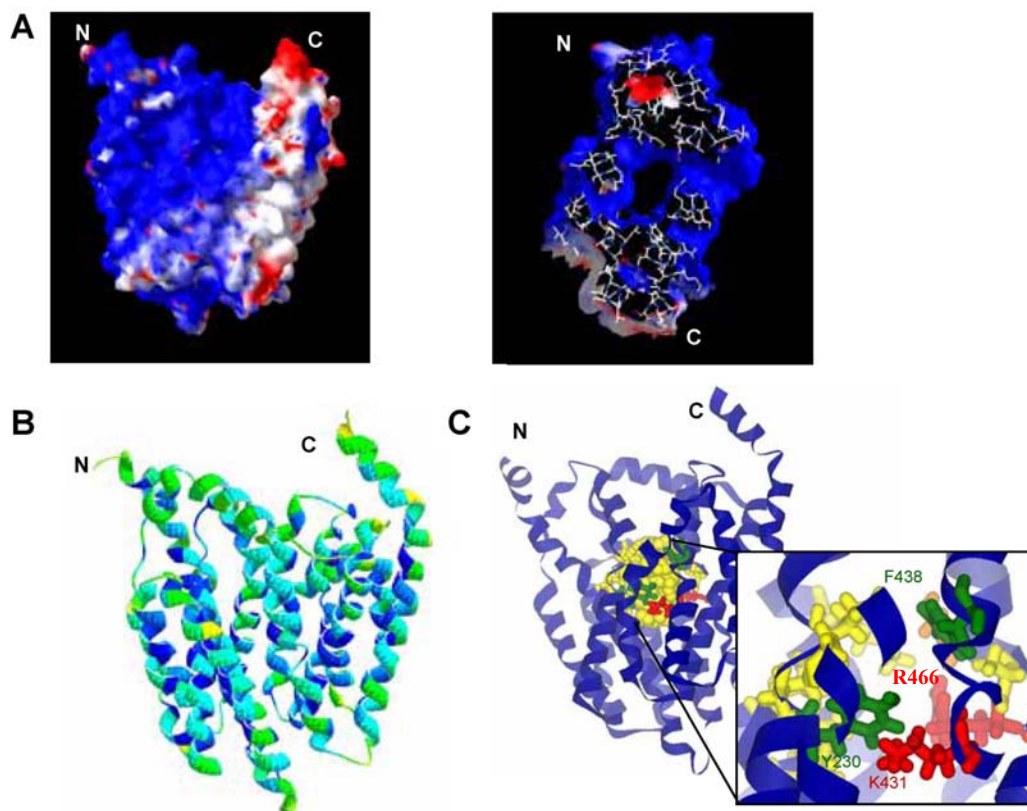


**Figure 1.4. A molecular model of hOAT1.** (A). Electrostatic potential map of the hOAT1 model. Two perspectives are shown, the first image depicts a horizontal view of the protein and the second image looks down on the cavity between the helices from the cytoplasm. Blue shading indicates large positive areas while red shading indicates large negative regions. (B). Solvent accessibility for the hOAT1 model. Blue depicts completely buried residues, while orange and yellow residues (mostly in loops) have greater than 50% of their surfaces accessible. (C). Putative active site of hOAT1 surrounded by helices 5, 7, 10 and 11. The inset depicts residues examined within this study along with residues 9 Å from the center of the predicted binding cavity for hOAT1. Basic: K431, R466 (red), Polar: S462, (orange) Aromatic: Y230, F438, (green) Aliphatic: L28, M31, A32, M207, I226, Q227, V229, A465 (yellow). (Perry et al., 2006)

According to this model:

The molecular surface indicates hOAT1 contains a large positive charge from the N-terminal side through the central cavity, due to basic amino acids. The putative active site for hOAT1 has a volume of 830 Å<sup>3</sup>, and has a large positive charge through the

central cavity due to basic amino acids. Arginine (R) 466 sits at the opening of the pocket while aromatic amino acids such as tryptophan (Y) and phenylalanine (F) surround the site. New residues additional residues Y230 (domain 5), K431 (domain 10) and F438 (domain 10) were identified and provided new aromatic and basic residues to test for model validation and potential impact on substrate transport.

## **1.4.2 Regulation**

### **1.4.2.1. Phosphorylation**

Organic anion transport in intact renal proximal tubular cells in animal model systems is reported to be downregulated by protein kinase C (PKC). All OAT isoforms cloned have several sites for PKC phosphorylation in the large intracellular loop between the sixth and seventh transmembrane domains.

Several studies have revealed that the activation of PKC decreases the transport activity of OATs (Lu et al., 1999; Soodvilai et al., 2004; Takeda et al., 2000; Uwai et al., 1998; Wolff et al., 2003; You et al., 2000). This inhibitory effect is also associated with altered substrate selectivity. The reduced OAT-mediated transport activity is rescued by PKC inhibitors. Furthermore, PKC-induced hOAT1 downregulation is achieved via carrier retrieval from the cell membrane. In addition to the sites for phosphorylation by PKC, OAT isoforms have putative sites for phosphorylation by protein kinase A (PKA), casein kinase II, or tyrosine kinase. Among these, protein kinases, including mitogen-activated protein kinase (MAPK), PKA, and tyrosine kinase, have been shown to be involved in the regulation of OAT transport functions (Sauvant et al., 2004; Soodvilai et al., 2004; Soodvilai et al., 2005). Epidermal growth factor (EGF) stimulates PAH and estrone sulfate transport in rabbit renal proximal tubules via MAPKs, and PGE<sub>2</sub> enhances basolateral PAH and estrone sulfate uptake via adenylate cyclase activation and causes PKA activation. A recent study has demonstrated that OAT3-mediated activity is also inhibited by tyrosine kinase and phosphatidylinositol 3-kinase (PI3K) (Soodvilai et al., 2005).

#### 1.4.2.2. Glycosylation

Glycosylation sites in the first extracellular loop between transmembrane domains (TMDs) 1 and 2 are conserved in OATs. Tunicamycin, an inhibitor of asparagine-linked glycosylation, inhibits PAH transport activity in mOAT1-transfected COS7 cells. Immunofluorescence revealed that the mOAT1 protein remained mainly in the intracellular compartment after tunicamycin treatment (Kuze et al., 1999). This indicated that glycosylation of the mOAT1 protein is necessary for proper trafficking of the protein to the plasma membrane. Other experiments have demonstrated that disruption of N39 (one of the glycosylated sites) in mice resulted in complete loss of transport activity of OAT1 without affecting its surface expression (Tanaka et al., 2004a). Thus, glycosylation could also be responsible for substrate recognition. Recently, a study investigated how the addition/acquisition and processing/modification of N-linked oligosaccharides play a role in the functional maturation of OAT4 using a novel approach (Zhou et al., 2005). Inhibition of acquisition of oligosaccharides in OAT4 by mutating asparagine to glutamine and by tunicamycin treatment was combined with wild-type OAT4 expression in a series of mutant CHO-Lec cells defective in different steps of glycosylation processing. Zhou et al., demonstrated that both the disruption of glycosylation sites by mutagenesis and the inhibition of glycosylation by tunicamycin treatment resulted in a nonglycosylated OAT4, which was unable to target to the cell surface. In contrast, OAT4 synthesized in mutant CHO-Lec cells carrying different structural forms of sugar moieties (mannose-rich in Lec1 cells, sialic acid-deficient in Lec2 cells, and sialic acid/galactose-deficient in Lec8 cells) was able to traffic to the cell surface. However, OAT4 expressed in CHO-Lec1 cells had significantly lower binding affinity for its substrates than did that expressed in parental CHO cells. These results provided novel information that addition/acquisition of oligosaccharides but not the processing of added oligosaccharides participates in the membrane insertion of OAT4. Processing of added oligosaccharides from mannose-rich type to complex type is important for enhancing the binding affinity of OAT4 for its substrates. Glycosylation could therefore serve as a means to specifically regulate

OAT4 function *in vivo* and in principle these findings could also be used for investigating the role of glycosylation in hOAT1.

#### **1.4.2.3 Gender differences**

Gender differences in mRNA and/or protein expression have been reported for OAT1 (Buist et al., 2002; Ljubojevic et al., 2004), OAT2 (Buist et al., 2002; Kobayashi et al., 2002a; Kobayashi et al., 2002b), OAT3 (Buist et al., 2002; Kobayashi et al., 2002a; Ljubojevic et al., 2004), and Urat1 (Hosoyamada et al., 2004), suggesting that some OAT family members are regulated by sex hormones. The mouse OAT1 mRNA levels were found to be higher in the male kidney than in the female kidney, and the rat OAT2 mRNA expression level was found to be higher in the female kidney than in the male kidney or liver. In contrast, the mouse OAT2 mRNA levels were found to be high in both male and female kidneys and low in the male liver. Rat OAT3 mRNA expression was detected in the male liver. The mouse Urat1 mRNA levels were found to be higher in the male kidney than in the female kidney.

#### **1.4.2.4 Oligomerization**

Only one study so far has provided information on the structural assembly of a cloned OAT to date. Using combined approaches of chemical cross-linking, gel filtration chromatography, co-immunoprecipitation, cell surface biotinylation, and metabolic labeling Hong *et al.* demonstrated for the first time that hOAT1 exists in the plasma membrane as homooligomeric complexes, possibly trimer, and higher order of oligomer (Hong et al., 2005).

### **1.5 Aims of the present study**

The primary aim of this study was to evaluate the structure-activity relationships in the human Organic Anion Transporter 1. Towards this goal, charged and conserved amino acid residues within the transmembrane domains of the transporter would be mutated and functionally characterized in order to ascertain their contribution in substrate

binding and translocation. Another part of the study sought to fill gaps in the current knowledge of the physiology of  $\text{OA}^-$  transport by OAT1. This would involve determining the effect of pH, interaction with Krebs cycle intermediates and investigation of the chloride mediated regulation of hOAT1.



## 2. MATERIALS

### 2.1 Oligonucleotide Primers

Sequence specific primers for sequence analysis and for site-directed mutagenesis were obtained from MWG Biotech AG (Ebersberg, Germany) and are listed in Table 2.1 below.

Amino-acid replacement	Primer Name	5' to 3' Mutation Primer Sequence
<b>R466K</b>	R466K-fw	GGCAGCACCATGGCC <b>AA</b> AGTGGGCAGCATCGTG
	R466K-rev	CACGATGCTGCCCACT <b>TTT</b> GGCCATGGTGCTGCC
<b>R466D</b>	R466D-fw	GGCAGCACCATGGCC <b>GAC</b> GTGGGCAGCATCGTG
	R466D-rev	CACGATGCTGCCCACT <b>GTC</b> GGCCATGGTGCTGCC
<b>R466N</b>	R466N-fw	GGCAGCACCATGGCC <b>AAC</b> GTGGGCAGCATCGTG
	R466N-rev	CACGATGCTGCCCACT <b>GTT</b> GGCCATGGTGCTGCC
<b>K382A</b>	K382A-fw	GGACCTGCCTGCC <b>GCG</b> CTTGTGGGCTTCCTTGTC
	K382A-rev	GACAAGGAAGCCCACAAGC <b>GCG</b> GCAGGCAGGTCC
<b>K382R</b>	K382R-fw	GGACCTGCCTGCC <b>GCG</b> CTTGTGGGCTTCCTTGTC
	K382R-rev	GACAAGGAAGCCCACAAGC <b>GCG</b> GCAGGCAGGTCC
<b>K382R/R466K</b>	K382R/R466K-fw	Mutation primer: K382R-fw; plasmid: R466K mutant
	K382A/R466D-rev	Mutation primer: K382R-rev; plasmid: R466K mutant
<b>K431R</b>	K431R-fw	CTTGCTGTGCTGGGG <b>GCG</b> GGTGTCTGGCTGCC
	K431R-rev	GGCAGCCAGACAACCC <b>GCG</b> CCCCAGCACAGCAAG
<b>K431D</b>	K431D-fw	GCTGTGCTGGGG <b>GAT</b> GGTGTCTGGCTGCCTCC
	K431D-rev	GGAGGCAGCCAGACAACC <b>ATC</b> CCCCAGCACAGC
<b>K431R/R466K</b>	K431R/R466K-fw	Mutation primer: K431R-fw; plasmid: R466K mutant
	K431R/R466K-rev	Mutation primer: K431R-rev; plasmid: R466K mutant
<b>D378A</b>	D378A-fw	TGATCTTTGGTGCTGTGG <b>CC</b> CCTGCCTGCCAAGC
	D378A-rev	GCTTGGCAGGCAG <b>GGC</b> CACAGCACCAAAGATCA
<b>D378R</b>	D378R-fw	TGATCTTTGGTGCTGTGG <b>CC</b> CCTGCCTGCCAAGC
	D378R-rev	GCTTGGCAGGCAG <b>GGC</b> CACAGCACCAAAGATCA
<b>D378R/R466D</b>	D378R/R466D-fw	Mutation primer: D378R-fw; plasmid: R466D mutant
	D378R/R466D-rev	Mutation primer: D378R-rev; plasmid: R466D mutant
<b>D378K/K431D</b>	D378R/K431D-fw	Mutation primer: D378R-fw; plasmid: K431D mutant
	D378R/K431D-rev	Mutation primer: D378R-rev; plasmid: K431D mutant

**Table 2.1 Oligonucleotide primers used in this study.** The codon is written in bold and the nucleotide replacements are underlined. Abbreviations used are: fw = forward; rev = reverse; Sequence details: A = adenosine, G = guanosine, C = cytosine, T = thymine; amino acid short-forms: R = arginine, K = lysine, D = aspartate, A = alanine, N = asparagine.

## 2.2 Enzymes

The restriction enzyme NOT I used for linearizing plasmid DNA was purchased from New England Biolabs Inc (Beverly, MA, USA). DNA polymerase *Pfu* DNA Polymerase, used for amplification of the entire plasmid in mutation PCRs, was purchased from Stratagene (La Jolla, CA, USA).

## 2.3 Chemicals and radiochemicals

All chemicals were of reagent grade. *p*-[*glycyl*-2-<sup>3</sup>H]aminohippurate ([<sup>3</sup>H]PAH) 5 μCi/ml, 1 to 5 Ci/mmol was obtained from Perkin Elmer, Boston, MA. [1,5-<sup>14</sup>C]glutaric acid ([<sup>14</sup>C]GA) 100 μCi/ml, 55 mCi/mmol was obtained from MP Biomedicals, Heidelberg, Germany. [<sup>3</sup>H(G)]-ochratoxin A ([<sup>3</sup>H]OCTX A) 1 mCi/ml, 7.2 Ci/mmol was obtained from Moravek Biochemicals Inc., Brea, CA. Unlabeled *p*-aminohippurate (PAH), glutaric acid (GA), adipic acid (AA) and malonic acid (MA) were obtained from Sigma, St. Louis, MO. 6-carboxy fluorescein (6-CF) [3',6'-dihydroxy-3-oxospiro (isobenzofuran-1(3H),9'-(9H)xanthene)-6-carboxylic acid] was purchased from Molecular Probes (Leiden, The Netherlands).

## 2.4 Cell lines

Originally the T-REx<sup>TM</sup>-HEK 293 cells (Human embryonic kidney, adherent fibroblastoid cells in monolayers) from Invitrogen Life technologies (Karlsruhe, Germany), were designed for use with the T-REx<sup>TM</sup> System (Invitrogen, Life Technologies) and they stably express the tetracycline (Tet) repressor. These T-REx<sup>TM</sup>-HEK293 cells were stably transfected with hpcDNA6/TR-based expression constructs, containing hOAT1 or only vector (negative control), and the dual selection made with Geneticin<sup>®</sup> and blasticidin by Dr. Ugele, Universitäts-Frauenklinik, München.

## 2.5 Buffers

The compositions of buffers used in the experimental procedures described under methods are given below.

<b>Buffers used</b>	<b>Composition</b>
TBE buffer	45 mM Tris, 45 mM borate, and 1 mM EDTA
TAE buffer	0.04 M Tris, 0.001 M EDTA-Na <sub>2</sub> -salt and 0.02 M acetic acid
Oocyte Ringer solution (ORI)	90mM NaCl, 3mM KCl, 2mM CaCl <sub>2</sub> , 1mM MgCl <sub>2</sub> , 5mM HEPES/Tris, pH 7.6
Cl <sup>-</sup> free ORI	90mM Na gluconate, 3mM K gluconate, 2mM Ca gluconate, 1mM Mg gluconate, 5mM HEPES/Tris, pH 7.6
Oocytes Barth's solution	88 mM NaCl, 1 mM KCl, 0.3 mM Ca(NO <sub>3</sub> ) <sub>2</sub> , 0.41 mM CaCl <sub>2</sub> , 0.82 mM MgSO <sub>4</sub> , 15 mM HEPES, 10 mg/l gentamicin, pH 7.6
Mammalian Ringer (MR) solution	130 mM NaCl, 4 mM KCl, 1 mM CaCl <sub>2</sub> , 1 mM MgSO <sub>4</sub> , 20 mM HEPES, 1mM NaH <sub>2</sub> PO <sub>4</sub> , and 18 mM glucose, pH 7.4
Cl <sup>-</sup> free MR	130 mM Na gluconate, 4 mM K gluconate, 1 mM Ca gluconate, 1 mM MgSO <sub>4</sub> , 1mM NaH <sub>2</sub> PO <sub>4</sub> , 20 mM HEPES, and 18 mM glucose, pH 7.4
Phosphate buffered saline (PBS)	150 mM NaCl, 10 mM Na <sub>2</sub> HPO <sub>4</sub> , 2.5 mM KCl, 1.5 mM KH <sub>2</sub> PO <sub>4</sub> , pH 7.2

**Table 2.2 Buffers that were used in this study.**

## 2.6 Cell culture media and supplements

Dulbecco's modified Eagle's medium (DMEM), fetal calf serum, Dulbecco's modified Eagle's medium nutrient mixture F-12 HAM, Phosphate Buffered Saline (PBS), and Penicillin/Streptomycin 10000U were from Gibco/Invitrogen Life Technologies (Karlsruhe, Germany). 35 mm, 100 mm, 145 mm culture Petri dishes, 25 cm<sup>2</sup> flasks, 45 cm<sup>2</sup> flasks and 75 cm<sup>2</sup> flasks were from Falcon (Lincoln Park, NJ USA). Six-well, 24-well, 96 well culture plates, cryopreservation vials, and sterile filters 0.2 µm were purchased from Nunc (Wiesbaden, Germany).

## 2.7 Plasmid vectors

*pcDNA3.1* – The functional FLAG-tagged hOAT1 used in this study was created in the following way. The hOAT1 coding region was subcloned into the untranslated regions (UTR) of the flounder sodium/ dicarboxylate cotransporter (fNaDC-3), which can be well expressed in oocytes. For this, the *Bam*HI and *Xba*I sites of the fNaDC-3 vector (pSport1) were disrupted by site-directed mutagenesis. The hOAT1 reading frame and the fNaDC-3 UTR separated by the vector were then amplified. The primers used in this amplification incorporated *Bam*HI and *Xba*I sites for hOAT1, to enable subsequent subcloning. The hOAT1 coding region flanked by *Bam*HI and *Xba*I restriction sites, which had been subcloned into pPCR-Script (Stratagene, La Jolla, CA), and the fNaDC-3 UTR/pSport1 amplificate were then sequentially digested with *Bam*HI and *Xba*I and were ligated together with T4 DNA ligase. For expression in mammalian cells, hOAT1 was subcloned into the *Kpn*I and *Not*I sites of pcDNA3.1 (Invitrogen, Calsbad, CA) (see Fig. 2.1) (Wolff et al., 2003).

*Epitope tagging* – for immunocytochemical detection, a FLAG epitope was introduced in the large first extracellular loop between amino acid residues 107 and 108, with primers containing the FLAG sequence flanked by regions complementary to adjacent regions of hOAT1 (MWG Biotech).

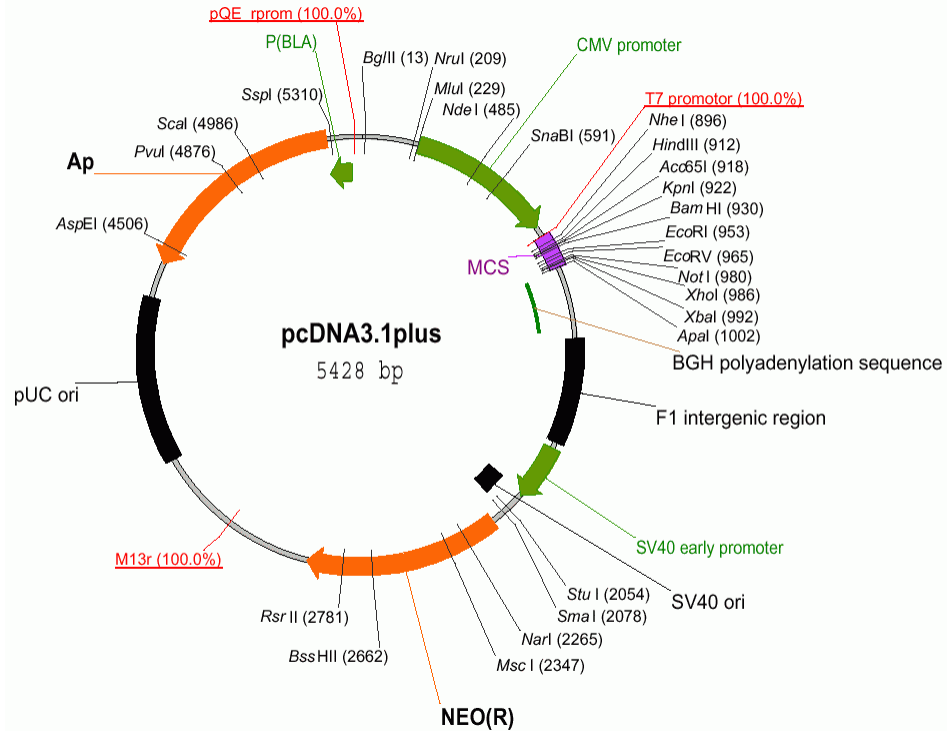


**Figure 2.1** Structure of the pcDNA3.1 vector. The vector contains the following elements: Human cytomegalovirus immediate-early (CMV) promoter for high-level expression in a wide range of mammalian cells, Multiple cloning sites in the forward (+) and reverse (-) orientations to facilitate cloning, and neomycin resistance gene for selection of stable cell lines.

## 2.8 Bacteria

Bacteria strains used for maintenance of plasmid constructs are listed in the Table 2.2 below.

Strain	Company	Genotype
INVaF.	Invitrogen	F', endA1, recA1, hsdR17 (rk -, mk +), supE44, thi-1, gyrA96, relA1, $\Phi$ 80lacZ $\Delta$ M15 $\Delta$ (lacZYA-argF)U169
TOP10F	Invitrogen	F'f, mcrA, $\Delta$ (mrr-hsdRMS-mcrBC), $\Phi$ 80lacZ $\Delta$ M15 $\Delta$ lacX74, deoR, recA1, araD139, $\Delta$ (ara-leu)7697, galU, galK, rpsL (StrR), endA1, nupG
XL1-Blue	Stratagene	recA1, endA1, gyrA96, thi-1, hsdR17, supE44, relA1, lac [F. proAB lacIq $\Delta$ M15 Tn10 (Tetr)]

**Table 2.3** Bacterial (*E.coli*) strains used in the study.

## 2.9 Kits

All kits used are listed in Table 2.4 below.

<b>A. Nucleic acid purification</b>	
MinElute Gel Extraction Kit	QIAGEN (Hilden, Germany)
QIAquick PCR Purification Kit	
QIAprep Spin Miniprep Kit	
NucleoSpin Plasmid Kit	Macherey-Nagel (Düren, Germany)
<b>B. Mutagenesis</b>	
QuikChange Site-directed Mutagenesis Kit	Stratagene (La Jolla, CA, USA)
<b>C. cRNA synthesis</b>	
T7 mMessage mMachine Kit	Ambion (Austin, TX, USA)

**Table 2.4 Kits used in this study.**

## 2.10 Software

Listed below are the software and online servers used to analyze raw sequence data, perform sequence alignments, identify putative secondary structures of protein sequences and consensus sequences for enzyme recognition sites, and primer design.

<b>Software</b>		
<b>Program</b>	<b>Use</b>	<b>Reference</b>
Chromas	sequence reading program	Technelysium Pty Ltd
Generunner	primer design	Hastings Software Inc
Microsoft Excel	evaluation of uptake and efflux experiments	Microsoft Corporation
SigmaPlot	statistical analyses	Jandel Corporation
LSM	image processing	Zeiss
ImageJ	image analysis	NIH
Reference Manager	managing of bibliographic references	Wintertree Software Inc

**Online sequence analysis servers**

<b>Program</b>	<b>Use</b>	<b>Reference</b>
Entrez Browser	sequence retrieval	<a href="http://www.ncbi.nlm.nih.gov/Entrez/">http://www.ncbi.nlm.nih.gov/Entrez/</a>
MAP	multiple sequence alignments	<a href="http://genome.cs.mtu.edu/map.html">http://genome.cs.mtu.edu/map.html</a>
TopPred 2	secondary structure prediction	<a href="http://www.biokemi.su.se/~server/toppred2/">http://www.biokemi.su.se/~server/toppred2/</a>
Webcutter	restriction maps	<a href="http://www.medkem.gu.se/cutter/">http://www.medkem.gu.se/cutter/</a>
Translation tool	N sequence to aa sequence	<a href="http://www.expasy.ch/tools/dna.html">http://www.expasy.ch/tools/dna.html</a>
Blast	Sequences alignments	<a href="http://www.ncbi.nlm.nih.gov/BLAST/">http://www.ncbi.nlm.nih.gov/BLAST/</a>
ClustalW	Sequences alignments	<a href="http://www.ebi.ac.uk/clustalw/">http://www.ebi.ac.uk/clustalw/</a>

**Table 2.5 Software used in this study****2.11 Equipment**

All equipment are listed in table 2.4 below

<b>Appliance</b>	<b>Model</b>	<b>Manufacturer</b>
Automated DNA sequencer	ABI Prism	Applied Biosystems (Laguna Beach CA, USA)
Centrifuges	Biofuge fresco 5417R	Heraeus (Osterode, Germany) Eppendorf (Hamburg, Germany)
Circulating water baths	D8	Haake (Karlsruhe, Germany)
Dissection microscope	Stemi1000	Zeiss (Jena, Germany)
Gel chamber	Midi	MWG-Biotech (Ebersberg, Germany)
Gel documentation	Gel Print 2000 I	Biophotonics (Ann Arbor, MI, USA)
Electroporator	Easyject	Equibio (Monchelsea, England)
Nanoliter injector		World Precision Instruments (Sarasota FL, USA)
Microwave	Privileg 8017	Quelle Schikedanz (Fürth, Germany)
pH meter	pH-Meter 611	Orion Research Inc (Beverly MA, USA)
Scintillation counter	1500 Tri-Carb	Packard Instrument Co (Meriden CT, USA)
Shaking incubator	3031	GFL (Burgwedel, Germany)
Spectrophotometer	GeneQuant II	Pharmacia (Uppsala, Sweden)
Speed vacuum	SVC 100E	Savant (Holbrook NY, USA)

concentrator

Thermocycler                      PTC-200                      MJ Research (Watertown MI, USA)

UV transilluminator              TM40                      UVP Inc (Upland, CA, USA)

Vortexer                              MS1                      IKA (Staufen, Germany)

---

**Table 2.6 Equipment used in this study.**



### 3. METHODS

#### 3.1. Molecular biological methods

##### 3.1.1 Site-Directed Mutagenesis

The QuikChange™ Site-Directed Mutagenesis Kit (Stratagene) was the method of choice for the introduction of single base mutations into hOAT1 Loop-FLAG clone (loop flag indicates that the FLAG epitope was introduced within the first large extracellular loop of hOAT1) (also see section 2.1). The FLAG tag is a short, hydrophilic 8-amino acid peptide. Because of its hydrophilic nature, the FLAG peptide is better located on the surface of the fusion protein. As a result, the FLAG peptide is easily accessible for detection with antibodies. In addition, because of the small size of the FLAG peptide tag, it did not obscure other epitopes, domains, or alter function, secretion, or transport of the fusion protein (hOAT1 Loop-FLAG). The QuikChange kit allows site-specific mutation in any double-stranded plasmid, thus eliminating the need for subcloning into M13-based bacteriophage vectors and for ssDNA rescue. The basic procedure involves a double-stranded DNA (dsDNA) vector with an insert of interest and two synthetic oligonucleotide primers containing the desired mutation. The oligonucleotide primers, each complementary to opposite strands of the vector, extend during temperature cycling by means of *Pfu* DNA polymerase (Table 2.1). This generates a mutant plasmid with staggered nicks, and the template can be removed by digestion with *DpnI* (a methylation-dependent endonuclease, which reacts only with the methylated template plasmid isolated from bacteria, target sequence: 5'-G<sup>m6</sup>ATC-3'). The nicked vector DNA incorporating the desired mutation can be then transformed into *E. coli*, where the nicks are repaired.

For introducing of each specific mutation, the mutagenic oligonucleotide primers were designed individually according to the desired nucleotide base substitution. The following consideration was taken for designing mutagenic primers: both primers contained the desired mutation and annealed to the same sequence on opposite strands of the plasmid; they were between 30 and 33 bases in length with the melting

temperature ( $T_m$ ) of around 78°C; the desired nucleotide base substitution was situated in the middle of the primer with approximately 15 bases of correct sequence on both sides; primers had a minimum GC content of 40% and terminated in C or G bases.

### Reagents used

<i>Pfu</i> DNA polymerase	2.5 U/ $\mu$ l
10x reaction buffer	100 mM KCl, 100 mM (NH <sub>4</sub> ) <sub>2</sub> SO <sub>4</sub> , 200 mM Tris-HCl (pH8.8), 20 mM MgSO <sub>4</sub> , 1% Triton X-100, 1 mg/ml BSA
Oligonucleotide primers	Forward and reverse primers, specific for each mutation, 125 ng/ $\mu$ l
dNTP mix	Composition not supplied by manufacturer
<i>Dpn I</i> restriction enzyme	10 U/ $\mu$ l
Competent cells	<i>Epicurian Coli</i> XL1-Blue supercompetent cells, 50 $\mu$ l
SOC medium	10 mM NaCl, 2.5 mM KCl, 10 mM MgCl <sub>2</sub> , 10 mM MgSO <sub>4</sub> , 20 mM Glucose, 2% Tryptone, 0.5% Yeast Extract

All primers, used for mutagenesis are listed in the materials section. The cycling reaction mix consisted of 5 $\mu$ l of 10x reaction buffer, 50 ng of template plasmid (2 $\mu$ l of 25ng/ $\mu$ l diluted plasmid DNA), 125 ng of each oligonucleotide primer, 1 $\mu$ l of dNTP mix, 1 $\mu$ l of *Pfu* DNA polymerase (2.5 U/ $\mu$ l) and ddH<sub>2</sub>O was added to a final volume of 50 $\mu$ l. Cycling parameters were: 95°C for 30 seconds, followed by 18 cycles of: 95°C for 30 seconds, 55°C for 1 minute, and 68°C for 13 minutes. Following temperature cycling, the reaction was placed on ice for cooling to less than 37°C. Afterwards, the template DNA was digested by adding of 1 $\mu$ l of the *Dpn I* restriction enzyme (10 U/ $\mu$ l) to amplification reaction and incubation at 37°C for 1 hour. Once *Dpn I* digestion was complete, 1  $\mu$ l of the extension mix was added to pre-thawed Epicurian Coli<sup>®</sup> XL1-Blue super-competent cells, gently mixed and incubated on ice for 30 min. The cells were then exposed to a 45 seconds heat shock at 42°C, and then transferred immediately on ice. After 2 minutes incubation on ice, 500  $\mu$ l SOC medium was added and the tube with cells were shaken horizontally at 37°C at 220 rpm for 1-2 hours. Afterwards, 200

$\mu$ l aliquot was spread on a pre-warmed LB agar plate, supplemented with ampicillin (specific for the plasmid used) and incubated at 37°C overnight. On the following day colonies were picked and cultured in LB medium (overnight). Plasmid DNA was isolated and sequenced to verify the presence of desired mutation.

### 3.1.2 cRNA synthesis

cRNAs for the oocyte microinjection were synthesized by means of the T7 mMESSAGE mMACHINE kit (for hOAT1 in pcDNA3.1(+) plasmid). These kits enable the synthesis of large amounts of capped RNA from a linearized cDNA template, by incorporation of cap analog (m<sub>7</sub>G(5')ppp(5')G) during polymerization reaction. Capped RNA mimics most eukaryotic mRNAs found *in vivo*, because it has a 7-methyl guanosine cap structure at the 5' end. mMESSAGE mMACHINE reactions include cap analog [m<sub>7</sub>G(5')ppp(5')G] in an ultra high-yield transcription reaction. The cap analog is incorporated only as the first or 5' terminal G of the transcript because its structure precludes its incorporation at any other position in the RNA molecule.

#### Reagents used

Enzyme Mix	Buffered 50% glycerol containing RNA polymerase, SUPERase•In, and other components
10x Transcription Buffer	T7 Reaction Buffer, salts, buffer, dithiothreitol, and other ingredients
2x Ribonucleotide Mix	T7 kit: 15 mM ATP, CTP, UTP, 3mM GTP and 12 mM Cap Analog; SP6 kit: 10 mM ATP, CTP, UTP, 2mM GTP and 8mM Cap Analog
TURBO DNase	RNase-free (2 U/ $\mu$ l), supplied in 50% glycerol buffer
Template DNA	Linearized with <i>NotI</i> restriction enzyme
Precipitation solution	7.5 M LiCl, 75 mM EDTA
Water	nuclease free provided with the kit

Before cRNA synthesis, the double-stranded DNA template should be digested to completion with a suitable restriction enzyme that cleaves distal to the promoter, downstream of the insert to be transcribed. *NotI* was the restriction enzyme of choice. The composition of digestion reaction was: 5 $\mu$ g of template cDNA, 3  $\mu$ l of 10x

NEBuffer 3 (100 mM NaCl, 50 mM Tris-HCl, 10 mM MgCl<sub>2</sub>, 1 mM dithiothreitol, pH 7.9 at 25°C), 3 µl of 10x BSA (to final concentration of 100µg/ml), 2.5 µl of 10U/µl *NotI* restriction enzyme (5-fold overdigest condition) and H<sub>2</sub>O to a final volume of 30µl. Digestion was carried out at 37°C for 3 hours, and its efficiency was checked on agarose gel. The linearized product was purified by ethanol precipitation, re-suspended in 10µl of nuclease-free H<sub>2</sub>O and measured for the DNA concentration. For the cRNA synthesis, transcription reaction was assembled at room temperature, and consisted of: 2µl of 10x reaction buffer, 10 µl of 2x ribonucleotide mix, 1 µg of linear template DNA, 2µl of enzyme mix, and nuclease-free H<sub>2</sub>O to a final volume of 20µl. The reaction was incubated at 37°C for 2 hours, after with template DNA was removed by the addition of 1 µl Rnase-free TURBO DNase and incubation at 37°C for 15 minutes. Following incubation, the synthesized cRNA was precipitated by adding of 30 µl of nuclease-free H<sub>2</sub>O, 30 µl of LiCl precipitation solution, and chilling the sample at -20°C for at least 2 hours. Afterwards, the cRNA was collected by centrifugation for 30 min at 4°C, 2 times washed and re-centrifuged with 1 ml of 70% ethanol. After removal of the ethanol, the cRNA was dried at room temperature for ~ 20 minutes and re-suspended in 20 µl of nuclease-free H<sub>2</sub>O. The concentration was determined and adjusted to either 1 µg/µl (23 ng of cRNA per 23 nl injection volume). The cRNA samples were stored at -80°C.

### **3.1.3 Restriction digestion**

Restriction digestion was used as a part of linearization of cDNA template in the procedure of site-directed mutagenesis. Plasmid DNA had to be linearized with a restriction enzyme downstream of the insert to be transcribed since circular plasmid templates will generate extremely long, heterogeneous RNA transcripts because RNA polymerases are very processive.

---

**Reagents used**

---

DNA template	1-5 $\mu$ g
10x Enzyme Buffer	10% v/v; composition depends on enzyme used
100x BSA	1% v/v; added when necessary for enzyme activity
Restriction Enzyme	2-5 U/ $\mu$ g DNA; less than 10% of the final reaction volume
Nuclease-free H <sub>2</sub> O	Up to required volume

---

After setting, the reaction was incubated at 37°C for 1-4 hours, depending on efficiency of enzyme used. The completion of digestion was controlled through gel electrophoresis.

**3.1.4 DNA isolation and purification****3.1.4.1 Agarose gel electrophoresis**

Agarose gel electrophoresis was used for visualization or/and isolation of DNA after PCR amplification. Agarose gels were cast at concentrations of 0.7% to 1.5%, depending on the size of the DNA molecule to be separated. Agarose was dissolved in TBE buffer (45 mM Tris, 45 mM borate, 1 mM EDTA) by heating in a microwave for ~ 1 minute. After cooling to 60-70°C, 10mg/ml ethidium bromide solution was added to a final concentration of 0.5  $\mu$ g/ml, mixed thoroughly, and the solution was immediately poured into the mold. The gel was completely set after 30-45 minutes at room temperature and run at 60-100 V for 1-2 hours, depending on the size of the DNA to be separated. Results of electrophoresis were visualized using Dual Intensity Ultraviolet Transilluminator (UniEquip) and photo-documented. Required DNA fragments were excised with a scalpel from gel, and isolated using the NucleoSpin<sup>®</sup> Gel Extraction kit (Macherey-Nagel) or the MinElute<sup>™</sup> Gel Extraction kit (Qiagen), according to the protocols provided.

**3.1.4.2 Isolation of plasmid DNA**

*E.coli* colonies, transformed with the plasmid of interest (as described previously under section 3.1.1), were cultured overnight in 5-7 ml of LB medium (10 g/l trypton, 5 g/l

yeast extract, 10 g/l NaCl, pH adjusted to 7.3 with NaOH, medium sterilized by autoclaving), containing 100µg/ml ampicillin. Cells from 3-6 ml of culture, depending on culture density, were harvested by centrifugation. Plasmid DNA was isolated by the principle of SDS/alkaline lysis, according to the manufacturer's instructions (NucleoSpin Plasmid kit; Macherey-Nagel). Therefore, the cells were resuspended in 250 µl of buffer A1, containing RNase, and lysed by addition of 250 µl of A2 buffer, containing SDS. Once lysis had occurred, 300 µl of neutralizing buffer A3 was added and mixed until formation of precipitate. Afterwards the SDS precipitate and cell debris were pelleted by centrifugation at maximum speed for 10 min, and the supernatant was loaded onto a NucleoSpin Plasmid column. Contaminations were washed away by centrifuging first with 500 µl of pre-warmed to 50°C AW buffer and then 600 µl of ethanol-containing buffer A4. The remaining ethanol was removed by additional centrifugation for 2 minutes and drying at 37°C for 5 minutes. Finally, plasmid DNA was eluted with 50 µl of buffer AE (5 mM Tris-HCl, pH 8.5) by centrifuging the column for 1 minute.

#### **3.1.4.3 Ethanol precipitation**

Precipitation with ethanol was used as the rapid technique for concentrating nucleic acids. Therefore 3M sodium acetate (pH 5.2) to a final concentration of 0.3 mM and 5 volumes of ice-cold ethanol were added to the DNA solution. After mixing the ethanolic solution was placed on -20°C for 15-30 minutes to allow precipitation of DNA. Afterwards DNA was recovered by centrifugation at 4°C at maximum speed for 20 minutes and supernatant was carefully removed without disturbing the pellet of nucleic acid. The pellet was washed 2 times by recentrifuging with 250 µl of 70% ethanol at 4°C at maximum speed for 5 minutes, and dried at room temperature or 37°C until the last traces of fluid were evaporated. DNA was dissolved in the desired volume of Nuclease-free water or TE buffer (pH 8.0).

#### **3.1.5 DNA sequencing and analysis**

The sequencing was performed by automated dye terminator cycle sequencing method (Applied Biosystems), at a centralized facility within the university. In this method a

premix solution, containing four dideoxynucleotides (ddNTPs), each labeled with a different fluorescent dye, and unlabeled desoxynucleotides was mixed with the template DNA and one sequencing primer. Therefore in the sequencing reaction DNA fragments of different size labeled at their 3'-ends with base specific fluorescent dyes were synthesized. After ethanol precipitation and denaturation, the probes were loaded on the gel (4.75% polyacrylamide DNA sequencing gel) and electrophoretically separated in the sequence service laboratory. The fluorescence of dye-containing polynucleotides was stimulated by 40 mW argon laser (488 nm and 514 nm) and the fluorescent signal was identified by the detector system of the DNA sequencer (automatic sequencer: ABI Prism, Applied Biosystems) and quantified.

#### Composition of sequencing reaction

DNA template	300-400 ng
Primer	10 pmol
Sequencing premix	2.5 $\mu$ l (Ready Reaction BigDye Terminator Kit: AmpliTag® DNA polymerase FS, thermostabile pyrophosphate, dNTPs, dITP, BigDye labeled ddNTPs and buffer with not specified composition (PE Biosystems))
HPLC H <sub>2</sub> O	To make up 10 $\mu$ l

The sequencing reaction comprised 25 cycles of: 96°C for 30 seconds, 50°C for 50 seconds and 72°C for 4 minutes. After completing of reaction, amplification products were precipitated by addition of 1/10 volume of 3M Na acetate and 5 volumes  $\mu$ l of 100% ethanol, followed by centrifugation for 20 minutes at 14000 U. Supernatant was discarded carefully, without disturbing the pellet. Afterwards the product was washed with adding of 250  $\mu$ l of 70% ethanol and centrifugation for 10 minutes at 14,000 U. Supernatant was removed completely and pellet was air dried and finally resuspended in 30  $\mu$ l of HPLC grade H<sub>2</sub>O. The sequence was assembled and analyzed with various software packages, as listed in Table 2.4. Sequence homology searches were performed using the BLAST network service.

## 3.2 Cell biological methods

### 3.2.1 Expression of hOAT1 in *Xenopus laevis* oocytes

The *Xenopus laevis* oocyte expression system was used for functional characterization the mutations produced in hOAT1. Oocytes were injected with cRNA synthesized from the cDNA of interest (wt or mutant hOAT1) and, after a 3 day expression period, uptake assays were carried out as described below. Figure 3.1 illustrates a schematic representation of the oocyte assay system.

#### 3.2.1.1 Preparation of oocytes

##### Reagents used

---

Barth's	88 mM NaCl, 1 mM KCl, 0.3 mM Ca(NO <sub>3</sub> ) <sub>2</sub> , 0.41 mM CaCl <sub>2</sub> , 0.82 mM MgSO <sub>4</sub> , 15 mM HEPES, 12 µg/ml gentamycin, pH set at 7.6 with NaOH
ORI (oocyte Ringer's solution)	90 mM NaCl, 3 mM KCl, 2 mM CaCl <sub>2</sub> , 1 mM MgCl <sub>2</sub> , 5 mM HEPES, pH set at 7.6 with 1 mM Tris

---

Individual stage V-VI oocytes were defolliculated by collagenase treatment. It involved overnight incubation of several ovarian lobes in 20 ml Barth's solution containing 0.5 mg/ml collagenase (Type CLSII, Biochrom KG) at 18°C. On the following day, oocytes were washed several times with oocyte Ringer's solution (ORI), incubated for 10 min in Ca<sup>2+</sup> free medium and then washed again 2-3 times with ORI solution. Oocytes were sorted and the "healthy" looking oocytes were used for the cRNA injection.



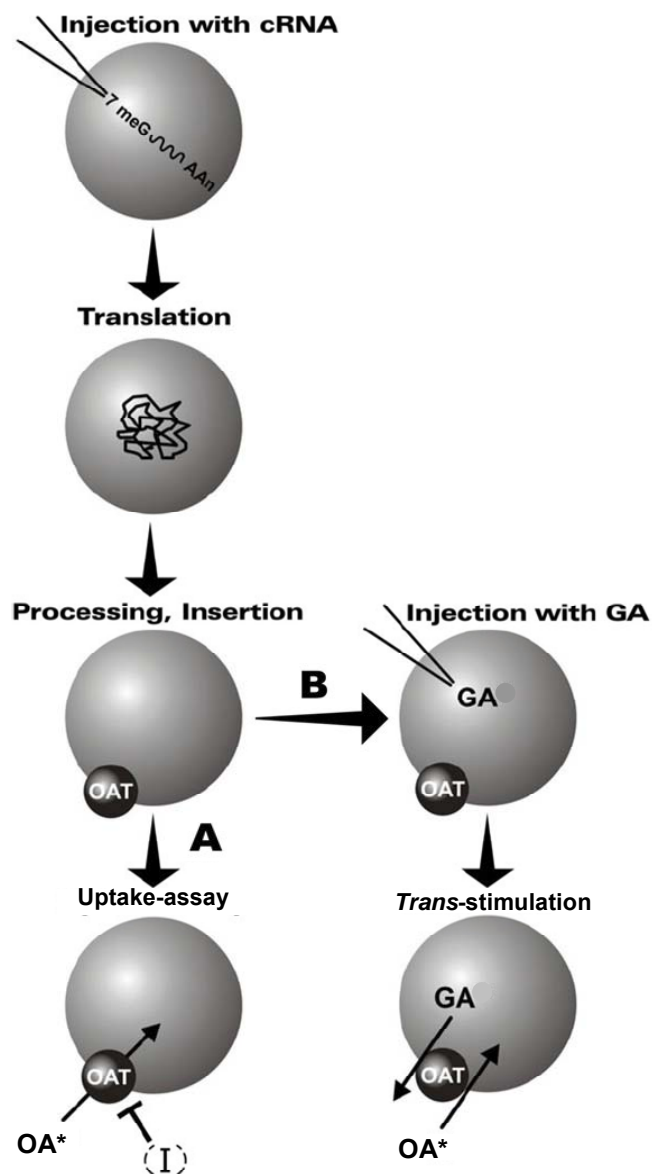


**Figure 3.1 Schematic representation of the oocyte assay system.** *Xenopus laevis* oocytes are injected with in vitro synthesized cRNA, with cap and poly-A tail. Then follows the expression period, necessary for translation of the polypeptide encoded by the cRNA, its processing and insertion into membrane. On the 3<sup>rd</sup> day, the functions of transporter could be studied by: (A) uptake assay, when the uptake of radioactively labeled substrates (OA\*) in the absence or presence of inhibitor compounds (I) was measured or (B) *trans*-stimulation, when oocytes were preloaded by injecting with glutaric acid (GA), and then *trans*-stimulation of labeled OA\* (PAH) uptake was measured.

### 3.2.1.2 Oocyte injection

cRNA were injected into the oocyte cytoplasm using a nanoliter microinjector with glass capillaries (World Precision Instruments). Oocytes were injected with 20-30 ng of cRNA in a 23-46 nl volume, or the equivalent volume of water as a control. Oocytes were arranged on a specially designed plastic support chamber with grooves to facilitate the injection process. Injection was carried out in ORI solution, and upon injection, the oocytes were incubated for three days at 18°C in Barth's solution. On the third day after injection, surviving oocytes were sorted to remove unhealthy or matured oocytes and used for transport assays.

### 3.2.1.3 Transport experiments

The selected oocytes were divided into groups of 9-12 and after equilibration in ORI medium, transferred to a 10 ml vial with 1 ml of ORI uptake medium, containing radioactively labeled substrate. Radio-labeled substances used were: [<sup>3</sup>H]PAH (5 µCi/ml) (aminohippuric acid, *p*-[glycyl-2-<sup>3</sup>H]-, 1-5 Ci/mmol, NEN), [1,5-<sup>14</sup>C]glutaric acid ([<sup>14</sup>C]GA) 100 µCi/ml, 55 mCi/mmol, or [<sup>3</sup>H(G)]-ochratoxin A ([<sup>3</sup>H]OTA) 1 mCi/ml, 7.2 Ci/mmol. Uptake was assayed at room temperature for time periods of 15 minutes to 1 hour, as required. After completion of the incubation period, the uptake was terminated by aspiration of the incubation medium and 3 x 4 ml washes with ice-cold ORI buffer. Individual oocytes were then transferred to 5 ml scintillation vials and dissolved in 100 µl of 1 N NaOH for 2 hours with shaking and, after neutralization with 100 µl of 1 N HCl and addition of 2.5 ml Lumasafe scintillation fluid (Lumac-LSC), the <sup>3</sup>H or <sup>14</sup>C content was assayed in a scintillation counter over 5 minutes.

### 3.2.1.4 Transport under chloride free conditions

Cl<sup>-</sup> free ORI was prepared by substitution with gluconate (90 mM Na<sup>+</sup>-gluconate, 3 mM K<sup>+</sup>-gluconate, 2 mM Ca<sup>2+</sup>-gluconate, 1 mM Mg<sup>2+</sup>-gluconate, 5 mM HEPES-Tris, pH 7.6). For transport assays in the absence of Cl<sup>-</sup>, oocytes were initially washed three times with Cl<sup>-</sup> free ORI over 15 min, and then incubated at room temperature for the

appropriate time periods, in the Cl<sup>-</sup> free ORI containing the radiolabel. Following the incubation, oocytes were washed with ice cold Cl<sup>-</sup> free ORI essentially and the same procedures as described in the previous section were followed.

### **3.2.1.5 *Cis*-inhibition experiments**

For *cis*-inhibition experiments 1mM malonic, glutaric or adipic acid solutions were prepared in ORI and pH was adjusted to 7.6. Uptake of [<sup>3</sup>H]PAH was assayed, in the presence of each dicarboxylate, at room temperature for 1 hour using uptake in [<sup>3</sup>H]PAH in ORI without any dicarboxylate as control. The same general protocol for transport experiments described in section 3.2.1.2 was followed.

### **3.2.1.6 *Trans*-stimulation experiments**

*Trans*-stimulation experiments were performed by injecting oocytes with 46 nl of 5 mM unlabeled glutaric acid solution in water (pH adjusted to 7.6). They were then washed and kept over ice for 15 minutes and then transferred to a 10 ml vial with 1 ml of ORI uptake medium, containing radioactively labeled substrate. Uptake of [<sup>3</sup>H]PAH was assayed over one hour. Uninjected oocytes and oocytes not preloaded with glutarate served as controls.

### **3.2.1.7 Kinetics**

Apparent K<sub>m</sub> determinations – An indirect approach was applied for determining changes in substrate affinity between mutant and wild type transporters under normal and chloride free conditions (Malo and Berteloot, 1991). For the determination of the kinetics of PAH transport in wt and mutant hOAT1, oocytes expressing the respective transporter were assayed for 1μM [<sup>3</sup>H]PAH uptake over 30 min in ORI with or without chloride and in the presence of increasing concentrations of unlabeled PAH (0-500 μM).

For both processes, the addition of unlabeled PAH inhibited uptake of [<sup>3</sup>H]PAH by a process adequately described by the Michaelis-Menten equation for competitive interaction of the labeled and unlabeled substrate:

$$V = \frac{V_{\max} [^*S]}{K_t + [^*S] + [S]} + C$$

where V is the rate of [<sup>3</sup>H]PAH transport from a concentration of labeled substrate equal to [<sup>\*</sup>S]; V<sub>max</sub> is the maximum rate of mediated PAH transport; K<sub>t</sub> is the PAH concentration that resulted in half-maximal transport (Michaelis constant); [S] is the concentration of unlabeled PAH in the transport reaction; and C is a constant representing the component of total PAH uptake that was not saturated (over the range of substrate concentrations tested) and presumably reflected the combined influence of diffusive flux, nonspecific binding, and/or incomplete washing.

### 3.2.2 Expression of hOAT1 in HEK293 cells

HEK-293 cells present the advantage of being of human origin rather than of canine (MDCK) or porcine (LLC-PK<sub>1</sub>) origin. We selected these well-differentiated human renal epithelial cells because previous studies have demonstrated their suitability in such type of physiological investigations and similar to findings with intact renal proximal tubular cells.

#### 3.2.2.1 Cultivation of HEK-293 cells stably transfected with hOAT1

Tetracycline-Regulated Expression (T-REx<sup>TM</sup>) HEK293 cells, stably expressing OAT1 were used for radioactive uptake inhibition studies as an expression system, alternative to *Xenopus laevis* oocytes. Originally, the T-Rex cells were designed for using with the T-REx<sup>TM</sup> System (Invitrogen, Life Technologies) and they stably express the tetracycline (Tet) repressor. These T-REx<sup>TM</sup>-HEK293 cells were stably transfected with hpcDNA6/TR-based expression constructs, containing OAT1 or only vector (negative control), and the dual selection made with Geneticin<sup>®</sup> and blasticidin by Dr. Ugele, Universitäts-Frauenklinik, München.

---

**Reagents used for cell culture maintenance**


---

T-REx culture medium	DMEM high glucose, 2mM L-glutamine, 1% Pen/Strep stock solution, 10% heat-inactivated FCS, 5 µg/ml blasticidin
“Milieu C”	1 mM EGTA, 85 mM NaCl, 17.5 mM NaHCO <sub>3</sub> , 3.9 mM KCl, 0.8 mM KH <sub>2</sub> PO <sub>4</sub> and 10 mM glucose
Freezing medium	45% of complete medium, 45% of conditioned medium (medium one day feed by the cells) and 10% DMSO
Polylysine solution	0.1 ml polylysine per 1 ml PBS
PBS buffer	0.9% NaCl, 10 mM sodium phosphate buffer, pH 7.2

---

HEK-293 cells were grown in 100 mm culture plates at 37°C with 5% CO<sub>2</sub>. Cells were cultivated routinely in T-REx culture medium, and passaged 1:5 every fourth or fifth day. Before splitting, medium was removed and cells were rinsed once with PBS. Then, 2.5 ml of pre-warmed EGTA-containing “milieu C” was added per 100\*20 mm culture dishes. After incubation at 37°C for 2-3 minutes (time required for detachment the cells from the plate), 2.5 ml of complete medium per culture dish was added and the cell suspension was transferred into a sterile 15 ml Falcon tube. The cells were collected by centrifugation at room temperature at 1000 rpm for 5 minutes. Supernatant was aspirated and cells were resuspended 1:2 in fresh complete medium, counted using the Hemacytometer (before the counting, 20 µl of cell suspension was diluted with 180 µl of medium for better accuracy) and seeded in the required density. Because of the property of the HEK293 cells to easily come off the plate, culture dishes were coated with polylysine (Sigma). Therefore, 200 µl of polylysine solution was pipetted onto each well of 24 well plates shortly before seeding and aspirated after a few minutes. Cells were seeded directly onto the polylysine-wet surface. For using in transport experiments cells were plated into the 24 well plates at the density of approximately  $2 \times 10^5$  cells per well upto 72 hours before the experiment.

**3.2.2.2 Uptake of radiolabeled substances in HEK-293 cells**

For the uptake experiments, confluent cell cultures were used. Therefore, cells were cultured in 24-well plates for at least 48 hours before the beginning of transport studies.

---

**Reagents used**


---

Mammalian Ringer solution	130 mM NaCl, 4 mM KCl, 1 mM CaCl <sub>2</sub> , 1 mM MgSO <sub>4</sub> , 20 mM HEPES, 1 mM NaH <sub>2</sub> PO <sub>4</sub> , 18 mM glucose, pH 7.4
Radio-labeled substrates	[ <sup>3</sup> H]ES (0.44 μCi/ml) (estrone sulfate, ammonium salt, [6,7- <sup>3</sup> H(N)]-, 40-60 Ci/mmol) and [ <sup>3</sup> H]PAH (5 μCi/ml) (aminohippuric acid, <i>p</i> -[glycyl-2- <sup>3</sup> H]-, 1-5 Ci/mmol, NEN),

---

Directly before uptake, cells were washed three times with 1 ml of mammalian Ringer solution, pre-warmed to 37°C. The transport media was pre-warmed mammalian Ringer solution, containing radioactively labeled substance (1 μM [<sup>3</sup>H]PAH or 1.8 nM [<sup>14</sup>C]glutarate). The volume of 500 μl of uptake solution was carefully added in each well, not directly on the cells, but on the well wall, not to cause cells detachment. Cells were incubated in the transport media at the room temperature for the required time period (usually 90 s). In the case of *trans*-stimulation experiments cells were passively preloaded by the addition of glutarate to a final concentration of 5mM directly to the culture medium. The cells were then left at 37°C for 2 hours, rinsed with warm mammalian Ringer and transport was initiated. After finishing the incubation, the uptake was terminated by aspiration of transport solution and washing the cells 3 times with 1 ml of ice-cold Ringer solution. Then 500 μl of 1 N NaOH was added in each well and the plates were incubated in this solution for 1 hour. After complete cells lysis, of 500 μl of 1 N HCl was added for neutralization and the solution was mixed. From this 1 ml of cell lysate, 100 μl were transferred into Eppendorf tubes for the subsequent protein estimation using the Bradford method. The Lumasafe scintillation fluid (2.5 ml) was added to the rest 900μl of solution and the <sup>3</sup>H or <sup>14</sup>C content was assayed in a scintillation counter over 5 minutes.

For measuring transport in Cl<sup>-</sup> free conditions, Cl<sup>-</sup> free mammalian Ringer's was prepared by substitution with gluconate (90 mM Na<sup>+</sup>-gluconate, 3 mM K<sup>+</sup>-gluconate, 2 mM Ca<sup>2+</sup>-gluconate, 1 mM Mg<sup>2+</sup>-gluconate, 5 mM HEPES-Tris, pH 7.6). Cells were initially washed three times with Cl<sup>-</sup> free MR, and then incubated at room temperature for the appropriate time periods, in the Cl<sup>-</sup> free MR containing the radiolabel.

### 3.2.2.3 Uptake of 6-CF in HEK-293 cells

For transport experiments using the fluorescent organic anion 6-CF essentially the same method as that in the uptake radiolabeled substrates was followed, with a few differences. Directly before the experiment, cells were washed three times with 1 ml of mammalian Ringer solution, pre-warmed to 37°C. The transport media comprised of 6-CF dissolved in MR in the appropriate concentration with the pH adjusted to 7.4. The volume of 500 µl of uptake solution was carefully added in each well, not directly on the cells, but on the well wall, not to cause cells detachment. Cells were incubated in the transport media at the room temperature for the required time period (usually 90 sec). After finishing the incubation, the uptake was terminated by aspiration of transport solution and washing the cells 3 times with 1 ml of ice-cold Ringer solution. Then 1 ml of 1 N NaOH was added in each well and the plates were incubated in this solution for 1 hour with shaking. After complete cells lysis, HCl was not added for neutralization as 6-CF needs a basic pH to produce fluorescence. From this 1 ml of cell lysate, 100 µl were transferred into Eppendorf tubes for the subsequent protein estimation using the Bradford method. The remaining 900µl was used to assess intracellular 6-CF accumulation. Fluorescence was measured in a fluorescence spectrophotometer (Hitachi, Tokyo, Japan) at 492-nm excitation/512-nm emission.

### 3.3 Immunocytochemistry

Immunocytochemistry involved the use of antibodies that recognize epitopes on the transporter, in this case the FLAG tag (the ‘primary antibody’) incorporated in the first large extracellular loop of hOAT1. A second antibody that recognizes antibodies generated in a particular animal species is then allowed to bind to the first antibody. This ‘secondary antibody’ has a fluorescent molecule attached to it so that it can be detected, for example by fluorescence confocal microscopy. In this way, the location and relative expression of transporters expressed on the surface of *Xenopus laevis* oocytes could be studied.

### 3.3.1 Immunocytochemical detection of mutant and wilt-type transporters

To study hOAT1 trafficking, oocytes were injected with the cRNA of wt or mutant hOAT1 or an equivalent volume of water (mocks). On day 3 after injection, they were manually devitellinized after 5 to 10 min of incubation in 200 mM K<sup>+</sup> aspartate (hypertonic) and then fixed in Dent's solution (80% methanol, 20% DMSO) overnight at -20°C. The fixative was washed out, and oocytes were incubated with mouse anti-FLAG M2 IgG monoclonal antibody (Sigma, Deisenhofen, Germany) (dilution 1:1000) in the presence of 10% goat serum at 4°C for 12 h. After being washed with phosphate-buffered saline, incubation with secondary Alexa 488 goat anti-mouse IgG antibody (Molecular Probes, Eugene, OR) (dilution 1:200) was performed at room temperature for 3 h. After being washed with phosphate-buffered saline, stained oocytes were postfixed with 3.7% paraformaldehyde for 30 min. Then an embedding procedure in acrylamide (Technovit 7100, Heraeus Kulzer, South Bend, IN) was carried out according to the manufacturer's instructions. Embedded oocytes were cut into 5- $\mu$ m sections by a microtome and mounted on glass slides. They were then covered with entellan (an adhesive mounting media) and a coverslip placed on top. Samples were stored at 4°C until fluorescence microscopy was performed.

### 3.3.2 Fluorescence microscopy

In fluorescence microscopy, the sample is itself the light source. The technique is used to study specimens, which can be made to fluoresce. The fluorescing areas can be observed in the microscope and shine out against a dark background with high contrast. The Alexa488 goat anti-mouse IgG antibody used as a secondary anti-body in this study has a green fluorescent dye conjugated to the goat anti-mouse IgG antibody that acts as a fluorophore making it visible under a fluorescence microscope (495 nm absorption and 519 nm emission wavelengths). Embedded oocytes were cut into 5- $\mu$ m sections and analyzed with a fluorescence microscope (Nikon Optiphot, Nikon, Natick, MA) to detect trafficking to the cell membrane.



### 3.4 Statistical analyses

All data presented are the means  $\pm$  SE of the number of observations indicated in the text or figure legends. 'n', is given as the number of experiments on oocytes from different donor animals, with the number of oocytes used per treatment in each individual experiment being 9-12. In case of experiments performed on cell lines 'n' denotes the number of experiments on cells from different passages with the number of wells used per treatment being 4-8. Statistical analysis was performed using SigmaPlot version 10 (Systat Software GmbH, Erkrath, Germany). Significant *p* values are indicated and were calculated by Student's *t* test or one way analysis of variance (ANOVA) where applicable.

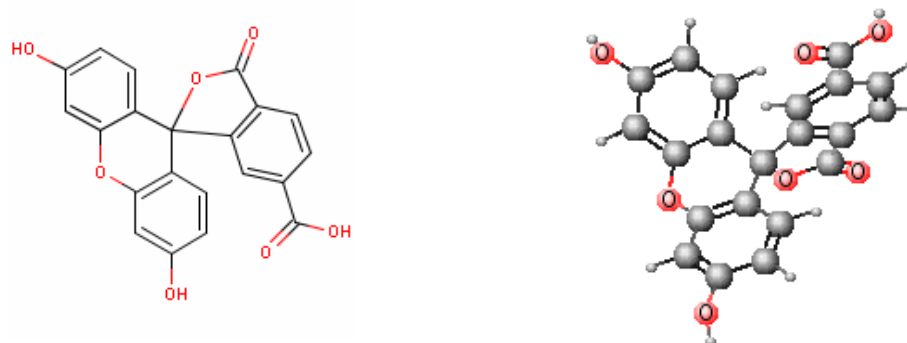
## 4. RESULTS

### 4.1. Use of a fluorescent organic anion to characterize hOAT1-mediated transport in a cell line stably expressing hOAT1.

HEK 293 (human embryonic kidney epithelial cell line) is a permanent line of primary human embryonal kidney transformed by sheared human adenovirus type 5 (Ad 5) DNA and was first described in 1977 (Graham et al., 1977). They have since been demonstrated to be a useful cell type to produce adenovirus, other viral vectors, and effectively glycosylated human recombinant proteins. HEK-293 cells present the advantage of being of human origin rather than of canine (MDCK) or porcine (LLC-PK<sub>1</sub>) origin. We selected these human renal epithelial cells because previous studies have demonstrated their suitability in such type of physiological investigations and similar to findings with intact renal proximal tubular cells (Ashokkumar et al., 2006; Bahn et al., 2005; Fernandes et al., 1999).

#### 4.1.1 Transport of 6-carboxy fluorescein (6-CF) in HEK-293 cells stably expressing hOAT1

6-carboxy fluorescein (6-CF), [3', 6'-dihydroxy-3-oxospiro(isobenzofuran-1(3H),9'-(9H)xanthene)-6-carboxylic acid)], a membrane impermeant derivative of carboxy fluorescein, is an organic anion at physiological pH and is known to be transported via OATs. The structure of 6-CF and physicochemical properties are described below. The fact that it is membrane impermeant and fluoresces makes it an ideal candidate to study OAT1-mediated transport especially since the need to work with radioactivity can be avoided. For all experiments HEK 293 cells stably transfected with hOAT1 (described in materials) were used and non-transfected cells served as negative controls.

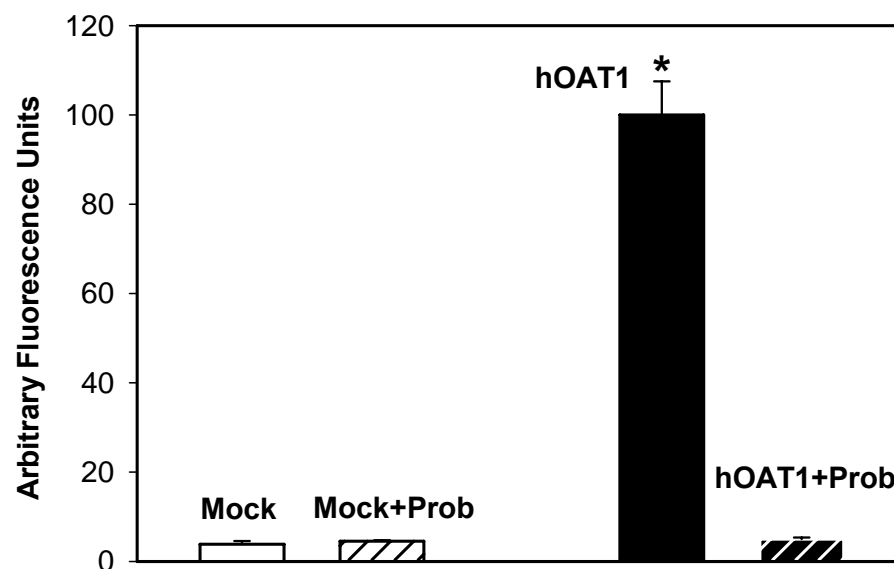


**Structure and physicochemical properties of 6-Carboxyfluorescein.** Mw: 376.319, Molecular formula:  $C_{21}H_{12}O_7$ , pKa: 6.5 ( about 1.5 ionized groups at pH 7.4), yellow orange solid soluble in pH > 6 water. Absorption 475 nm at neutral/acidic pH; 492 nm at basic pH. Emission 517 nm.

#### 4.1.1.1 Time course of 6-carboxy fluorescein uptake

In order to characterize hOAT1-mediated 6-CF transport in the stably transfected cell line, we first started with measuring the accumulation of 6-CF over time. 6-CF uptake was assayed over 10, 30, 60, 180, 120, 240, 600 and 1200 seconds and relative fluorescence measured, after lysing the cells in 1N NaOH, in a fluorimeter (lysis solution was not neutralized as 6-CF fluoresces at basic pH only). Results showed rapid and linear uptake for up to 240 seconds using  $\mu$ 5M CFI in mammalian Ringer's (MR) (Fig. 4.1 B). Therefore, 2 minutes (120 seconds) was taken as the time for further determinations of  $K_m$ . Mock cells which served as controls did not appreciably accumulate 6-CF over this time frame and furthermore the uptake of 6-CF could also be inhibited by probenecid (Fig. 4.1 A). Therefore, the uptake was determined to be hOAT1-mediated.

A.



B.

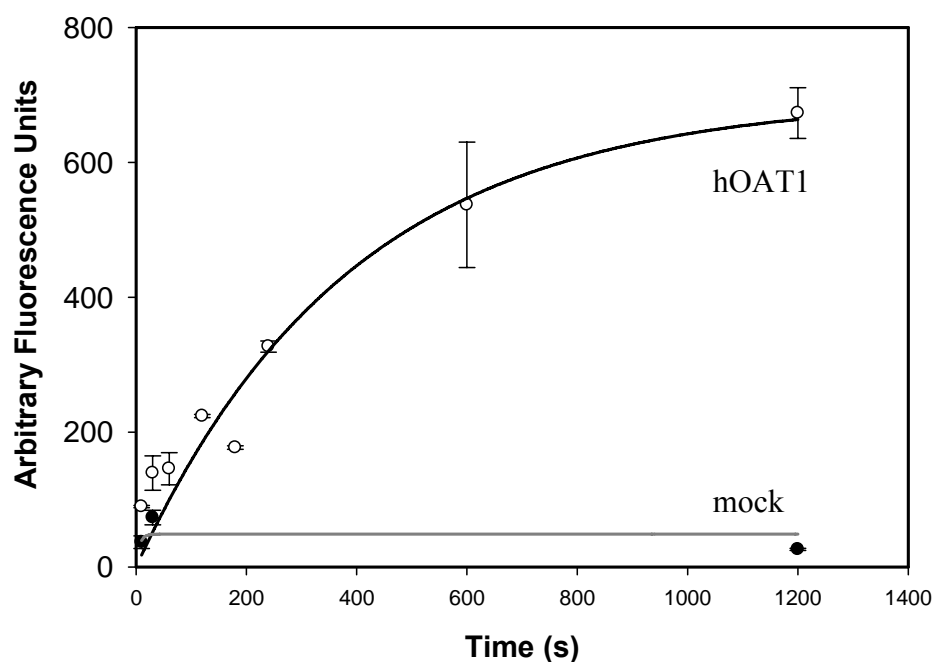


**Figure 4.1 hOAT1-mediated 6-CF uptake in stably transfected HEK-293 cells. (A) Probenecid sensitive transport of 6-CF. (B) Time course of 6-CF uptake.** The uptake of 5  $\mu$ M 6-CF dissolved in MR was assayed at room temperature for 2 min (A) or 30 to 1200 s (B) in hOAT1- or non (mock)- transfected cells. Uptake was terminated by washing with ice cold MR and cells were lysed with 1ml 0.5 N NaOH. Fluorescence was measured at 492-nm excitation/512-nm emission and is reported as average from 4-8 wells in each group. The figures show mean  $\pm$  SE values from 2 experiments each (\*  $p < 0.05$  as compared to mock)

#### 4.1.1.2 Determination of $K_m$ of hOAT1 for 6-CF

Figure 4.2 shows the concentration dependence of hOAT1 for 6-CF obtained from 3 separate experiments. The  $K_m$  value, calculated from Sigma Plot 10, indicates that 6-CF is a high affinity substrate of hOAT1 with a  $K_m$  of  $5.5 \pm 2.1 \mu\text{M}$ . This is consistent with other reported  $K_m$  values for hOAT1, for example  $3.93 \mu\text{M}$  reported by Cihlar T and Ho E.S in another stably transfected cell line (Cihlar and Ho, 2000).

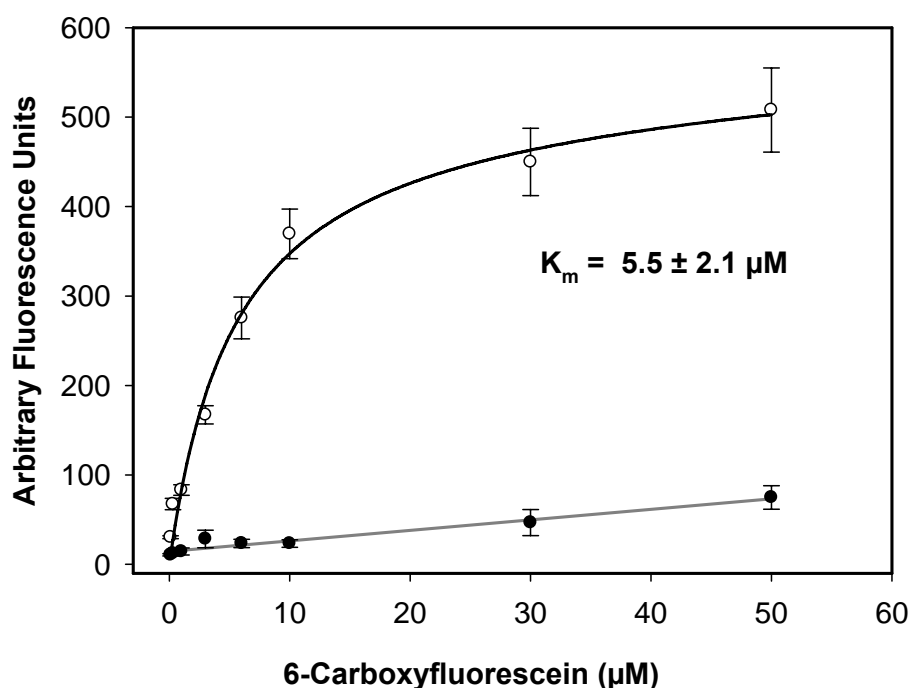


**Figure 4.2 Concentration dependence of 6-CF transport for hOAT1.** The uptake of increasing concentrations of 6-CF was assayed for 2 min in HEK-293 cells stably expressing hOAT1 (white circles) or no transporter (mocks) (black circles). Uptake was terminated by washing with ice cold MR and cells were lysed with 1ml 0.5 N NaOH. Fluorescence was measured at 492-nm excitation/512-nm emission and is reported as average from 4-8 wells in each group. The figure shows the mean  $\pm$  SE values from 3 experiments.

#### 4.2 Interaction of hOAT1 with intermediates of Krebs cycle

It has been established that OAT1 is an exchanger that is functionally coupled to  $\text{Na}^+/\text{K}^+$  ATPase and sodium dicarboxylate transporter 3 (NaDC3), which generate the necessary driving forces for  $\text{OA}^-/\alpha$ -ketoglutarate exchange via OATs (see Introduction

Fig. 1.1). Since  $\alpha$ -ketoglutarate is a dicarboxylate that is present intracellularly in a high concentration as a product of metabolism through Krebs cycle, we sought to investigate whether other byproducts of Krebs cycle also interact with hOAT1. We hypothesized that if these substances were transported through hOAT1 then they would inhibit the uptake of 6-CF from the *cis* side (called *cis*-inhibition).

#### **4.2.1 *Cis*-inhibition by Krebs cycle intermediates**

Based on the  $K_m$  value of about 5.5  $\mu$ M and linear uptake for upto 4 minutes, a 6-CF concentration of 2  $\mu$ M and uptake for 2 minutes was used for these *cis*-inhibition studies. The substances tested were:  $\alpha$ -ketoglutarate, malate, citrate, and succinate at concentrations of 1 and 10 mM each. Results show that the inhibition of 6-CF uptake was most marked with  $\alpha$ -ketoglutarate (the physiologically preferred substrate and exchange partner of hOAT1) and followed the order:  $\alpha$ -ketoglutarate > succinate > citrate > malate (Fig. 4.3). The inhibitions are summarized in Table 4.1. In the presence of 1mM test compound a significant inhibition was seen for all the compounds tested. The maximal *cis*-inhibitory effect of  $\alpha$ -ketoglutarate could already be seen at 1 mM concentration and only a slight increase in inhibition was seen at 10 mM ( $95.9 \pm 1.4$  vs.  $96.69 \pm 0.6$  %). Malate produced the least inhibition at 1 mM. At 10 mM the inhibition was increased further but was not significant. Citrate and succinate showed significant inhibition at 1 mM concentrations and the inhibition were increased significantly at 10mM concentration (see table 4.1).

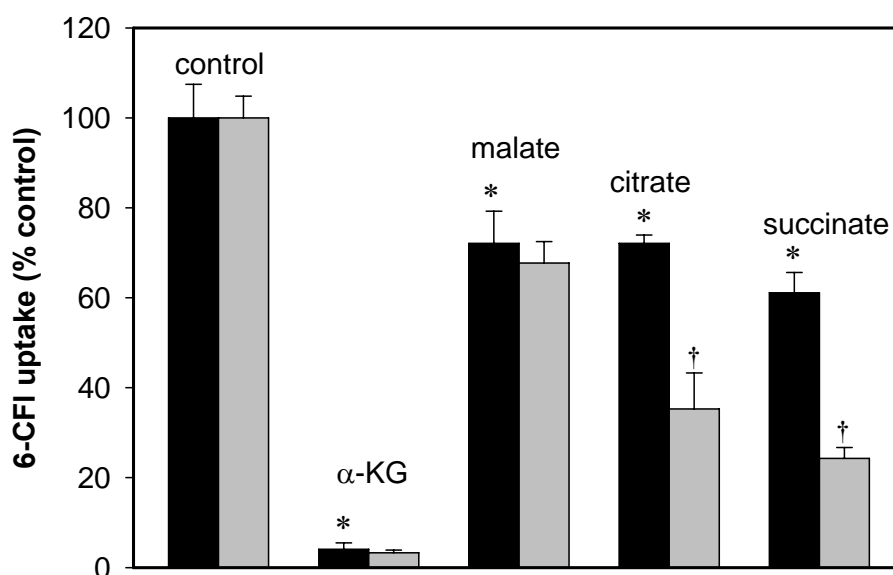


**Figure 4.3 Influence of Krebs cycle intermediates on 6-CF transport by hOAT1.** The figure above shows percent uptake of 2 $\mu$ M 6-CF over 2 minutes in the presence of 1 mM (black bars) or 10 mM (grey bars) of the substance indicated above the bar. Uptake was terminated by washing with ice cold MR and cells were lysed with 1ml 0.5 N NaOH. The values are compared to the uptake of 2 $\mu$ M 6-CF only (control). Uptake by non-transfected cells was subtracted and mean  $\pm$  SEM values are shown from 3 experiments (\* $p$ <0.05 vs. control, † $p$ <0.05 vs. uptake in the presence of 1mM test compound).

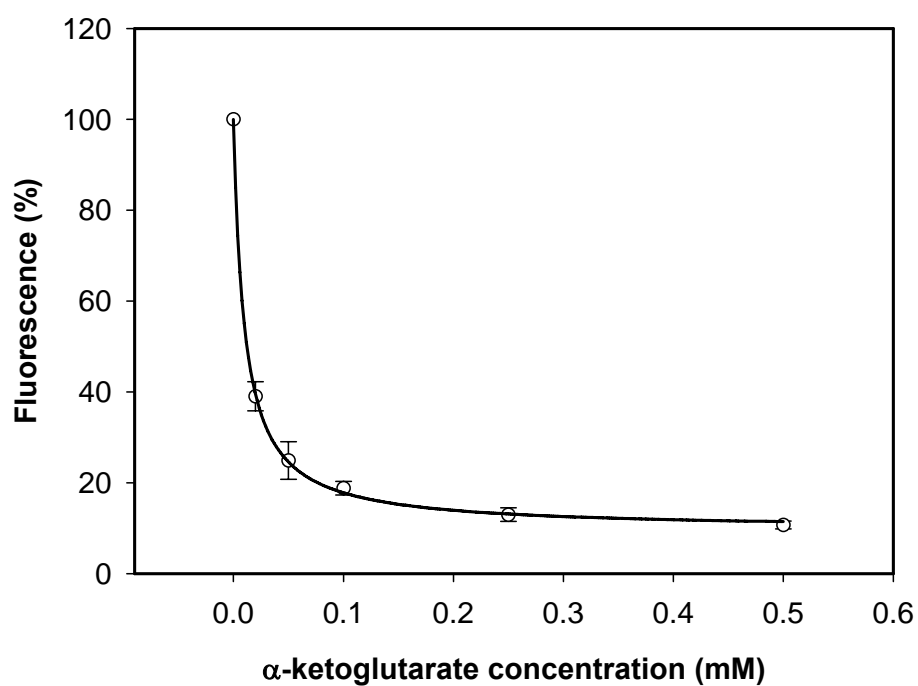
Test compound	% Inhibition vs. control	
	1 mM	10 mM
$\alpha$ -ketoglutarate	95.90 $\pm$ 1.4*	96.69 $\pm$ 0.6*
malate	27.92 $\pm$ 7.2*	32.27 $\pm$ 4.8†
citrate	27.90 $\pm$ 1.9*	64.74 $\pm$ 8.0
succinate	38.90 $\pm$ 4.5*	75.72 $\pm$ 2.4†

**Table 4.1. Cis-inhibition of 6-CF uptake by Krebs cycle intermediates.** Shown are the % inhibition of 6-CF uptake produced upon addition of 1 or 10 mM of test compound (\* $p$ <0.05 vs. 6-CF uptake, † $p$ <0.05 vs. uptake in the presence of 1mM of test compound,  $n = 3$ )

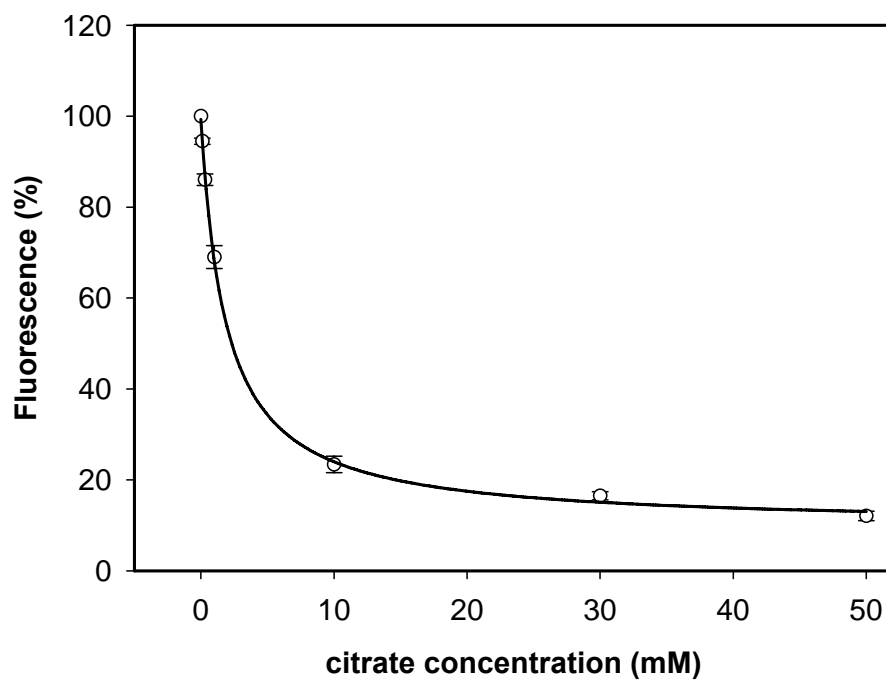
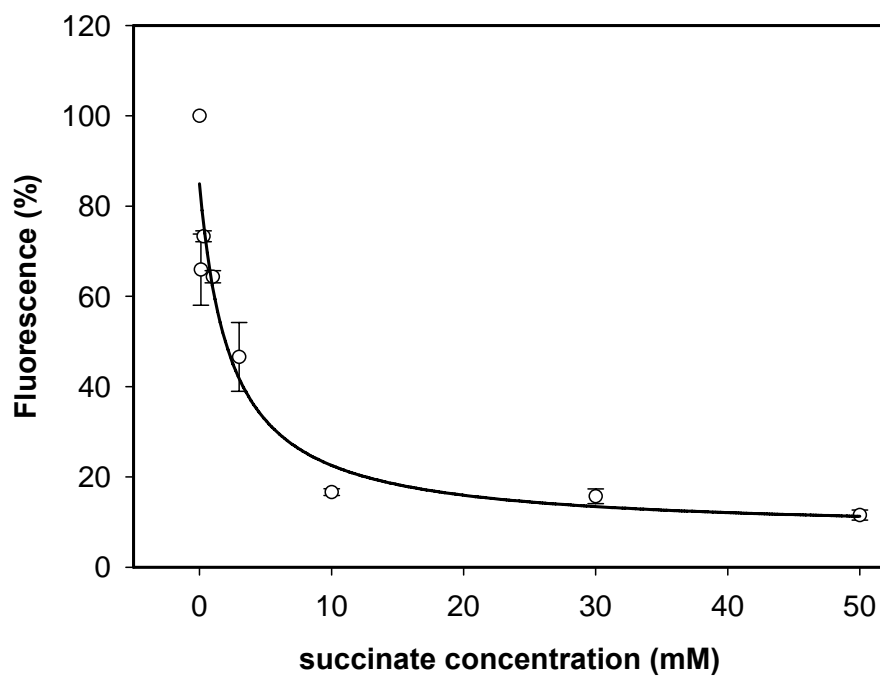
#### 4.2.2 IC<sub>50</sub> determination of Krebs cycle intermediates

Since significant *cis*-inhibition was seen with the compounds tested, we chose to determine their IC<sub>50</sub> values. The IC<sub>50</sub> values obtained are summarized in Table 4.2. Since malate did not produce significant inhibition even at 10 mM and even further up during attempts to determine its IC<sub>50</sub>, only the inhibition at 1 and 10 mM is reported (see Fig. 4.4 : A, B, and C, and Table 4.2).

##### A. $\alpha$ -ketoglutarate





**B. Citrate****C. Succinate**

**Figure 4.4** IC<sub>50</sub> determination of Krebs cycle intermediates. A-  $\alpha$ -ketoglutarate; B- succinate; C- citrate. Values shown are mean  $\pm$  SEM of one representative experiment.

	IC <sub>50</sub>
<b><math>\alpha</math>-ketoglutarate</b>	9.9 $\pm$ 0.0005 $\mu$ M
<b>malate</b>	N.D
<b>citrate</b>	1.90 $\pm$ 0.09 mM
<b>succinate</b>	2.37 $\pm$ 1.23 mM

**Table 4.2 IC<sub>50</sub> values of the inhibition of 6-CF uptake by Krebs cycle intermediates.** Values shown are mean  $\pm$  SEM of 3 independent experiments. N.D: not determinable.

#### 4.3 The influence of pH and chloride on hOAT1, characterized in stably transfected HEK-293 cells

##### *Time course of PAH and glutarate uptake*

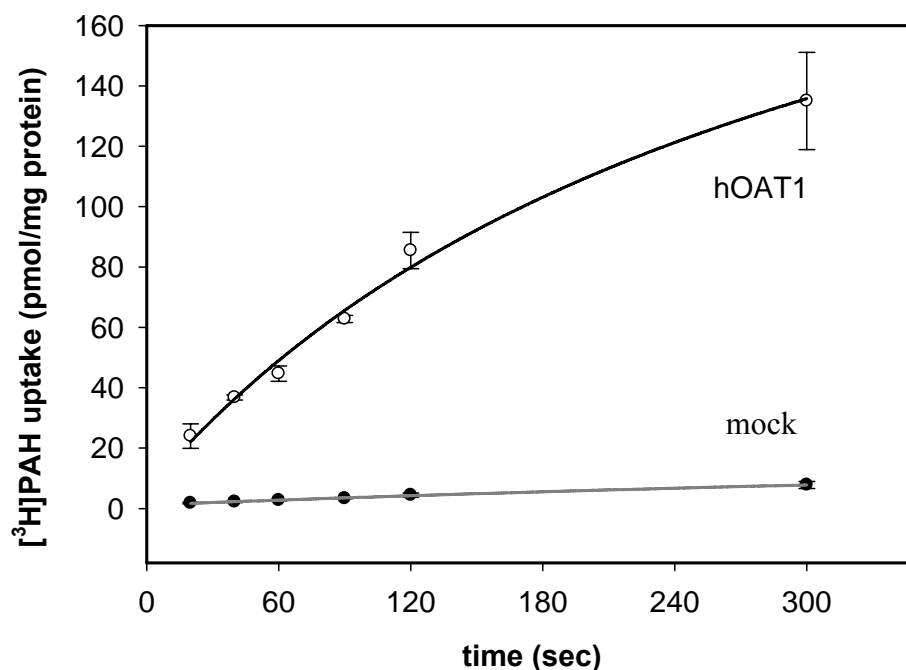


**Figure 4.5 Time course of PAH uptake in hOAT1 stably transfected HEK-293 cells.** Uptake of 1  $\mu$ M [<sup>3</sup>H]PAH was assayed at different time points upto 5 min. Uptake was terminated by washing with ice cold MR. Following uptake cells were washed, lysed and assessed for radioactivity. Y-axis values represent the average uptake calculated as pmols/mg protein. Values shown are mean  $\pm$  SEM from two experiments.

In Figure 4.5 the hOAT1-mediated incorporation of labeled PAH in HEK-293 cells is shown. The process was determined to be linear upto 2 minutes using 1  $\mu\text{M}$  [ $^3\text{H}$ ]PAH in the uptake buffer. A similar time course was performed for 1.8  $\mu\text{M}$  [ $^{14}\text{C}$ ]glutarate and is shown in Figure 4.6. The 90 second time point was chosen in both cases for further investigations.

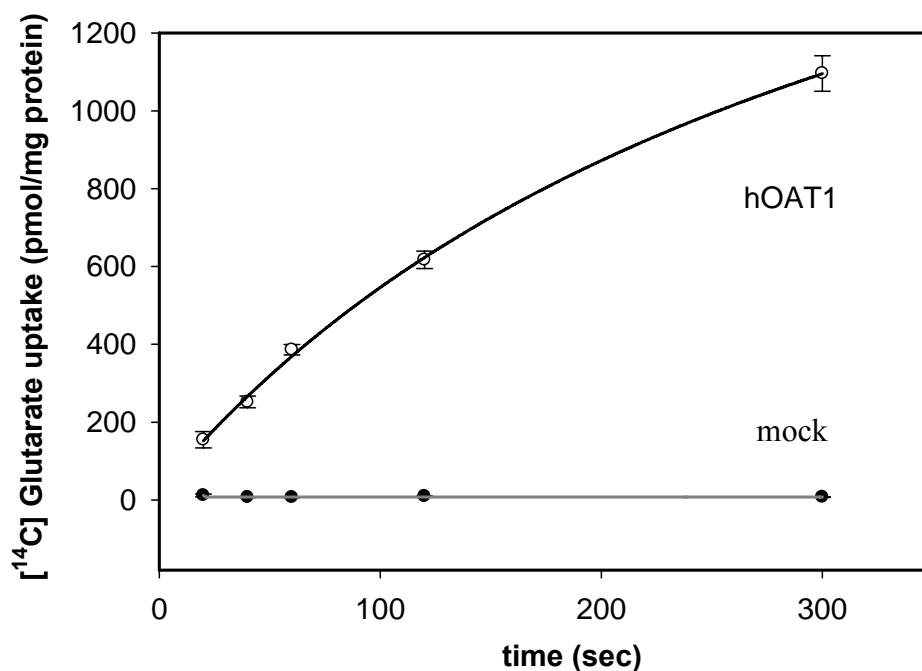


**Figure 4.6 Time course of glutarate uptake in hOAT1 stably transfected HEK-293 cells.** Uptake of 1.8  $\mu\text{M}$  [ $^{14}\text{C}$ ]Glutarate was assayed at different time points upto 5 min. Uptake was terminated by washing with ice cold MR. Following uptake cells were washed, lysed and assessed for radioactivity. Y-axis values represent the average uptake calculated as pmols/mg protein. Values shown are mean  $\pm$  SEM from two experiments.

#### 4.3.1 Stimulation of hOAT1-mediated transport by acidic pH

There have been references to the stimulation of the “PAH transport system” under acidic pH (Eveloff J 1987). We tested the effect of lowering pH upon PAH and glutarate transport in HEK-293 cells stably transfected with hOAT1. A significant stimulation of both PAH (91.14 %) and glutarate (62.09 %) uptake was observed under acidic conditions (Fig. 4.7) whereas no significant difference was seen in the null-transfected HEK-293 cells. The effect of increasing the hOAT1-mediated PAH and

glutarate uptake by lowering the pH could be due to the ability of hOAT1 to exchange for hydroxyl ions for which there exists an outwardly directed gradient at acidic extracellular pH.

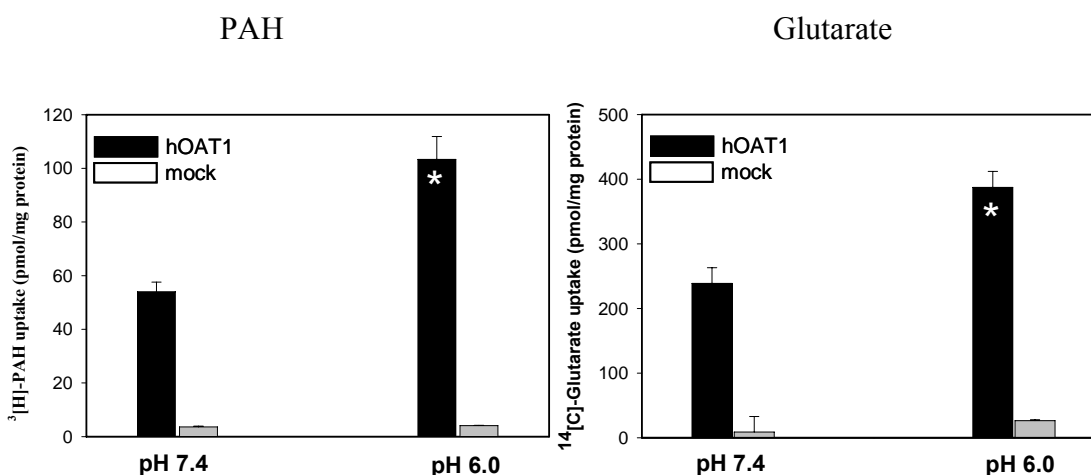


**Figure 4.7 Stimulation of hOAT1-mediated transport by acidic pH.** The uptake of 1  $\mu$ M [<sup>3</sup>H]PAH (left panel) or 1.8  $\mu$ M [<sup>14</sup>C]glutarate (right panel) was assayed over 2 minutes at pH 7.4 and 6. Uptake was terminated by washing with ice cold MR. Following uptake cells were washed, lysed and assessed for radioactivity. Values represent the average uptake calculated as pmols/mg protein and are mean  $\pm$  SEM from three experiments (\* $p$ <0.05 vs. uptake at pH 7.4)

#### 4.3.2 Stimulation of hOAT1-mediated transport by chloride

The following sets of observations were concerned with investigating chloride dependence in hOAT1. Inhibition of hOAT1 mediated PAH transport upon substitution of chloride with the anion gluconate has been reported for a number of the cloned OATs (Hosoyamada et al., 1999; Race et al., 1999; Wolff et al., 2003). While OAT1 and OAT3 have been reported to be dependent on chloride such that the rate of transport decreases in the absence of chloride, other transporters like hOAT4 have been reported to be stimulated under chloride free conditions suggesting Cl/OA exchange (Hagos et al., 2006). PAH (2-[(4-aminobenzoyl)amino]acetic acid) is a monovalent organic anion at physiological, pH. So far it had only been established that PAH transport is chloride dependent in OATs rather than organic anion transport. The aim of these studies and subsequent studies later on was to establish whether transport of other

substrates was also stimulated by chloride. For this reason glutarate was chosen which a divalent organic anion at physiological pH. As shown in figure 4.8 in the absence of chloride PAH transport went down by 70.6 % and glutarate transport by 93.6 %, whereas no significant difference was seen in the null-transfected HEK-293 cells.

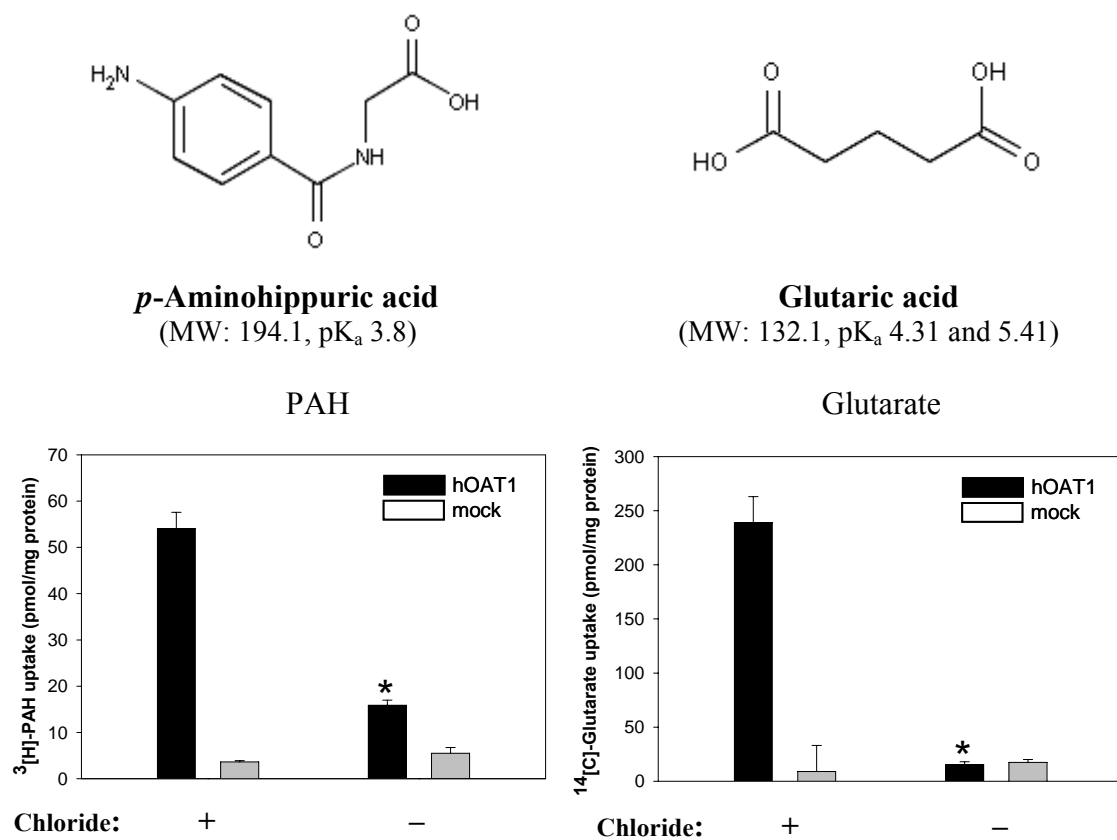
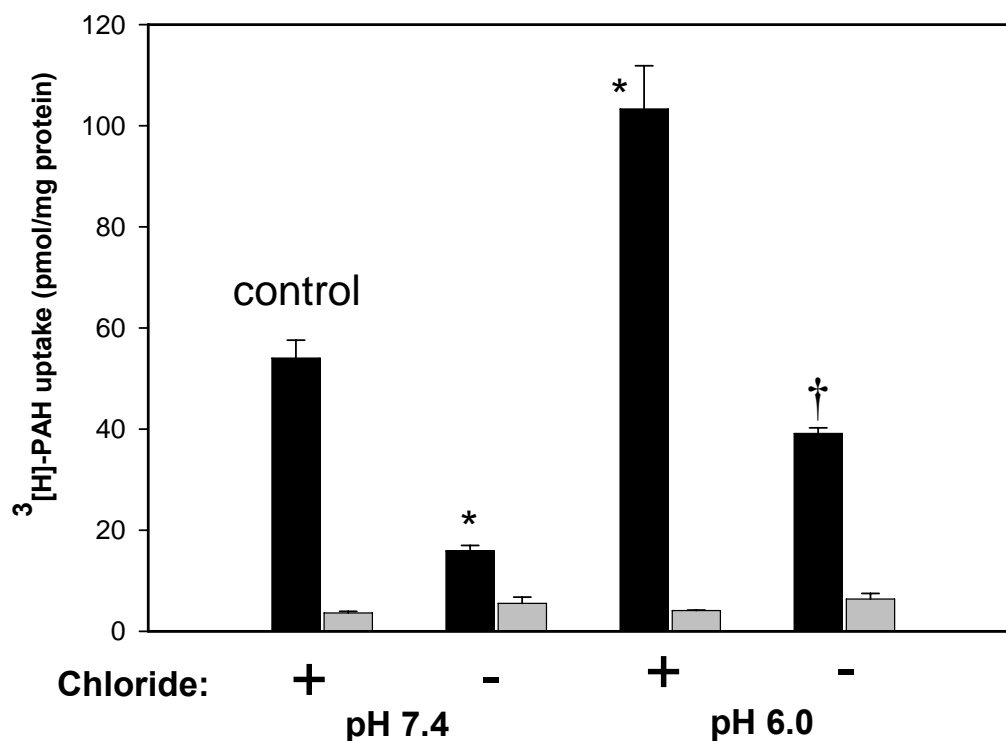


**Figure 4.8 Stimulation of hOAT1-mediated transport by chloride.** The uptake of 1  $\mu$ M [ $^3$ H]PAH (left panel) and 1.8  $\mu$ M [ $^{14}$ C]glutarate (right panel) was assayed over 2 minutes in the presence (+) or absence (-) of chloride. Uptake was terminated by washing with ice cold MR. Following uptake cells were washed, lysed and assessed for radioactivity. Values represent the average uptake calculated as pmols/mg protein and are mean  $\pm$  SEM from three experiments (\* $p$ <0.05 vs. in the presence of chloride)

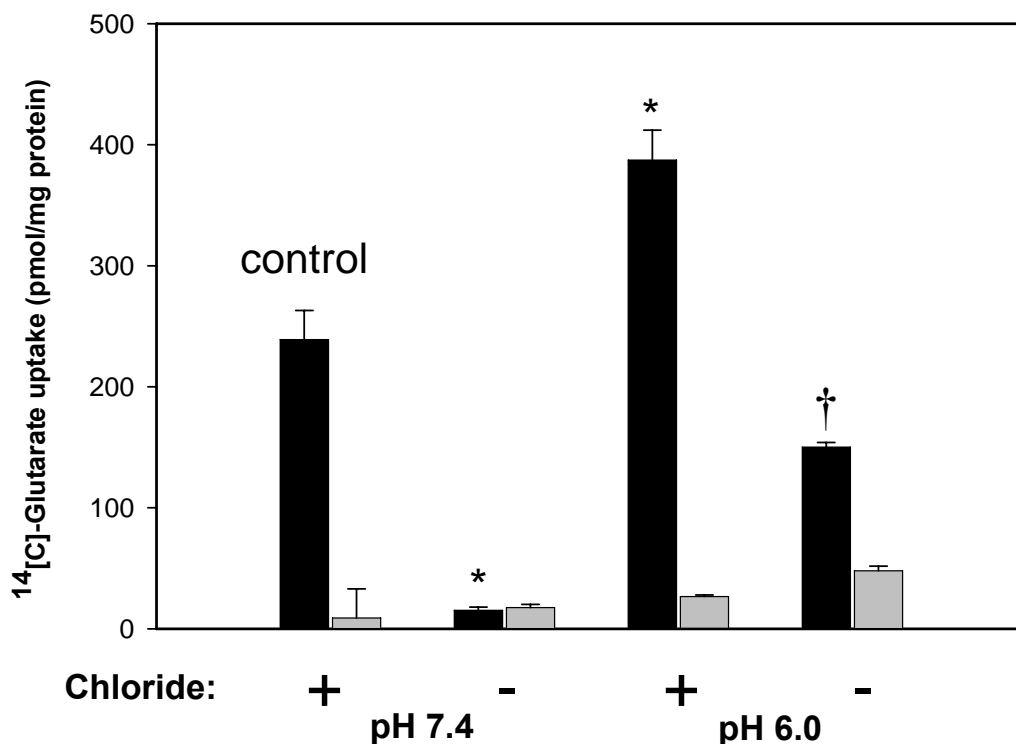
### 4.3.3 Combined effects of pH and chloride replacement upon hOAT1-mediated transport

Figure 4.9 and 4.10 show hOAT1-mediated uptake of radiolabeled PAH or glutarate by HEK-293 cells stably expressing hOAT1, at pH 7.4 and 6.0, and in the presence and

absence of chloride. In the absence of chloride PAH transport went down by 70.6 % and glutarate transport was reduced by 93.6 %. However, for both PAH and glutarate the lowered transport under chloride free conditions could be significantly stimulated upon acidification of the external medium. The resultant stimulations were 91.14 % and 62.09 % for PAH and glutarate, respectively.



**Figure 4.9 Uptake of PAH by HEK-293 cells stably expressing hOAT1, at pH 7.4 and 6.0, and in the presence and absence of chloride.** The uptake of  $1\mu\text{M}$  [ $^3\text{H}$ ]PAH was assayed over 2 minutes in the presence (+) or absence (-) of chloride and at pH 7.4 and 6.0 in hOAT1 (black bars)- or non (grey bars)- transfected cells. Transport was terminated by washing with ice cold MR. Following uptake cells were washed, lysed and assessed for radioactivity. Values represent the average uptake calculated as pmols/mg protein and are mean  $\pm$  SEM from three experiments (\* $p < 0.05$  vs. control, † $p < 0.05$  vs. uptake at pH 6.0)



**Figure 4.10 Uptake of glutarate by HEK-293 cells stably expressing hOAT1, at different pH and in the presence and absence of chloride.** The uptake of  $1\mu\text{M}$  [ $^{14}\text{C}$ ]glutarate was assayed over 2 minutes in the presence (+) or absence (-) of chloride and at pHs 7.4 and 6.0 in hOAT1 (black bars)- or non (grey bars)- transfected cells. Transport was terminated by washing with ice cold MR. Following uptake cells were washed, lysed and assessed for radioactivity. Values represent the average uptake calculated as pmols/mg protein and are mean  $\pm$  SEM from three experiments (\* $p < 0.05$  vs. control, † $p < 0.05$  vs. uptake at pH 6.0)

#### 4.3.4 Effect of increasing chloride concentration on PAH uptake by HEK-293 cells stably transfected with hOAT1

In order to quantify the effect of chloride, hOAT1-mediated uptake of labeled PAH was measured by sequentially increasing chloride concentration from 0 mM to 200 mM. As in the previous experiments the chloride salts in the buffer were replaced by the respective gluconate salt. When uptake at 130 mM (that present in mammalian ringer) of chloride, was set to 100% and plotted versus chloride concentration in the uptake buffer, a sigmoidal relation was observed (Fig. 4.11). Half maximal transport could be seen at a chloride concentration of  $103.45 \pm 20.5$  mM with a Hill coefficient of  $2.72 \pm 0.99$ , which indicates a positive co-operativity in the binding of chloride.

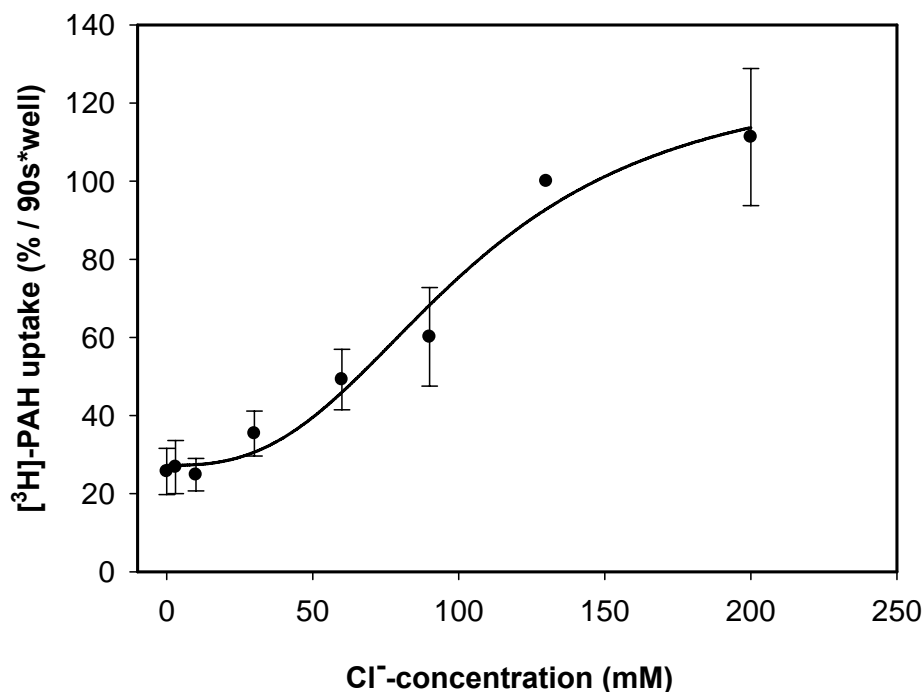


**Figure 4.11 Stimulation of hOAT1 mediated PAH transport by chloride.** The uptake of 1 $\mu$ M [<sup>3</sup>H]PAH was assayed over 2 minutes in MR with 0 to 200 mM of chloride. Uptake at 130 mM chloride was set to 100%. Transport was terminated by washing with ice cold MR. Following uptake cells were washed, lysed and assessed for radioactivity. Values represent the average uptake and are mean  $\pm$  SEM from three experiments.

We have shown in the previous experiments that presence of chloride stimulates both PAH and exchange partner glutarate, transport. Acidification of the uptake buffer leads to further increase in transport, both in the presence and absence of chloride. The next step was to ascertain whether *trans*-stimulation could be observed with either substrate in the absence of chloride as well. In Fig. 4.12 are seen the *trans*-stimulatory effects of PAH and glutarate preloading observed in the absence and presence of chloride. An increase in transport of radiolabeled PAH was observed by both PAH and glutarate preloading. However, in the absence of chloride a *trans*-stimulatory effect was considerably more with PAH preloading than with glutarate preloading.



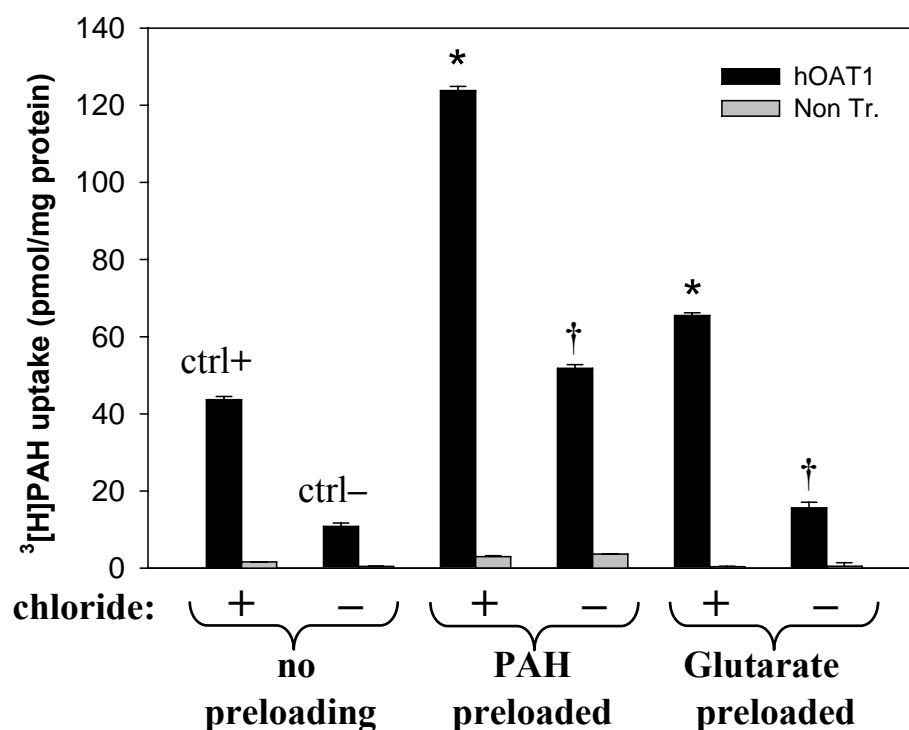


**Figure 4.12** Effects of PAH and glutarate preloading on hOAT1-mediated [<sup>3</sup>H]PAH uptake in the presence and absence of chloride. The uptake of 1 μM [<sup>3</sup>H]PAH was assayed over 2 minutes in the presence (+) or absence (-) of chloride in hOAT1 (black bars)- or non (grey bars)- transfected cells, with and without PAH or glutarate preloading (indicated). ctrl+ and ctrl- represent uptakes in non-preloaded cells in the presence and absence of chloride, respectively. Values represent the average uptake calculated as pmols/mg protein and are mean ± SEM from three experiments (\*p < 0.05 vs. ctrl+, †p < 0.05 vs. ctrl-).

#### 4.4 Mutational analysis of hOAT1

Mutational analysis of hOAT1 was undertaken in an attempt to elucidate the contribution of positive charges in substrate binding and the overall transport process. To this end a combination of point mutations were generated, and the effect of these alterations on hOAT1-mediated uptake was observed. Mutations of interest were then further characterized in order to determine the effect of the mutation on transporter activity and membrane trafficking.

#### **4.4.1 Alignments and sequence characteristics of OATs: identifying important amino acid residues**

As a first step towards mutational analyses, the online tool ClustalW (<http://www.ebi.ac.uk/clustalw/>) was used to generate the protein sequence alignments of all the known and characterized OATs with a view to identify the conserved and charged amino acids within the transmembrane domains (TMDs) of hOAT1.

In order to identify key residues that may be involved in substrate binding and translocation in the human OAT1 we reasoned that, since anions are negatively charged, positive charges embedded within transmembrane helices of the transporter should be involved. Through sequence alignment of all mammalian OATs we could identify positively charged amino acids that were completely conserved amongst all OATs. Upon close examination of the alignment of the related OATs and OCTs we found that certain cationic amino acid residues within/close to (putative) transmembrane domains that are conserved in all members of OATs, are substituted in OCTs for a residue of opposite or neutral charge. Three positions satisfy this criterion completely in hOAT1; the H (histidine) at position 34, the K (lysine) at position 382, and R (arginine) at position 466 in hOAT1, align with isoleucine (neutral), alanine (neutral) and aspartate (positive) residues found at the corresponding positions in OCTs. The figure below shows parts of an alignment of OAT1 and OCT1 from different species.



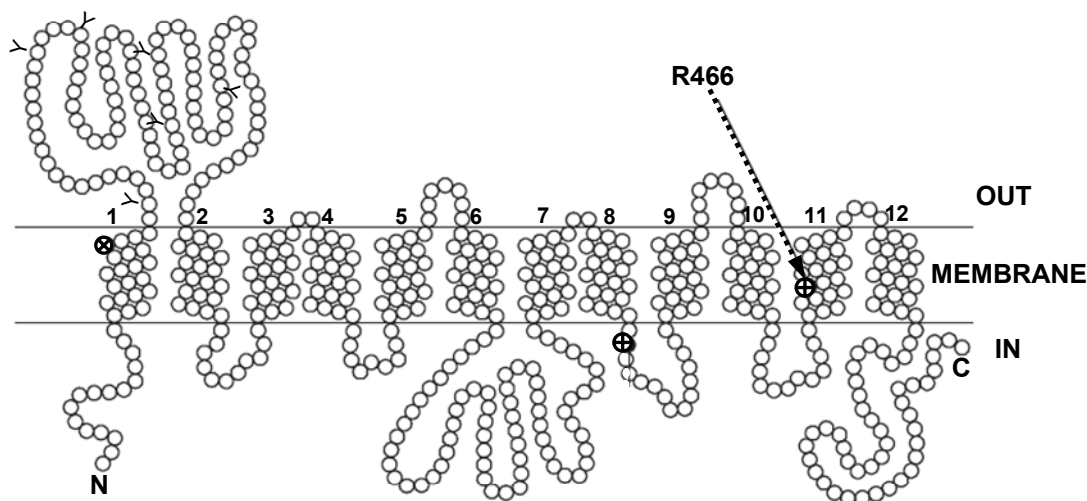


**Figure 4.14 Secondary structure model of human OAT1 and conservation of the arginine residue.** The currently accepted topological model of hOAT1 shows 12 transmembrane helices with N- and C-termini located intracellularly. The dotted arrow indicates the position of arginine 466 in the 11<sup>th</sup> transmembrane helix. The conserved, positively charged amino acids and histidine residue that are oppositely charged or neutral in OCTs, are indicated by  $\oplus$  and  $\otimes$ , respectively.

#### 4.4.2 Generation of R466 mutants

We chose first to investigate the role of R466 since secondary structure analysis predicted that this residue lies approximately at the center of TMD 11, a segment that is known to be critical for the functioning of hOAT1 (hOAT1-3 and 4 isoforms lacking this TMD are nonfunctional) and is also replaced by an *opposite* charge in OCT1s (Figs. 4.13 and 4.14). We therefore investigated what effect charge conservative, *i.e.* replacing arginine (R) 466 with lysine (K), and then non-conservative *i.e.* replacing R466 with oppositely charged aspartate (D) or neutral asparagines (N), would have on the transporter. These mutants, were sequenced to ensure polymerase fidelity, and expressed in oocytes (Fig. 4.15 below is shown as an example of successful mutageneses).

```

seq_1      ATCTTCCTGTATACTGGGGAAGTGTATCCCACAATGATCCGGCAGACAGGCATGGGAATG 154
seq_2      ATCTTCCTGTATACTGGGGAAGTGTATCCCACAATGATCCGGCAGACAGGCATGGGAATG 152
seq_3      ATCTTCCTGTATACTGGGGAAGTGTATCCCACAATGATCCGGCAGACAGGCATGGGAATG 142
seq_4      ATCTTCCTGTATACTGGGGAAGTGTATCCCACAATGATCCGGCAGACAGGCATGGGAATG 174
R466K_Fw
hOAT1_orf  ATCTTCCTGTATACTGGGGAAGTGTATCCCACAATGATCCGGCAGACAGGCATGGGAATG 1380

seq_1      GGCAGCACCATGGCCCGAGTGGGCAGCATCGTGAGCCCACTGGTGAGCATGACTGCCGAG 214
seq_2      GGCAGCACCATGGCCCGAGTGGGCAGCATCGTGAGCCCACTGGTGAGCATGACTGCCGAG 212
seq_3      GGCAGCACCATGGCCAAA GTGGGCAGCATCGTGAGCCCACTGGTGAGCATGACTGCCGAG 202
seq_4      GGCAGCACCATGGCCAAA GTGGGCAGCATCGTGAGCCCACTGGTGAGCATGACTGCCGAG 234
R466K_Fw   GGCAGCACCATGGCCAAA GTGGGCAGCATCGTG----- 33
hOAT1_orf  GGCAGCACCATGGCCCGAGTGGGCAGCATCGTGAGCCCACTGGTGAGCATGACTGCCGAG 1440
*****

seq_1      CTCTACCCCTCCATGCCTCTCTTCATCTACGGTGCTGTTCTGTGGCCGCCAGCGCTGTC 274
seq_2      CTCTACCCCTCCATGCCTCTCTTCATCTACGGTGCTGTTCTGTGGCCGCCAGCGCTGTC 272
seq_3      CTCTACCCCTCCATGCCTCTCTTCATCTACGGTGCTGTTCTGTGGCCGCCAGCGCTGTC 262
seq_4      CTCTACCCCTCCATGCCTCTCTTCATCTACGGTGCTGTTCTGTGGCCGCCAGCGCTGTC 294
R466K_Fw
hOAT1_orf  CTCTACCCCTCCATGCCTCTCTTCATCTACGGTGCTGTTCTGTGGCCGCCAGCGCTGTC 1500

```

**Figure 4.15 Identification of successful mutations.** Mutations were confirmed by sequencing and aligning with the open reading frame of hOAT1 and the mutagenesis primer. The above alignment shows the R466K mutation as an example. Sequence 3 and 4 which have the mutation align perfectly with the mutation primer (and the rest with the wild type hOAT1) whereas unsuccessful mutations do not align perfectly with the mutation primer. The codons are boxed and successful mutations are shown in red. Abbreviations used are: seq\_1- sequence 1 and so on; R466K\_Fw- forward primer used for mutagenesis; and hOAT1\_orf- open reading frame of hOAT1.

#### 4.4.3 Functional characterization of R466 mutants

##### 4.4.3.1 PAH transport by R466 mutants

When expressed in *Xenopus laevis* oocytes, the wild type human OAT1 transports the model anion, *p*-aminohippurate (PAH) with high affinity. The results of uptake experiments involving each mutant are shown in Fig 4.16. In comparison with wild-type hOAT1, R466K-, R466D- and R466N- mediated uptakes of PAH were considerably lower. Amongst all the R466 mutants, percent uptakes relative to that by wild-type hOAT1 were  $12.11 \pm 1.0$  % for R466K,  $6.46 \pm 0.84$  % for R466D, and  $5.84 \pm 0.75$  % for R466N respectively. Uptake by mocks was  $3.0 \pm 0.32$  %. Hence, amongst the mutants, the mutant R466K which had the most conservative mutation showed maximal transport of PAH.

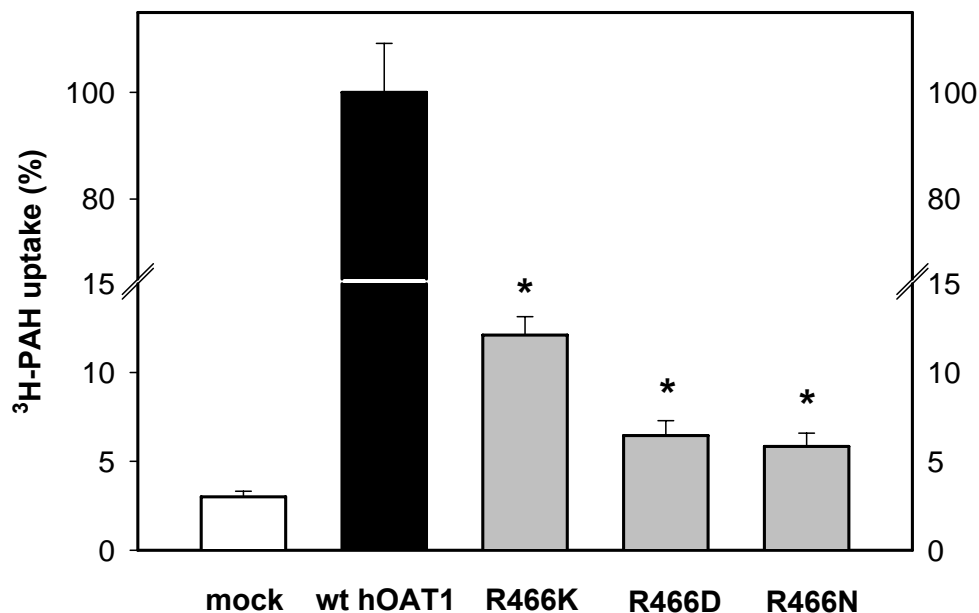


**Figure 4.16 Effect of mutating arginine 466 to lysine (R466K), aspartate (R466D) or asparagine (R466N) on the uptake of PAH.** Oocytes were injected with the wild-type (black) or mutant (grey) hOAT1 cRNA, or an equivalent volume of water (mock, white). After three days of incubation, the uptake of 1  $\mu$ M [<sup>3</sup>H]PAH was determined for 30 min. Values shown are means  $\pm$  SEM from three separate experiments with 10-12 determinations each (\*  $p < 0.05$  as compared to mock).

#### 4.4.3.2 *Trans*-stimulation of PAH transport by mutations of arginine 466

Physiologically, OAT1 exchanges extracellular organic anions with intracellular  $\alpha$ -ketoglutarate. Therefore oocytes preloaded with glutarate, the non-metabolizable analogue of  $\alpha$ -ketoglutarate should be able to stimulate PAH uptake. As shown in Fig. 4.17 this preloading significantly stimulated hOAT1-mediated PAH uptake into wt-hOAT1 cRNA injected oocytes. This increase in PAH uptake is termed *trans*-stimulation, because glutarate was offered from the *trans*-side, and labelled PAH from the *cis*-side, of the oocyte's cell membrane. When the same experiment was done on the mutants, a *trans*-stimulation of PAH uptake by intracellular glutarate was observed with the mutant R466K only, and not with R466D or R466N. This suggested that the replacement of arginine 466 by lysine did not impair the interaction of OAT1 with glutarate, however, a replacement of arginine by the oppositely charged aspartate (R466D) or neutral asparagine (R466N), not only decreased PAH uptake below that

observed with R466K, but in addition abolished the *trans*-stimulation by glutarate (Fig. 4.17).

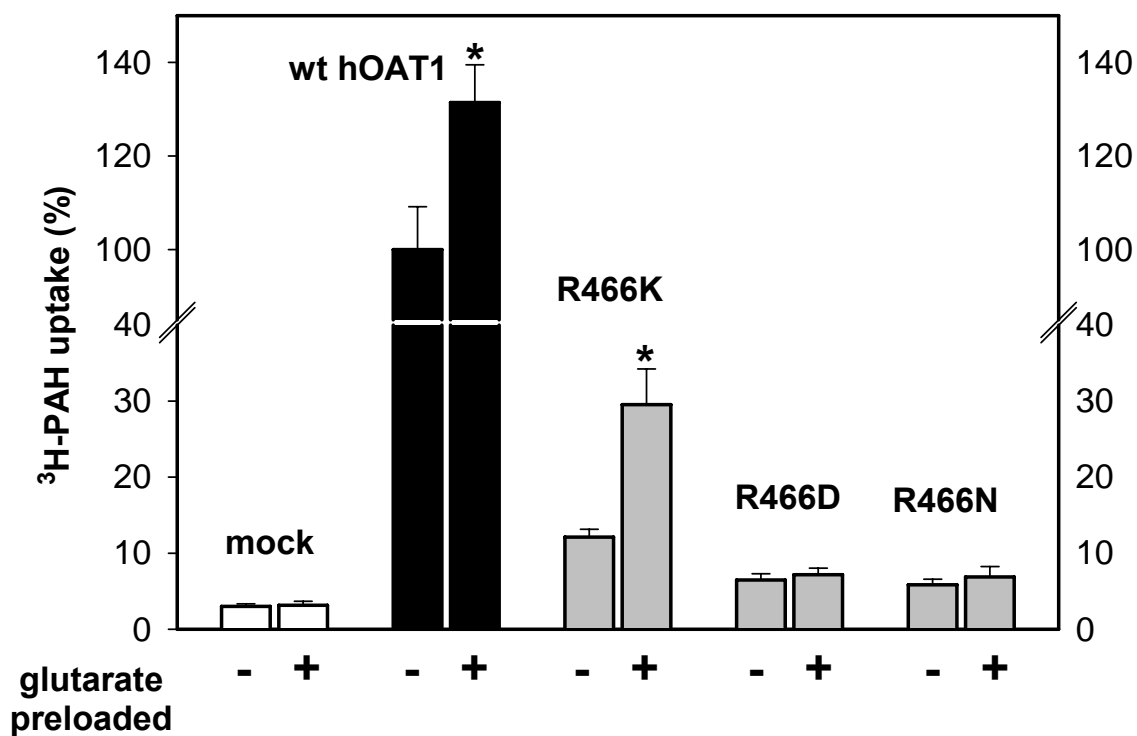


**Figure 4.17 *Trans*-stimulation of PAH uptake by intracellular glutarate.** Oocytes expressing no transporter (mock, white), wt hOAT1 (black) or the mutants (grey) R466K, R466D or R466N, were microinjected with 46 nl of 5 mM unlabeled glutarate (indicated by “+” below the panel) or uninjected (designated by “-”). Thereafter, oocytes were rinsed with ORI, and after 15 min uptake of 1  $\mu$ M [<sup>3</sup>H]PAH was assayed for 1 hour. Percent [<sup>3</sup>H]PAH uptake by non-preloaded (control), wt-hOAT1 (set to 100%) or mutants is shown. Values shown are means  $\pm$  SEM from three separate experiments with 9-12 determinations under each experimental condition (\*  $p < 0.05$  versus non-preloaded control group).

#### 4.4.3.3 Membrane trafficking of the R466 mutants

Since the lowered transport rate because of the mutations could also be the result of a decreased expression of this mutant at the cell membrane, we used the loop-FLAG epitope in the wt hOAT1 and its mutants, to detect the protein at the cell membrane using anti-FLAG antibodies. As shown in Fig. 4.18, mock oocytes did not show any immunoreactivity, excluding a non-specific labelling of endogenous proteins by anti-FLAG antibodies. Oocytes expressing the flag-tagged wt OAT1 revealed a clear

fluorescence labelling at their plasma membrane. Likewise, the mutants R466K, R466D and R466N (also Fig. 4.18) appeared at the plasma membrane. Hence, the low transport rate by the mutants was not due to a strongly decreased expression of the transporter protein at the cell membrane.

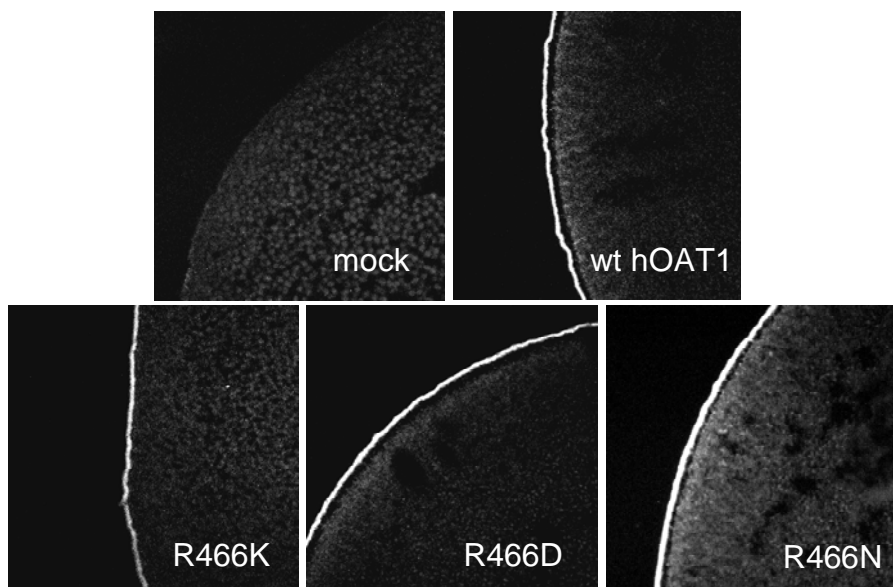


**Figure 4.18 Effect of mutating arginine 466 to lysine (R466K), aspartate (R466D) or asparagines (R466N) on transporter expression at the cell membrane.** Immunocytochemical detection of wt hOAT1 and mutants R466K, R466D and R466N in *Xenopus laevis* oocytes is shown. Devitellinized oocytes expressing no transporter (mock) or wt hOAT1, R466K, R466D or R466N containing a FLAG epitope were immunostained with anti-FLAG mouse IgG, followed by secondary Alexa 488 goat anti-mouse IgG. Thereafter, the oocytes were embedded in acrylamide, and 5  $\mu\text{M}$  sections were analysed by fluorescence microscopy.

#### 4.4.4 Characterization of the R466K mutant

The mutant R466K of hOAT1 was singled out for further characterization as it was the only one which showed appreciable PAH uptake and could also function as an exchanger.

##### 4.4.4.1 PAH transport by the R466K mutant

The transport of labelled PAH by the mutant R466K has been shown earlier in section 2.3.1 “PAH transport by R466 mutants”. 1  $\mu\text{M}$  [ $^3\text{H}$ ]PAH uptake into wt-hOAT1 expressing oocytes was  $2.7 \pm 0.4$  pmol/oocytes  $\cdot$  30min and that by mutant R466K was



$0.30 \pm 0.05$  pmol/oocytes  $\cdot$  30min. These values represent approximately 31 fold and 3.5 fold increases in PAH uptake over mocks by wt- and mutant R466K-hOAT1 expressing oocytes, respectively.

#### 4.4.4.2 *Trans*-stimulation by glutarate

The charge conservative mutation R466K was the only one which could be *trans*-stimulated by intracellular glutarate. This has been shown earlier in figure 4.17 and a part of it is repeated here to maintain continuity. In figure 4.19 below this *trans*-stimulatory effect can be seen, when 46 nL of 5 mM glutarate was preinjected into oocytes. This lead to a 1.3 fold and 2.4 fold increase in PAH uptake in wt and R466K cRNA injected oocytes, respectively.

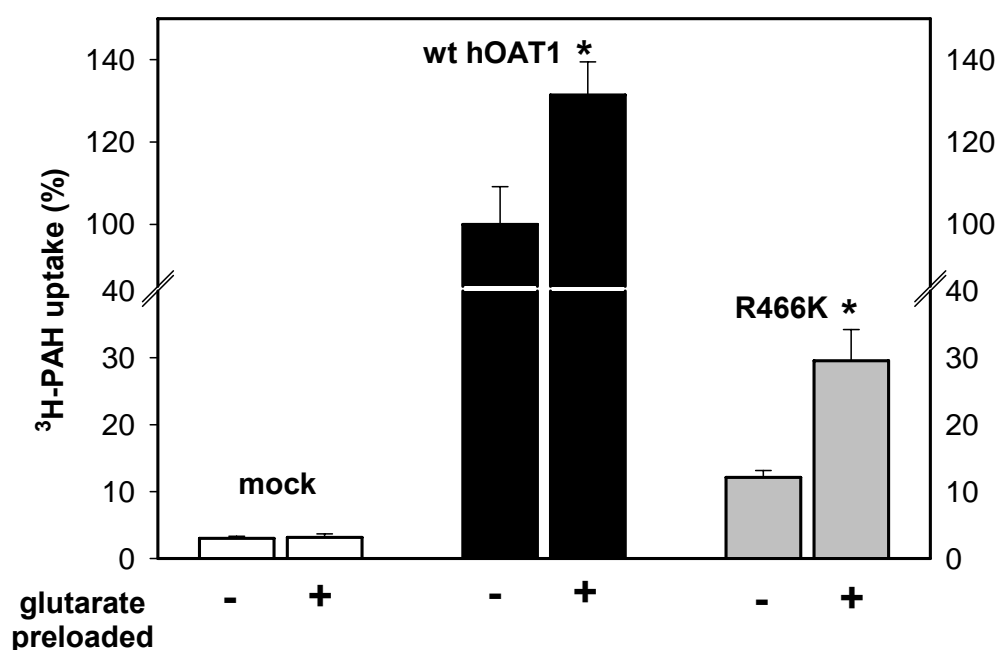


**Figure 4.19 *Trans*-stimulation of PAH uptake in the mutant R466K.** Oocytes expressing no transporter (mock, white), wt hOAT1 (black) or the mutant R466K (grey), were microinjected with 46 nl of 5 mM unlabeled glutarate (indicated by “+” below the panel) or uninjected (designated by “-”). Thereafter, oocytes were rinsed with ORI, and after 15 min uptake of 1  $\mu\text{M}$  [ $^3\text{H}$ ]PAH was assayed for 1 hour. Percent [ $^3\text{H}$ ]PAH uptake by non-preloaded (control), wt-hOAT1 (set to 100%) or mutant is shown. Values shown are means  $\pm$  SEM from three separate experiments with 9-12 determinations under each experimental condition (\*  $p < 0.05$  versus non-preloaded control group).

#### 4.4.4.3 *Cis*-inhibition

Another signature of the OATs1 is that PAH transport is *cis*-inhibitable by dicarboxylates with a minimum chain length of 4-5 carbon atoms. We next tested how the mutant R466K interacts with dicarboxylates of different chain lengths. This would also reflect any change in substrate selectivity that the mutant may have. Figure 4.20 (left panel), left panel, shows the effect of 1 mM malonate (3 carbons backbone), glutarate (5 carbons) and adipate (6 carbons) on hOAT1-mediated PAH transport. Malonate slightly inhibited the uptake of PAH, whereas glutarate and adipate completely abolished it. This result is in agreement with fig. 4.3 and the previously observed dependence of inhibition on the chain length of dicarboxylates. Similar to the wild type, the mutant R466K was slightly, but not significantly inhibited by malonate (Figure 4.20, right panel) whereas, glutarate and adipate significantly decreased PAH uptake.

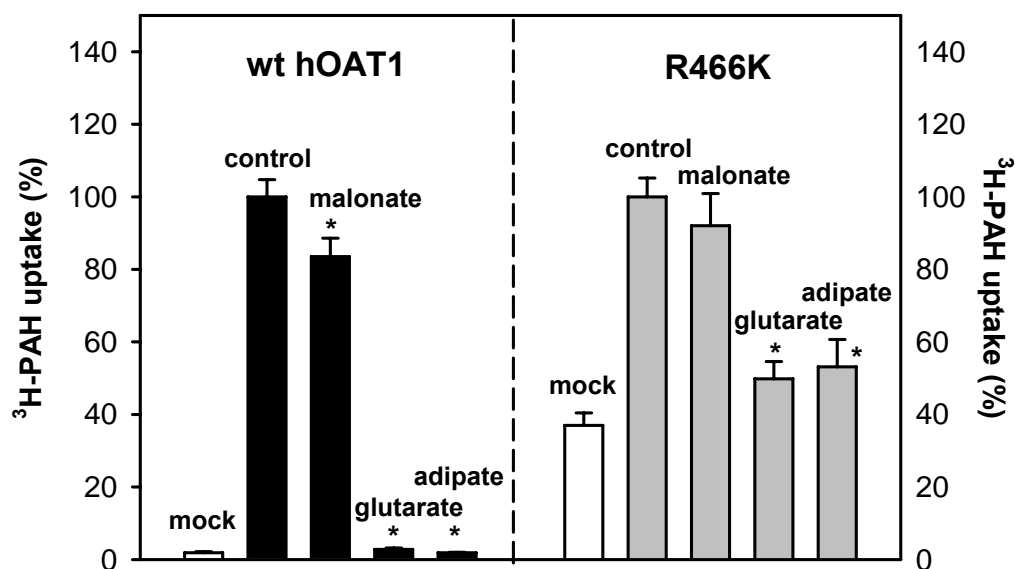


**Figure 4.20** Effect of dicarboxylates of different chain lengths on PAH uptake by wild type hOAT1 (left) and mutant R466K (right). Oocytes expressing no transporter (mock, white), wt-hOAT1 (black) or mutant R466K (grey) were incubated for 1 hour with 1  $\mu$ M [ $^3$ H]PAH in the presence of 1 mM of unlabeled malonate (3 carbons), glutarate (5 carbons), or adipate (6 carbons). [ $^3$ H]PAH uptake into wt- or R466K-expressing oocytes under control condition (no dicarboxylates present in the incubation medium) was set to 100% in their respective panels. Values shown are means  $\pm$  SEM from three separate experiments with 9-12 determinations under each experimental condition (\*  $p < 0.05$  versus control).

---

#### 4.4.4.4 The effect of chloride upon wt- or mutant R466K-hOAT1 mediated transport

The characterization of mutant R466K revealed, so far, that it seemed to be similar to the wild-type hOAT1 in all regards except that it became slower. Therefore we decided to test the chloride dependence of the transporter since hOAT1 it was established in experiments with the hOAT1-stably transfected cell line that the transporter is stimulated by chloride and therefore becomes slow in the absence of chloride (see section 4.3). Upon removal of chloride, PAH uptake by the wt OAT1 was decreased by ~87% from  $2.7 \pm 0.4$  pmol/oocytes · 30min to  $0.35 \pm 0.09$  pmol/oocytes · 30min, but was still significantly higher than PAH uptake in mock cells (Fig. 4.21 left panel). In mock cells, chloride removal had no effect, excluding non-specific effects on the oocytes. As opposed to the wild type, chloride removal in R466K-expressing oocytes did not alter PAH uptake (Fig. 4.21 right panel). PAH uptake by R466K was  $0.30 \pm 0.05$  pmol/oocytes · 30min in the presence of chloride, and  $0.30 \pm 0.06$  pmol/oocytes · 30min in its absence. Thereby, PAH uptakes by wt in the absence of chloride, and by R466K in the presence of absence of chloride were of the same magnitude, suggesting that arginine 466 is required for the chloride mediated stimulation of hOAT1.

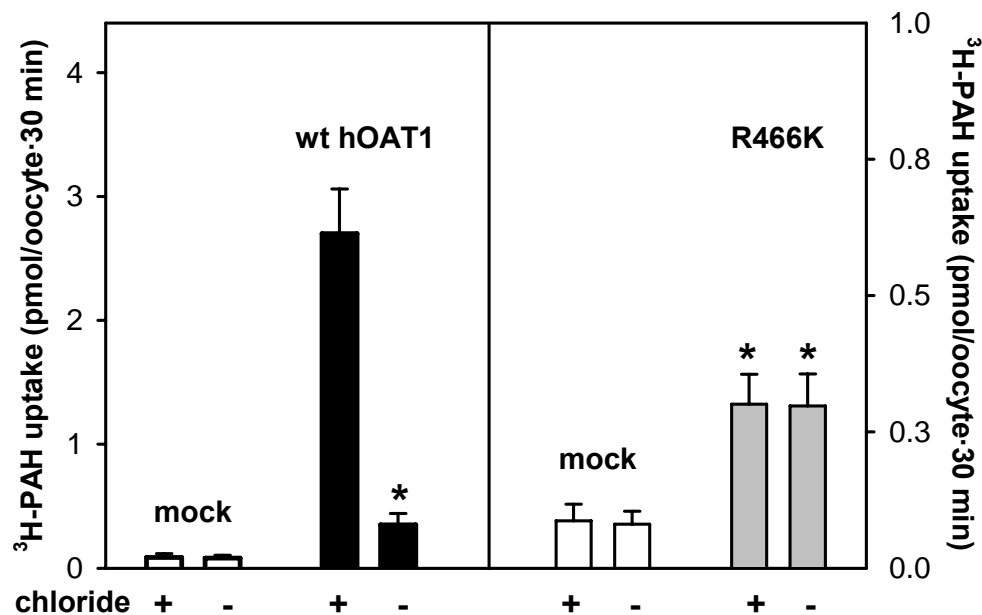


**Figure 4.21 Effect of chloride on PAH uptake by wt hOAT1 and mutant R466K.** The uptake of 1  $\mu\text{M}$  [ $^3\text{H}$ ]PAH was measured for 1 hr in oocytes Ringer buffer (chloride +) or in a buffer in which all chloride was substituted with gluconate (chloride -). Values shown are means  $\pm$  SEM from three separate experiments with 9-12 determinations under each experimental condition. Note the different scales for the left and right panels (\*  $p < 0.05$  versus mock).

To verify these results more conclusively we measured chloride dependence of wild type and mutant R466K under simulated  $V_{\text{max}}$  conditions using a total PAH concentration of 100  $\mu\text{M}$ ; comprising 5  $\mu\text{M}$  labelled and 95  $\mu\text{M}$  unlabeled PAH. To account for non-specific uptake we subtracted uptake in the presence of 10 mM unlabeled PAH. As shown in Figure 4.22, hOAT1 mediated PAH uptake was reduced by  $> 80\%$  in wt hOAT1 in the absence of chloride, but remained unchanged for the mutant R466K.

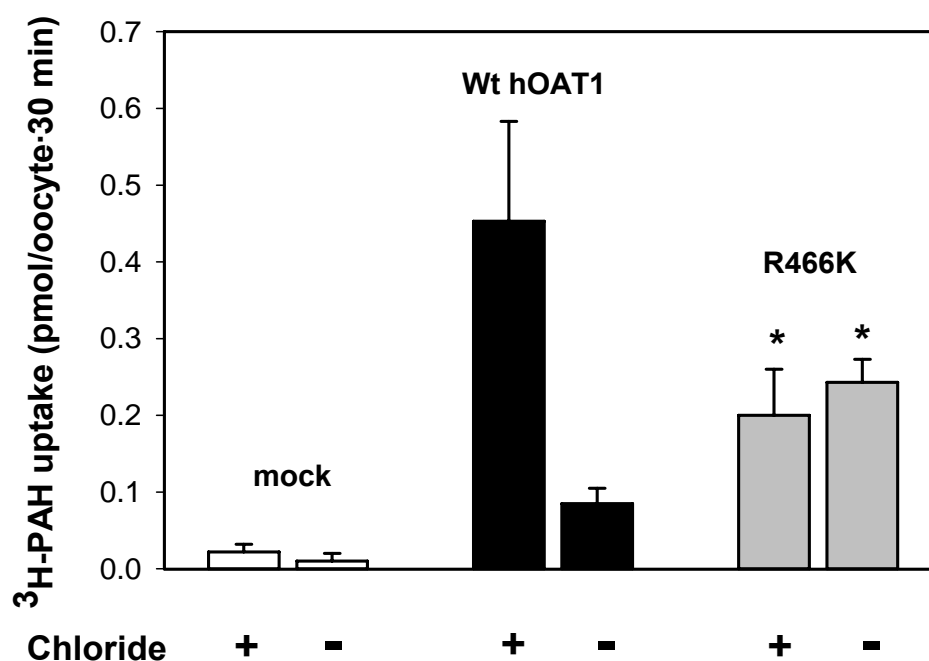


**Fig. 4.22 Effect of chloride on PAH uptake under  $V_{\max}$  conditions.** The uptake of 5  $\mu\text{M}$  [ $^3\text{H}$ ]-PAH was measured for 1 hr in oocytes Ringer buffer (chloride +) or in a buffer in which all chloride was replaced by gluconate (chloride -); an additional 95  $\mu\text{M}$  unlabeled PAH was also added to the uptake buffer to make the total PAH concentration equal to 100 $\mu\text{M}$ . Finally, the saturable component (uptake in the presence of 10mM unlabeled PAH) was subtracted from each data set. Values shown are means  $\pm$  SEM from three separate experiments with 9-12 determinations under each experimental condition. (\*  $p < 0.05$  versus wild type).

#### 4.4.4.5 The effect of chloride upon wt- or mutant R466K-hOAT1 mediated transport of other substrates

The mutation of R466 may influence the chloride sensitivity of only the PAH uptake, or of organic anion transport in general. Therefore we investigated the effect of chloride on the uptake of radiolabeled glutarate (Fig. 4.23, left panel) and ochratoxin A (right panel), two compounds with unrelated chemical structures. Chloride removal clearly reduced glutarate uptake as well as ochratoxin A uptake in wt-expressing oocytes. However, mutant R466K uptakes of both glutarate and ochratoxin A, were found no longer to be dependent on the presence or absence of chloride. These results suggest that optimal transport of PAH, glutarate, and ochratoxin A requires chloride in wt

hOAT1, but not in the mutant R466K. It is important to note that Fig. 4.23 (left panel) also shows the direct transport of radiolabeled glutarate by mutant R466K.

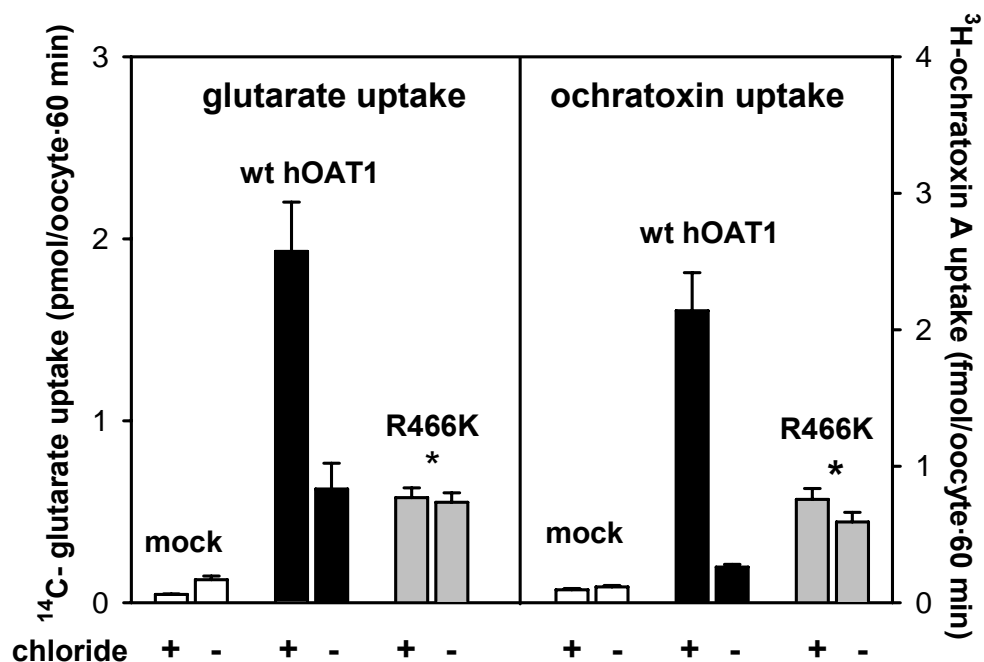


**Figure 4.23 Chloride-sensitivity of glutarate and ochratoxin A transport by wt OAT1 and mutant R466K.** The uptake of  $1.8 \mu\text{M}$  [ $^{14}\text{C}$ ]glutarate (left panel) or of  $200 \text{ nM}$  [ $^3\text{H}$ ]ochratoxin A (right panel) was assayed following 1 hr incubation of mock oocytes or oocytes expressing wt hOAT1 or mutant R466K in oocytes Ringer solution (chloride +) or in a buffer in which all chloride was replaced by gluconate (chloride -). Values shown are means  $\pm$  SEM from three separate experiments with 9-12 determinations under each experimental condition. (\*  $p < 0.05$  versus mock).

#### 4.5 Kinetic analyses of wt and R466K-hOAT1

The strongly decreased hOAT1-mediated uptake of PAH in the absence of chloride, and by R466K both in the presence and absence of chloride, could also be due to a decrease in affinity for PAH, apart from decreased surface expression. Having ruled out surface expression as a possible reason, we proceeded to determine  $K_m$  and  $V_{max}$  of PAH uptake by both the mutant and wild-type hOAT1 in the presence and absence of chloride.

#### 4.5.1 Determinations of $K_m$ of mutant R466K and wild type hOAT1 for PAH, in the presence and absence of chloride

An indirect approach was applied for determining changes in affinity between mutant and wild type transporters, and between normal and chloride free conditions. For the determination of the kinetics of PAH transport in wt and mutant R466K, oocytes expressing the respective transporter were assayed for  $1\mu\text{M}$  [ $^3\text{H}$ ]PAH uptake over 30 min in ORI with or without chloride and in the presence of increasing concentrations of unlabeled PAH (0-500  $\mu\text{M}$ ) (see Methods section for details). With the wt hOAT1, the  $K_m$  was  $3.1 \pm 0.8\mu\text{M}$  in the presence of chloride, and  $4.0 \pm 1.5\mu\text{M}$  in its absence (Fig. 4.24 A and 4.25 A). Hence, chloride removal did not affect the apparent affinity of OAT1 for PAH. The decrease in uptake by chloride removal must, therefore, be due solely to a decrease in  $V_{\text{max}}$ . on the other hand, the mutant R466K exhibited an apparent  $K_m$  for PAH of  $6.4 \pm 0.2\mu\text{M}$  in the presence of chloride and  $4.5 \pm 1.1\mu\text{M}$  in its absence (Fig. 4.23 B and 4.25 B). Therefore, with the mutant, chloride removal did not change significantly the  $K_m$  for PAH. Since the apparent  $K_m$  values of wt and R466K did not differ significantly, the mutation itself appeared to have no impact on the affinity of OAT1 for PAH. Again, the decreased PAH uptake by R466K must be due to a decrease in  $V_{\text{max}}$ . Taken together, chloride removal does not affect the affinity of OAT1 to PAH, but, in the wt, decreases the maximal velocity.

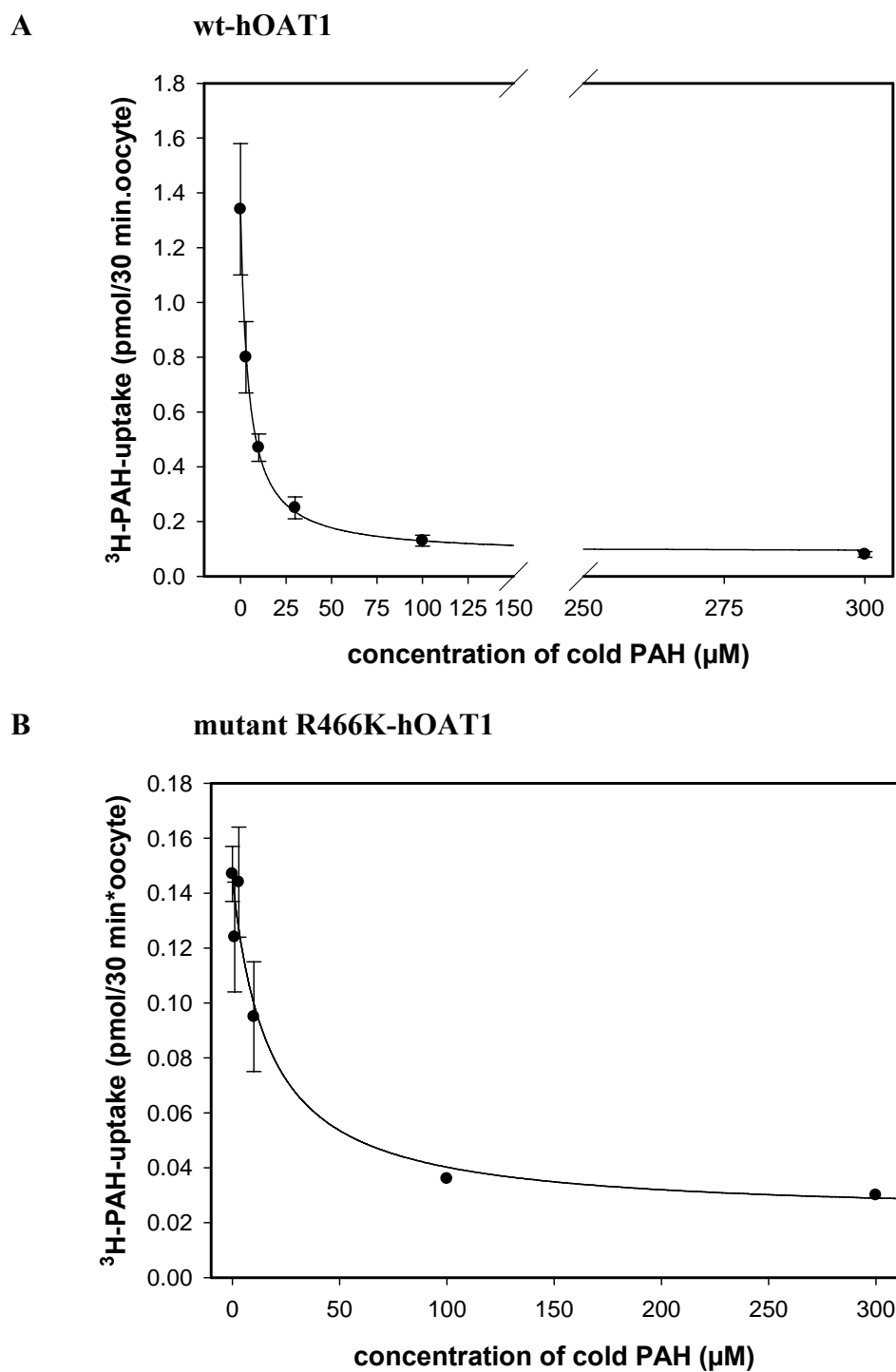


**Figure 4.24**  $K_m$  determination for PAH in (A) wt- and mutant (B) R466K- hOAT1 expressing oocytes, in the presence of chloride. Oocytes expressing the respective transporter were assayed for  $1\mu\text{M}$  [ $^3\text{H}$ ]PAH uptake over 30 min in ORI in the presence of increasing concentrations of unlabeled PAH (0-500  $\mu\text{M}$ ). A representative graph from each is shown above. Values shown are means  $\pm$  SEM.



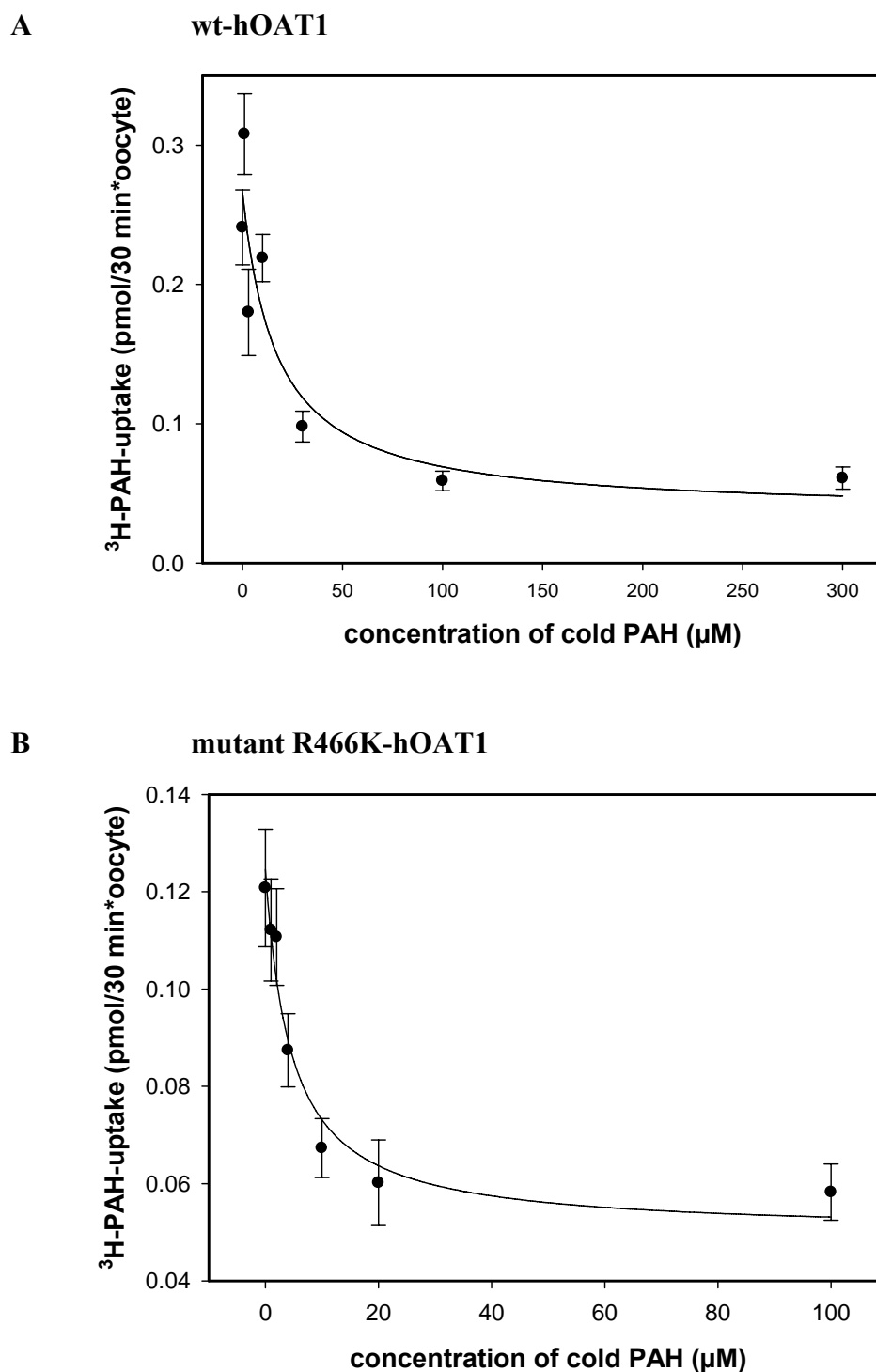


**Figure 4.25**  $K_m$  determination for PAH in (A) wt- and mutant (B) R466K- hOAT1 expressing oocytes, in the absence of chloride. Oocytes expressing the respective transporter were assayed for  $1\mu\text{M}$  [ $^3\text{H}$ ]PAH uptake over 30 min in chloride free ORI in the presence of increasing concentrations of unlabeled PAH (0-500  $\mu\text{M}$ ). A representative graph from each is shown above. Values shown are means  $\pm$  SEM.

---

**Kinetic parameters of wt hOAT1 and mutant R466K in the presence and absence of chloride**

<b>hOAT1</b>	<b>Uptake buffer</b>	<b>K<sub>m</sub> (μM)</b>	<b>V<sub>max</sub> (pmol/30min•oocyte)</b>
Wt	+ Cl <sup>-</sup>	3.1 ± 0.8	7.17 ± 2.11
	- Cl <sup>-</sup>	4.0 ± 1.5	0.99 ± 0.06
R466K	+ Cl <sup>-</sup>	6.4 ± 0.2	1.10 ± 0.15
	- Cl <sup>-</sup>	4.5 ± 1.1	0.55 ± 0.11

**Table 4.3** Transport kinetics of PAH in wt- and mutant R466K-hOAT1 expressing oocytes, in the presence (+ Cl<sup>-</sup>) and absence (- Cl<sup>-</sup>) of chloride. Values represent mean ± SEM from three separate experiments. (No significant difference in K<sub>m</sub> between groups by ANOVA, p < 0.05)

#### 4.6 Mutations of other charged residues in hOAT1

Following the characterization of the R466 mutations, we proceeded to mutate other charges in the transporter with the same strategies and aims. Shown below is the secondary structure model of hOAT1 with all the combinations of point-mutants and double mutants generated and functionally tested. The rationales for creating these mutants are explained in the sections to follow.

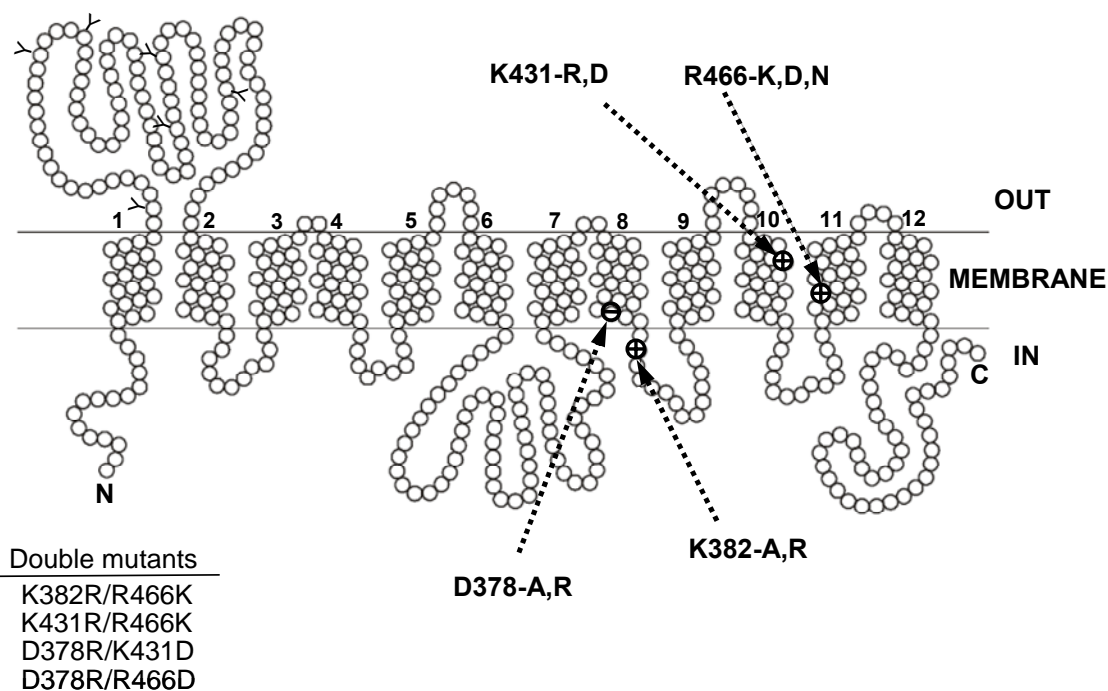


**Figure 4.26 Point mutations produced in hOAT1.** The figure above shows the currently accepted secondary structure model of hOAT1. Glycosylation sites are shown by “Y” symbols, for depicting amino acids the following abbreviations are used: A- alanine, D- aspartate, K- lysine, R- arginine. Positive and negative charges are marked as encircled “+” and “-” respectively. The mutations produced in this study are indicated by dotted arrows and the double mutations are given in the lower left-hand corner.

#### 4.6.1 Generation and functional testing of K382 mutants

The K382 mutant was produced since it was the second amino acid that satisfied the conditions we set for amino acids that may contribute towards substrate binding in hOAT1. K382 is cationic and is also completely conserved in all OATs and in OCTs the counterpart is a neutral alanine (A). We therefore made a mutant hOAT1 bearing this replacement, denoted as K382A, as well as a charge conservative replacement, denoted as K382R. When these mutants were tested for PAH transport it was found that PAH accumulation was not significantly different from mocks. Immunocytochemistry, however, showed that both these mutants were still expressed on the cell membrane

(Fig. 4.27). This suggests to us that this residue is also key for transporter activity since no change at this position could be tolerated.

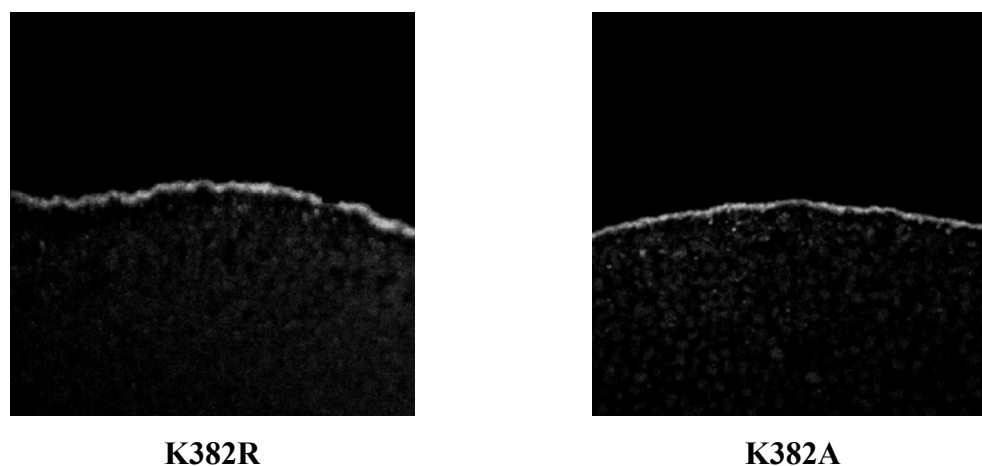


**Figure 4.27 Effect of mutating lysine 382 to arginine (mutant K382R) or alanine (mutant K382A) on expression at the cell membrane.** Immunocytochemical detection of K382R and K382A in *X. laevis* oocytes is shown. Devitellinized oocytes expressing no transporter (mock), wt hOAT1, K382R, or K382A containing a FLAG epitope were immunostained with anti-FLAG mouse IgG, followed by secondary Alexa 488 goat anti-mouse IgG. Thereafter, the oocytes were embedded in acrylamide, and 5  $\mu$ M sections were analysed by fluorescence microscopy.

#### 4.6.2 Generation and functional testing of R466K+K382R double mutant

Having already identified R466 and K382 as key residues we then proceeded to test whether the deficiency in length of arginine made in the R466K mutant could be compensated (in substrate binding) by increasing the length of lysine 382. We therefore made a double mutant R466K+K382R. When tested for PAH transport this mutant was also non-functional, with uptake not significantly over mock. In this case too, immunocytochemistry revealed that this double-mutant was still expressed on the cell membrane (Fig. 4.28).

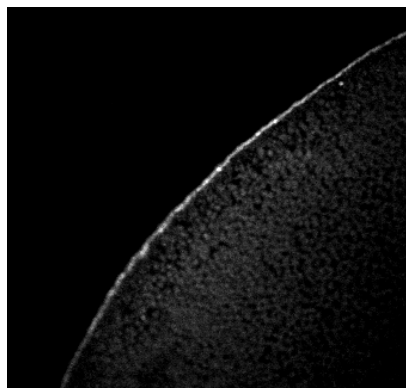


**Figure 4.28 Effect of the double mutation R466K+K382R on hOAT1 expression at the cell membrane.** Immunocytochemical detection of the double mutation R466K+K382R in *X. laevis* oocytes is shown. Devitellinized oocytes expressing hOAT1 bearing double mutation R466K+K382R and containing a FLAG epitope were immunostained with anti-FLAG mouse IgG, followed by secondary Alexa 488 goat anti-mouse IgG. Thereafter, the oocytes were embedded in acrylamide, and 5  $\mu$ M sections were analysed by fluorescence microscopy.

#### 4.6.3 Generation and functional testing of mutations in other charged residues

Other residues of interest in hOAT1 are lysine at position 431 (K431, TMD 10) and aspartate at position 378 (D378, TMD 8). K431 could potentially be important for substrate recognition because it is also a conserved charged residue within TMD 10. On the other hand D378 is a conserved negatively charged residue within TMD 8. We tested for several possibilities to ascertain the possible functional roles of these residues. The mutant K431R was generated, functionally tested and found to be inactive. Thereafter, the double mutant K431R+R466K was generated and it was seen whether the K431R mutant could be rescued as in the case of the R466K+K382R mutation (see section 4.6.2). This mutant was inactive as well.

Considering that with all three, even the subtle, mutations that were made in cationic residues lead to greatly reduced transport function it could be possible that these residues are involved in structural stabilization of the transporter through interaction with an anionic residue. hOAT1 has a conserved cationic residue in TMD 8. The molecular model of hOAT1 proposed by Perry *et. al* predicts that this cationic residue D378 may form salt bridges with R466 or K431. We therefore made the mutations in which these residues were exchanged to test this interaction. However, upon functional

testing no significant PAH transport could be measured in the double mutants D378R+R466K and D378K+K431R. The results of PAH transport by all the mutations mentioned above are shown in the combined figure below.

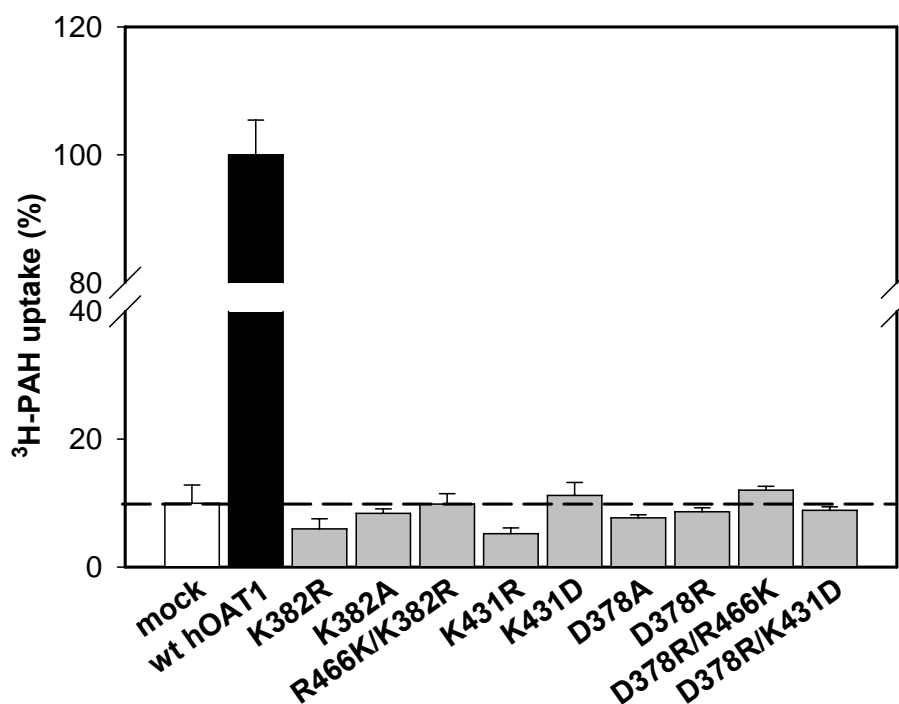


**Figure 4.29 PAH transport by following mutation of other conserved charged residues in hOAT1 in various combinations.** Oocytes were injected with the wild-type (black) or mutant (grey) hOAT1 cRNA, or an equivalent volume of water (mock, white). After three days of incubation, the uptake of 1  $\mu$ M [<sup>3</sup>H]PAH was determined for 30 min. Values shown are means  $\pm$  SEM from at least two separate experiments with 10-12 determinations each. Except for wild-type hOAT1, none of the other PAH uptakes were significantly higher than mock.

## 5. DISCUSSION

### 5.1 Characterizing hOAT1-mediated transport in stably transfected HEK-293 cells

#### 5.1.1 Use of 6-carboxyfluorescein as a substrate for hOAT1-mediated transport studies

It has been demonstrated earlier that renal proximal tubules are able to accumulate fluorescein (Miller et al., 1996; Sullivan et al., 1990). The accumulation was inhibited by probenecid and various competing organic anions, suggesting that fluorescein and possibly some other fluorescent anions may be substrates for the OAT system and, thus, serve as suitable probes to assess hOAT1 transport activity (Sullivan and Grantham, 1992).

A fluorescence based assay for characterizing hOAT1 mediated transport was first demonstrated by Cihlar and Ho in 2000. They developed a fluorescence-based, 96-well format assay using CHO cells stably expressing hOAT1, which allowed for the evaluation of interactions between small molecules and hOAT1. The assay was based on the inhibition of the transport of 6-carboxyfluorescein (6-CF), which was identified as one of several fluorescent organic anions. The relative inhibition potency of various known hOAT1 substrates determined using the 6-carboxyfluorescein based inhibition assay correlated well with their  $K_m$  values, indicating that this fluorescent assay exhibited a proper specificity for hOAT1 (Cihlar and Ho, 2000).

We used the stably transfected HEK-293 cell line (HEK293-hOAT1) to characterize hOAT1 mediated transport of 6-CF because HEK-293 cells present the advantage of being of human origin rather than of rodent (CHO), canine (MDCK), or porcine (LLC-PK<sub>1</sub>) origin and are well-differentiated human renal epithelial cells. Previous studies have also demonstrated their suitability in such type of physiological investigations and were similar to findings with intact renal proximal tubular cells (Ashokkumar et al., 2006; Bahn et al., 2005; Fernandes et al., 1999). In our experiments the stably transfected cells were capable of accumulating hOAT1 substrates to levels many fold higher than those non-transfected cells. The expressed transporter exhibited the

expected substrate specificities as well as susceptibility to inhibitors and functioned as an organic anion/dicarboxylate exchanger.

As demonstrated by the time-course curve in Fig. 4.1, the fluorescent signal of 6-CF in the cell lysate (after the transport assay) shows an approximately linear time dependence during the first 4 min of the incubation. The transport was almost completely brought down to the level of mocks by the addition of 100  $\mu$ M probenecid demonstrating that most 6-CF was transported via hOAT1 (Fig. 4.1A). The high efficiency and low background of hOAT1-mediated transport of 6-CFL allowed these experiments to be performed in the 24-well plates at room temperature. To determine the affinity of 6-CF toward hOAT1, kinetic parameters of the transport were analyzed. Using a 2 min endpoint, a  $K_m$  value of 5.5  $\mu$ M, was estimated (Fig. 4.2). This is in agreement with other reported  $K_m$  values of 6-CF for hOAT1 (Cihlar and Ho, 2000).

### **5.1.2 Interaction of hOAT1 with intermediates of Krebs cycle**

This system was then used to characterize the interaction of Krebs cycle intermediates with hOAT1 in the HEK293-hOAT1 cell line. Krebs cycle intermediates such as succinate, citrate, and  $\alpha$ -ketoglutarate are transferred across plasma membranes of cells in the proximal tubule epithelium, by secondary active transporters that couple the downhill movement of sodium to the concentrative uptake of substrate. Several transporters have been identified in isolated membrane vesicles and cells based on their functional properties, suggesting the existence of at least three or more  $\text{Na}^+$ /dicarboxylate cotransporter proteins in a given species (Pajor, 1999). In human kidneys, di- and tricarboxylates are taken up from both the luminal and the basolateral side through sodium-coupled transport systems, thereby allowing maintenance of intracellular concentrations of dicarboxylates three- to fourfold higher than those in the plasma. In humans this job is done by NaDC3 and NaDC1 in the basolateral and luminal membranes respectively (Burckhardt et al., 2005; Markovich and Murer, 2004). By  $\text{Na}^+$ -coupled uptake, NaDC-3 provides intracellular  $\alpha$ -ketoglutarate used for organic anion/dicarboxylate exchange through OAT1 and OAT3. Recently the substrate



specificity of the human analogue of NaDC3 was tested and it was reported that the dicarboxylates glutarate,  $\alpha$ -ketoglutarate, succinate, malate, fumarate and oxaloacetate were appreciably translocated as indicated by the respective substrate-induced currents. In contrast tricarboxylates, in the Krebs cycle like citrate, iso-citrate and cis-aconitate showed a considerably slower translocation (Burckhardt et al., 2005). We tested  $\alpha$ -ketoglutarate, malate, citrate and succinate for interaction with 6-CF transport and found that only  $\alpha$ -ketoglutarate *cis*-inhibited 6-CF transport in the micro-molar range with an  $IC_{50}$  of about 10  $\mu$ M, followed by citrate ( $IC_{50}$ : 1.9mM) and succinate ( $IC_{50}$ : 2.4mM) and malate did not produce a significant inhibition. Therefore we conclude that only  $\alpha$ -ketoglutarate is the intracellular exchange partner for hOAT1 among the Krebs cycle intermediates tested.

### **5.1.3 The influence of chloride substitution on hOAT1 mediated transport**

The HEK293-hOAT1 cell line was again used for testing the chloride and pH dependence of hOAT1 mediated transport. Previously, pH dependence data only existed in studies from vesicles prepared from basolateral membrane of the renal cortex (Eveloff, 1987). The inhibition of PAH transport upon chloride substitution was reported in studies that reported the initial cloning of the transporter (Hosoyamada et al., 1999; Race et al., 1999) and earlier in a study in renal cortex basolateral membrane vesicles (Pritchard, 1988). Our results established some key points. We report that OAT1 is stimulated by chloride and that chloride binding shows positive co-operativity with a Hill coefficient of about 2.7. Chloride dependent stimulation is applicable for substrates of OAT1 that are structurally very different, like PAH (monovalent), glutarate (divalent) and ochratoxin A (monovalent bulky), which has not been shown previously. We showed that in the absence of chloride (like in its presence) an acidic pH and preloading with the exchange partner could enhance substrate transport. Therefore functional properties were intact. Later on it is discussed that the affinity for PAH did not change in the absence of chloride.

## 5.2 Mutational analysis of hOAT1

### 5.2.1 Mutation of charged residues in hOAT1

Mutational analyses of hOAT1 in this study involved four charged amino acid residues, and mutations were made with different combinations of amino acid substitutions to test different hypotheses. R466 and K382 were selected because they were the only cationic amino acids in a transporter that predominantly transports anions, which were completely conserved amongst OATs, corresponding amino acids in the organic cation transporter were oppositely charged, and were within (R466) or at (K382) putative transmembrane helices of hOAT1. The third and fourth residues namely the cationic K431 and anionic D378 were selected based on correspondence with a group that was involved with producing a molecular model of hOAT1. According to them K431 could be involved in substrate binding and both K431 and both R466 and K431 could possibly form salt bridges with D378 and thereby play a structural role. Therefore we made the double mutation constructs R466D/D378R and K431D/D378K to see whether we could mimic this interaction (if it were there) by simply exchanging amino acids. Both sets of double mutants as well as the respective single mutations did not show PAH transport significantly above that by mocks. This showed that the purpose of these residues was not only to serve as charge neutralizing pairs. Coming back to the original residues identified by us, mutations K382A and K382R turned out to be non-functional as well with respect to PAH transport. In all, only the very subtle mutation where arginine at position 466 was replaced with lysine, R466K, showed transport capability (about 15% that of wild type hOAT1) that lent itself to further characterization and will be discussed in detail in the next section.

The residues mutated by us lie in the 8<sup>th</sup> and 11<sup>th</sup> transmembrane domains (TMDs) that we believe are domains involved in substrate recognition and translocation. The recent three-dimensional model of hOAT1 confirmed this hypothesis and inferences drawn from our mutational analyses fitted well with the proposals made by this model (Perry et al., 2006). Firstly, TMDs 8, 10 and 11 were shown to be involved in charge

recognition and substrate translocation. The residues R466 (TMD 11), K382 (TMD 8), and K431 (TMD 10) were recognized to be amongst the ones that formed the substrate binding site. Therefore, it is reasonable that all but the most subtle mutation produced in these critical residues translated into considerable loss of function.

### 5.2.2 Characterization of mutations produced in arginine at position 466

We showed that R466 is important for both, binding of dicarboxylates and conformational changes required for substrate translocation. Mutation of this positively charged residue R466 to a negative aspartate D or neutral asparagine N, led to severely reduced transport of PAH. No *trans*-stimulation of radiolabeled PAH influx could be seen upon preloading with the exchange partner glutarate, suggesting that interaction with dicarboxylates was abolished. In earlier studies with the flounder OAT1 (11) it was shown that this mutation led to loss of interaction with dicarboxylates and no *trans*-stimulation or *cis*-inhibition of PAH transport could be demonstrated along with a reduction of PAH affinity. Because of the extremely low uptake of R466D mutant in hOAT1 we were unable to measure affinity. Since in flounder OAT1 only a non-conservative R to D substitution was made in the present study we made a conservative mutation wherein the cationic arginine 466 in hOAT1 was mutated to lysine (K), another cationic amino acid. We report that this conservative mutation could rescue the R to D mutant in many ways. Firstly, the transport rate was increased; secondly, the affinity remained similar to the wild type transporter; thirdly *cis*-inhibition profile of the mutant by a series of dicarboxylates of increasing chain lengths remained qualitatively similar to the wild type; and fourthly, the mutant transported glutarate and could also be *trans*-stimulated by it.

The counterparts of R466 in hOAT1 have been investigated in other transporters of the SLC22 family, namely, in fOAT1 (mentioned previously), rOCT1 (26), mOAT3 (12) and rOCT2 (27). In the above cases, both, a conservative mutation *and*  $K_m$  determination was only made for hOAT1 (present study) and for rOCT1. In both cases it was found that  $K_m$  values remained same (PAH for OAT1 and MPP for OCT1) or

were decreased (choline, TEA, N<sup>1</sup>-methylnicotinamide for OCT1), whereas maximal transport rate ( $V_{\max}$ ) went down severely, suggesting that the arginine is key for conformational changes required for substrate translocation, which may explain the low turnover number and unaltered affinity (for PAH) in a charge conservative mutation. Since the low  $V_{\max}$  could have been due to reduced surface expression, we checked for membrane trafficking and found similar expression of the mutant and wild type transporters.

Since arginine is ~1.5 Å longer than lysine, and has a different pK<sub>a</sub> and hydrogen bonding profile, one possible explanation why lysine does not substitute for arginine is that R466 plays a role in conformational change via short range interactions and shortening the residue even by this little is not able to rescue the reduced turnover. The low turnover number indicates that this residue also contributes structurally to the transporter apart from its interaction with dicarboxylates. Due the broad substrate specificity of hOAT1, it is likely that a number of residues will contribute to substrate binding. The 3-dimensional model of hOAT1 proposes that hOAT1 has a large positively charged molecular surface from the N-terminal side through the central cavity, due to cationic amino acids and R466 sits at the opening of this pocket. The fact in the R466K mutant affinity for PAH remained unchanged and interaction with glutarate could be rescued by simply manipulating the charge implies that this residue is important for binding of dicarboxylates and may or may not be a player in PAH binding. Altogether, it can be concluded from the results that R466 is a charge recognizing residue in OAT1.

Our second set of observations were concerned with determining what role chloride plays in OATs. Chloride-dependent regulation has been reported for a number of the cloned OATs (6,18,28), and an earlier study using basolateral membrane (BLM) vesicles from rat kidney (29). While OAT1 and OAT3 have been reported to be dependent on chloride such that the rate of transport decreases in the absence of chloride, other transporters like hOAT4 have been reported to be stimulated under chloride free conditions suggesting Cl<sup>-</sup>/OA<sup>-</sup> exchange (Hagos et al., 2006). Firstly, we

quantified the transport of OAT1 substrates of different physicochemical properties namely: PAH (monovalent anion), glutarate (divalent anion), and OTA (bulky monovalent anion), all high affinity substrates of OAT1, in the presence and absence of chloride. For PAH we found that chloride removal brings down transport rate to ~13% of the original value. This was also the case for the other substrates namely, glutarate and ochratoxin A. Therefore, we conclude that the chloride effect is a general phenomenon on hOAT1 and not dependent upon the substrate.

Kinetic analyses of PAH transport in wild type hOAT1, in the presence and absence of chloride showed no significant change in affinity but greatly reduced  $V_{\max}$ . Since affinity for PAH did not change in the absence of chloride, it can be considered that chloride does not interact with the PAH binding site. There arise two ways of interpreting these findings. One, chloride is co-transported with organic anions via a binding site different from that of PAH; two, chloride binds to OAT1 but is not transported and serves other purposes important for turnover. The possibility of chloride transport has been tested in the earlier study by Pritchard, JB using basolateral membrane vesicles and it was found that  $^{36}\text{Cl}^-$  uptake by renal cortex basolateral vesicles was not altered by PAH transport nor could a chloride gradient (in > out) stimulate PAH entry. Therefore chloride is not co-transported. We favor the other possibility that chloride binding stimulates the transporter through conformational changes resulting in increased turnover of the transporter. That is why chloride depletion leads to lowered  $V_{\max}$  at unaltered  $K_m$ . Based on our results, it is likely that chloride exerts these effects through the amino acid arginine 466, since the mutant R466K essentially behaves like hOAT1 under chloride free conditions - it has similar affinity for PAH, it can be *cis*-inhibited and *trans*-stimulated by dicarboxylates, however it is not stimulated by chloride.

### 5.3 Outlook

To date at least 43 residues have been mutated and functionally tested for transport in different isoforms of the OATs, and more have been identified in the form of single nucleotide polymorphisms in the human population. These range from residues that are important for substrate binding and translocation, residues that modify substrate selectivity, and residues that are involved in glycosylation or regulation of the transporter through kinases. Species differences in OATs with respect to substrate selectivity and even membrane sorting have been identified. Role of OATs in drug-drug interactions has been recognized and screening for interaction with OATs for new drug entities has been made mandatory by drug regulatory authorities. Nonetheless, many questions remain to be answered. First, several uncharacterized (orphan) transporters in the SLC22A superfamily remain, and further investigation is therefore required to determine their functions. Second, knowledge of the mechanisms by which OATs are regulated is lacking. Third, clarification of the three-dimensional (3D) structures of OATs is necessary to understand the broad substrate recognition of OATs so that a valid pharmacophore may be proposed. Because of difficulties in the purification and crystallization of membrane transporter proteins, the 3D structures of transporters have yet to be clarified. Fourth, a comprehensive understanding of the apical exit pathway for organic anions in the kidneys and the PDZ interaction on apical OATs is an important issue. Finally, the pathological significance of OATs is of great interest. Originally, studies on OATs were focused on the molecular mechanisms that underlie the elimination of xenobiotics. However, recent studies have unveiled the reabsorptive roles of endogenous compounds, such as urate, for OAT isoforms. This implies that the fundamental roles of OATs are not restricted to pharmacological and toxicological roles. Thus, genetic defects of OATs might give rise to pathophysiological states.

---

**6. REFERENCES**

- Alebouyeh M, Takeda M, Onozato ML, Tojo A, Noshiro R, Hasannejad H, Inatomi J, Narikawa S, Huang XL, Khamdang S, Anzai N and Endou H (2003) Expression of human organic anion transporters in the choroid plexus and their interactions with neurotransmitter metabolites. *J Pharmacol Sci* **93**(4):430-436.
- Ashokkumar B, Vaziri ND and Said HM (2006) Thiamin uptake by the human-derived renal epithelial (HEK-293) cells: cellular and molecular mechanisms. *Am J Physiol Renal Physiol* **291**(4):F796-805.
- Asif AR, Steffgen J, Metten M, Grunewald RW, Müller GA, Bahn A, Burckhardt G and Hagos Y (2005) Presence of organic anion transporters 3 (OAT3) and 4 (OAT4) in human adrenocortical cells. *Pflugers Arch* **450**(2):88-95.
- Aslamkhan A, Han Y-H, Walden R, Sweet DH and Pritchard JB (2003) Stoichiometry of organic anion/dicarboxylate exchange in membrane vesicles from rat renal cortex and hOAT1-expressing cells. *Am J Physiol Renal Physiol* **285**(4):F775-783.
- Aslamkhan AG, Thompson DM, Perry JL, Bleasby K, Wolff NA, Barros S, Miller DS and Pritchard JB (2006) The flounder organic anion transporter fOat has sequence, function, and substrate specificity similarity to both mammalian Oat1 and Oat3. *Am J Physiol Regul Integr Comp Physiol* **291**(6):R1773-1780.
- Babu E, Takeda M, Narikawa S, Kobayashi Y, Enomoto A, Tojo A, Cha SH, Sekine T, Sakthisekaran D and Endou H (2002) Role of human organic anion transporter 4 in the transport of ochratoxin A. *Biochim Biophys Acta* **1590**(1-3):64-75.
- Bahn A, Ebbinghaus C, Ebbinghaus D, Ponimaskin EG, Füzesi L, Burckhardt G and Hagos Y (2004a) Expression studies and functional characterization of renal human organic anion transporter 1 isoforms. *Drug Metab Dispos* **32**(4):424-430.
- Bahn A, Hagos Y, Rudolph T and Burckhardt G (2004b) Mutation of amino acid 475 of rat organic cation transporter 2 (rOCT2) impairs organic cation transport. *Biochimie* **86**(2):133-136.
- Bahn A, Knabe M, Hagos Y, Rödiger M, Godehardt S, Graber-Neufeld DS, Evans KK, Burckhardt G and Wright SH (2002) Interaction of the metal chelator 2,3-dimercapto-1-propanesulfonate with the rabbit multispecific organic anion transporter 1 (rbOAT1). *Mol Pharmacol* **62**(5):1128-1136.
- Bahn A, Ljubojevic M, Lorenz H, Schultz C, Ghebremedhin E, Ugele B, Sabolic I, Burckhardt G and Hagos Y (2005) Murine renal organic anion transporters mOAT1 and mOAT3 facilitate the transport of neuroactive tryptophan metabolites. *Am J Physiol Cell Physiol* **289**(5):C1075-1084.

- Bahn A, Prawitt D, Buttler D, Reid G, Enklaar T, Wolff NA, Ebbinghaus C, Hillemann A, Schulten HJ, Gunawan B, Füzesi L, Zabel B and Burckhardt G (2000) Genomic structure and in vivo expression of the human organic anion transporter 1 (hOAT1) gene. *Biochem Biophys Res Commun* **275**(2):623-630.
- Bakhiya N, Stephani M, Bahn A, Ugele B, Seidel A, Burckhardt G and Glatt H (2006) Uptake of chemically reactive, DNA-damaging sulfuric acid esters into renal cells by human organic anion transporters. *J Am Soc Nephrol* **17**(5):1414-1421.
- Beery E, Middel P, Bahn A, Willenberg HS, Hagos Y, Koepsell H, Bornstein SR, Müller GA, Burckhardt G and Steffgen J (2003) Molecular evidence of organic ion transporters in the rat adrenal cortex with adrenocorticotropin-regulated zonal expression. *Endocrinology* **144**(10):4519-4526.
- Bleasby K, Hall LA, Perry JL, Mohrenweiser HW and Pritchard JB (2005) Functional consequences of single nucleotide polymorphisms in the human organic anion transporter hOAT1 (SLC22A6). *J Pharmacol Exp Ther* **314**(2):923-931.
- Boll M, Hergert M, Wagener M, Weber WM, Markovich D, Biber J, Clauss W, Murer H and Daniel H (1996) Expression cloning and functional characterization of the kidney cortex high-affinity proton-coupled peptide transporter. *Proc Natl Acad Sci U S A* **93**(1):284-289.
- Brandoni A, Anzai N, Kanai Y, Endou H and Torres AM (2006) Renal elimination of p-aminohippurate (PAH) in response to three days of biliary obstruction in the rat. The role of OAT1 and OAT3. *Biochim Biophys Acta* **1762**(7):673-682.
- Buist SC, Cherrington NJ, Choudhuri S, Hartley DP and Klaassen CD (2002) Gender-specific and developmental influences on the expression of rat organic anion transporters. *J Pharmacol Exp Ther* **301**(1):145-151.
- Burckhardt BC and Burckhardt G (2003) Transport of organic anions across the basolateral membrane of proximal tubule cells. *Rev Physiol Biochem Pharmacol* **146**:95-158.
- Burckhardt BC, Drinkuth B, Menzel C, König A, Steffgen J, Wright SH and Burckhardt G (2002) The renal Na<sup>+</sup>-dependent dicarboxylate transporter, NaDC-3, translocates dimethyl- and disulfhydryl-compounds and contributes to renal heavy metal detoxification. *J Am Soc Nephrol* **13**(11):2628-2638.
- Burckhardt BC, Lorenz J, Kobbe C and Burckhardt G (2005) Substrate specificity of the human renal sodium dicarboxylate cotransporter, hNaDC-3, under voltage-clamp conditions. *Am J Physiol Renal Physiol* **288**(4):F792-799.
- Burckhardt G, Bahn A and Wolff NA (2001) Molecular physiology of renal p-aminohippurate secretion. *News Physiol Sci* **16**:114-118.



- Burckhardt G and Wolff NA (2000) Structure of renal organic anion and cation transporters. *Am J Physiol Renal Physiol* **278**(6):F853-866.
- Cha SH, Sekine T, Fukushima JI, Kanai Y, Kobayashi Y, Goya T and Endou H (2001) Identification and characterization of human organic anion transporter 3 expressing predominantly in the kidney. *Mol Pharmacol* **59**(5):1277-1286.
- Cherrington NJ, Slitt AL, Li N and Klaassen CD (2004) Lipopolysaccharide-mediated regulation of hepatic transporter mRNA levels in rats. *Drug Metab Dispos* **32**(7):734-741.
- Choudhury D and Ahmed Z (2006) Drug-associated renal dysfunction and injury. *Nat Clin Pract Nephrol* **2**(2):80-91.
- Cihlar T and Ho ES (2000) Fluorescence-based assay for the interaction of small molecules with the human renal organic anion transporter 1. *Anal Biochem* **283**(1):49-55.
- Cihlar T, Lin DC, Pritchard JB, Fuller MD, Mendel DB and Sweet DH (1999) The antiviral nucleotide analogs cidofovir and adefovir are novel substrates for human and rat renal organic anion transporter 1. *Mol Pharmacol* **56**(3):570-580.
- Deguchi T, Kusuhara H, Takadate A, Endou H, Otagiri M and Sugiyama Y (2004) Characterization of uremic toxin transport by organic anion transporters in the kidney. *Kidney Int* **65**(1):162-174.
- Enomoto A, Takeda M, Taki K, Takayama F, Noshiro R, Niwa T and Endou H (2003) Interactions of human organic anion as well as cation transporters with indoxyl sulfate. *Eur J Pharmacol* **466**(1-2):13-20.
- Eraly SA, Hamilton BA and Nigam SK (2003) Organic anion and cation transporters occur in pairs of similar and similarly expressed genes. *Biochem Biophys Res Commun* **300**(2):333-342.
- Eraly SA, Vallon V, Vaughn DA, Gangoiti JA, Richter K, Nagle M, Monte JC, Rieg T, Truong DM, Long JM, Barshop BA, Kaler G and Nigam SK (2006) Decreased renal organic anion secretion and plasma accumulation of endogenous organic anions in OAT1 knock-out mice. *J Biol Chem* **281**(8):5072-5083.
- Eveloff J (1987) p-Aminohippurate transport in basal-lateral membrane vesicles from rabbit renal cortex: stimulation by pH and sodium gradients. *Biochim Biophys Acta* **897**(3):474-480.
- Feng B, Dresser MJ, Shu Y, Johns SJ and Giacomini KM (2001) Arginine 454 and lysine 370 are essential for the anion specificity of the organic anion transporter, rOAT3. *Biochemistry* **40**(18):5511-5520.

- Fernandes I, Beliveau R, Friedlander G and Silve C (1999) NaPO<sub>4</sub> cotransport type III (PiT1) expression in human embryonic kidney cells and regulation by PTH. *Am J Physiol* **277**(4 Pt 2):F543-551.
- Fujita T, Brown C, Carlson EJ, Taylor T, de la Cruz M, Johns SJ, Stryke D, Kawamoto M, Fujita K, Castro R, Chen CW, Lin ET, Brett CM, Burchard EG, Ferrin TE, Huang CC, Leabman MK and Giacomini KM (2005) Functional analysis of polymorphisms in the organic anion transporter, SLC22A6 (OAT1). *Pharmacogenet Genomics* **15**(4):201-209.
- George RL, Wu X, Huang W, Fei YJ, Leibach FH and Ganapathy V (1999) Molecular cloning and functional characterization of a polyspecific organic anion transporter from *Caenorhabditis elegans*. *J Pharmacol Exp Ther* **291**(2):596-603.
- Gorboulev V, Volk C, Arndt P, Akhoundova A and Koepsell H (1999) Selectivity of the polyspecific cation transporter rOCT1 is changed by mutation of aspartate 475 to glutamate. *Mol Pharmacol* **56**(6):1254-1261.
- Graham FL, Smiley J, Russell WC and Nairn R (1977) Characteristics of a human cell line transformed by DNA from human adenovirus type 5. *J Gen Virol* **36**(1):59-74.
- Groves CE, Munoz L, Bahn A, Burckhardt G and Wright SH (2003) Interaction of cysteine conjugates with human and rabbit organic anion transporter 1. *J Pharmacol Exp Ther* **304**(2):560-566.
- Hagos Y, Bahn A, Asif AR, Krick W, Sandler M and Burckhardt G (2002) Cloning of the pig renal organic anion transporter 1 (pOAT1). *Biochimie* **84**(12):1221-1224.
- Hagos Y, Steffgen J, Rizwan AN, Langheit D, Knoll A, Burckhardt G and Burckhardt BC (2006) Functional roles of cationic amino acid residues in the sodium-dicarboxylate cotransporter 3 (NaDC-3) from winter flounder. *Am J Physiol Renal Physiol* **291**(6):F1224-1231.
- Hasegawa M, Kusuhara H, Endou H and Sugiyama Y (2003) Contribution of organic anion transporters to the renal uptake of anionic compounds and nucleoside derivatives in rat. *J Pharmacol Exp Ther* **305**(3):1087-1097.
- Ho ES, Lin DC, Mendel DB and Cihlar T (2000) Cytotoxicity of antiviral nucleotides adefovir and cidofovir is induced by the expression of human renal organic anion transporter 1. *J Am Soc Nephrol* **11**(3):383-393.
- Hong M, Tanaka K, Pan Z, Ma J and You G (2006) Determination of the external loops and the cellular orientation of the amino- and the carboxyl termini of the human organic anion transporter hOAT1. *Biochem J*.
- Hong M, Xu W, Yoshida T, Tanaka K, Wolff DJ, Zhou F, Inouye M and You G (2005) Human organic anion transporter hOAT1 forms homooligomers. *J Biol Chem* **280**(37):32285-32290.

- Hong M, Zhou F and You G (2004) Critical amino acid residues in transmembrane domain 1 of the human organic anion transporter hOAT1. *J Biol Chem* **279**(30):31478-31482.
- Hosoyamada M, Ichida K, Enomoto A, Hosoya T and Endou H (2004) Function and localization of urate transporter 1 in mouse kidney. *J Am Soc Nephrol* **15**(2):261-268.
- Hosoyamada M, Sekine T, Kanai Y and Endou H (1999) Molecular cloning and functional expression of a multispecific organic anion transporter from human kidney. *Am J Physiol* **276**(1 Pt 2):F122-128.
- Ichida K, Hosoyamada M, Kimura H, Takeda M, Utsunomiya Y, Hosoya T and Endou H (2003) Urate transport via human PAH transporter hOAT1 and its gene structure. *Kidney Int* **63**(1):143-155.
- Ishikawa T, Tsuji A, Inui K, Sai Y, Anzai N, Wada M, Endou H and Sumino Y (2004) The genetic polymorphism of drug transporters: functional analysis approaches. *Pharmacogenomics* **5**(1):67-99.
- Jigorel E, Le Vee M, Boursier-Neyret C, Parmentier Y and Fardel O (2006) Differential regulation of sinusoidal and canalicular hepatic drug transporter expression by xenobiotics activating drug-sensing receptors in primary human hepatocytes. *Drug Metab Dispos* **34**(10):1756-1763.
- Jung KY, Takeda M, Kim DK, Tojo A, Narikawa S, Yoo BS, Hosoyamada M, Cha SH, Sekine T and Endou H (2001) Characterization of ochratoxin A transport by human organic anion transporters. *Life Sci* **69**(18):2123-2135.
- Khamdang S, Takeda M, Noshiro R, Narikawa S, Enomoto A, Anzai N, Piyachaturawat P and Endou H (2002) Interactions of human organic anion transporters and human organic cation transporters with nonsteroidal anti-inflammatory drugs. *J Pharmacol Exp Ther* **303**(2):534-539.
- Kimura H, Takeda M, Narikawa S, Enomoto A, Ichida K and Endou H (2002) Human organic anion transporters and human organic cation transporters mediate renal transport of prostaglandins. *J Pharmacol Exp Ther* **301**(1):293-298.
- Kobayashi Y, Hirokawa N, Ohshiro N, Sekine T, Sasaki T, Tokuyama S, Endou H and Yamamoto T (2002a) Differential gene expression of organic anion transporters in male and female rats. *Biochem Biophys Res Commun* **290**(1):482-487.
- Kobayashi Y, Ohshiro N, Shibusawa A, Sasaki T, Tokuyama S, Sekine T, Endou H and Yamamoto T (2002b) Isolation, characterization and differential gene expression of multispecific organic anion transporter 2 in mice. *Mol Pharmacol* **62**(1):7-14.
- Koepsell H and Endou H (2004) The SLC22 drug transporter family. *Pflugers Arch* **447**(5):666-676.

- Koh AS, Simmons-Willis TA, Pritchard JB, Grassl SM and Ballatori N (2002) Identification of a mechanism by which the methylmercury antidotes N-acetylcysteine and dimercaptopropanesulfonate enhance urinary metal excretion: transport by the renal organic anion transporter-1. *Mol Pharmacol* **62**(4):921-926.
- Kojima R, Sekine T, Kawachi M, Cha SH, Suzuki Y and Endou H (2002) Immunolocalization of multispecific organic anion transporters, OAT1, OAT2, and OAT3, in rat kidney. *J Am Soc Nephrol* **13**(4):848-857.
- Kuze K, Graves P, Leahy A, Wilson P, Stuhlmann H and You G (1999) Heterologous expression and functional characterization of a mouse renal organic anion transporter in mammalian cells. *J Biol Chem* **274**(3):1519-1524.
- Lacy SA, Hitchcock MJ, Lee WA, Tellier P and Cundy KC (1998) Effect of oral probenecid coadministration on the chronic toxicity and pharmacokinetics of intravenous cidofovir in cynomolgus monkeys. *Toxicol Sci* **44**(2):97-106.
- Ljubojevic M, Herak-Kramberger CM, Hagos Y, Bahn A, Endou H, Burckhardt G and Sabolic I (2004) Rat renal cortical OAT1 and OAT3 exhibit gender differences determined by both androgen stimulation and estrogen inhibition. *Am J Physiol Renal Physiol* **287**(1):F124-138.
- Lopez-Nieto CE, You G, Bush KT, Barros EJ, Beier DR and Nigam SK (1997) Molecular cloning and characterization of NKT, a gene product related to the organic cation transporter family that is almost exclusively expressed in the kidney. *J Biol Chem* **272**(10):6471-6478.
- Lu R, Chan BS and Schuster VL (1999) Cloning of the human kidney PAH transporter: narrow substrate specificity and regulation by protein kinase C. *Am J Physiol* **276**(2 Pt 2):F295-303.
- Malo C and Berteloot A (1991) Analysis of kinetic data in transport studies: new insights from kinetic studies of Na<sup>+</sup>-D-glucose cotransport in human intestinal brush-border membrane vesicles using a fast sampling, rapid filtration apparatus. *J Membr Biol* **122**(2):127-141.
- Markovich D and Murer H (2004) The SLC13 gene family of sodium sulphate/carboxylate cotransporters. *Pflugers Arch* **447**(5):594-602.
- Miller DS, Letcher S and Barnes DM (1996) Fluorescence imaging study of organic anion transport from renal proximal tubule cell to lumen. *Am J Physiol* **271**(3 Pt 2):F508-520.
- Monica Torres A, Mac Laughlin M, Muller A, Brandoni A, Anzai N and Endou H (2005) Altered renal elimination of organic anions in rats with chronic renal failure. *Biochim Biophys Acta* **1740**(1):29-37.

- Motohashi H, Sakurai Y, Saito H, Masuda S, Urakami Y, Goto M, Fukatsu A, Ogawa O and Inui K (2002) Gene expression levels and immunolocalization of organic ion transporters in the human kidney. *J Am Soc Nephrol* **13**(4):866-874.
- Motojima M, Hosokawa A, Yamato H, Muraki T and Yoshioka T (2002) Uraemic toxins induce proximal tubular injury via organic anion transporter 1-mediated uptake. *Br J Pharmacol* **135**(2):555-563.
- Motojima M, Hosokawa A, Yamato H, Muraki T and Yoshioka T (2003) Uremic toxins of organic anions up-regulate PAI-1 expression by induction of NF-kappaB and free radical in proximal tubular cells. *Kidney Int* **63**(5):1671-1680.
- Mulato AS, Ho ES and Cihlar T (2000) Nonsteroidal anti-inflammatory drugs efficiently reduce the transport and cytotoxicity of adefovir mediated by the human renal organic anion transporter 1. *J Pharmacol Exp Ther* **295**(1):10-15.
- Pajor AM (1999) Sodium-coupled transporters for Krebs cycle intermediates. *Annu Rev Physiol* **61**:663-682.
- Perry JL, Dembla-Rajpal N, Hall LA and Pritchard JB (2006) A three-dimensional model of human organic anion transporter 1: Aromatic amino acids required for substrate transport. *J Biol Chem*.
- Pombrio JM, Giangreco A, Li L, Wempe MF, Anders MW, Sweet DH, Pritchard JB and Ballatori N (2001) Mercapturic acids (N-acetylcysteine S-conjugates) as endogenous substrates for the renal organic anion transporter-1. *Mol Pharmacol* **60**(5):1091-1099.
- Pritchard JB (1988) Coupled transport of p-aminohippurate by rat kidney basolateral membrane vesicles. *Am J Physiol* **255**(4 Pt 2):F597-604.
- Quaglia NB, Brandoni A, Ferri A and Torres AM (2003) Early manifestation of nephropathy in rats with arterial calcinosis. *Ren Fail* **25**(3):355-366.
- Race JE, Grassl SM, Williams WJ and Holtzman EJ (1999) Molecular cloning and characterization of two novel human renal organic anion transporters (hOAT1 and hOAT3). *Biochem Biophys Res Commun* **255**(2):508-514.
- Reid G, Wolff NA, Dautzenberg FM and Burckhardt G (1998) Cloning of a human renal p-aminohippurate transporter, hROAT1. *Kidney Blood Press Res* **21**(2-4):233-237.
- Sakurai Y, Motohashi H, Ogasawara K, Terada T, Masuda S, Katsura T, Mori N, Matsuura M, Doi T, Fukatsu A and Inui K (2005) Pharmacokinetic significance of renal OAT3 (SLC22A8) for anionic drug elimination in patients with mesangial proliferative glomerulonephritis. *Pharm Res* **22**(12):2016-2022.

- Sauvant C, Hesse D, Holzinger H, Evans KK, Dantzer WH and Gekle M (2004) Action of EGF and PGE2 on basolateral organic anion uptake in rabbit proximal renal tubules and hOAT1 expressed in human kidney epithelial cells. *Am J Physiol Renal Physiol* **286**(4):F774-783.
- Sauvant C, Holzinger H and Gekle M (2006) Prostaglandin E2 inhibits its own renal transport by downregulation of organic anion transporters rOAT1 and rOAT3. *J Am Soc Nephrol* **17**(1):46-53.
- Schwenk M (1987) Drug transport in intestine, liver and kidney. *Arch Toxicol* **60**(1-3):37-42.
- Sekine T, Watanabe N, Hosoyamada M, Kanai Y and Endou H (1997) Expression cloning and characterization of a novel multispecific organic anion transporter. *J Biol Chem* **272**(30):18526-18529.
- Somogyi A (1996) Renal transport of drugs: specificity and molecular mechanisms. *Clin Exp Pharmacol Physiol* **23**(10-11):986-989.
- Soodvilai S, Chatsudthipong V, Evans KK, Wright SH and Dantzer WH (2004) Acute regulation of OAT3-mediated estrone sulfate transport in isolated rabbit renal proximal tubules. *Am J Physiol Renal Physiol* **287**(5):F1021-1029.
- Soodvilai S, Wright SH, Dantzer WH and Chatsudthipong V (2005) Involvement of tyrosine kinase and PI3K in the regulation of OAT3-mediated estrone sulfate transport in isolated rabbit renal proximal tubules. *Am J Physiol Renal Physiol* **289**(5):F1057-1064.
- Sugawara M, Mochizuki T, Takekuma Y and Miyazaki K (2005) Structure-affinity relationship in the interactions of human organic anion transporter 1 with caffeine, theophylline, theobromine and their metabolites. *Biochim Biophys Acta* **1714**(2):85-92.
- Sullivan LP, Grantham JA, Rome L, Wallace D and Grantham JJ (1990) Fluorescein transport in isolated proximal tubules in vitro: epifluorometric analysis. *Am J Physiol* **258**(1 Pt 2):F46-51.
- Sullivan LP and Grantham JJ (1992) Specificity of basolateral organic anion exchanger in proximal tubule for cellular and extracellular solutes. *J Am Soc Nephrol* **2**(7):1192-1200.
- Sun H, Frassetto L and Benet LZ (2006) Effects of renal failure on drug transport and metabolism. *Pharmacol Ther* **109**(1-2):1-11.
- Sun W, Wu RR, van Poelje PD and Erion MD (2001) Isolation of a family of organic anion transporters from human liver and kidney. *Biochem Biophys Res Commun* **283**(2):417-422.

- Sweet DH (2005) Organic anion transporter (Slc22a) family members as mediators of toxicity. *Toxicol Appl Pharmacol* **204**(3):198-215.
- Sweet DH, Chan LM, Walden R, Yang XP, Miller DS and Pritchard JB (2003) Organic anion transporter 3 (Slc22a8) is a dicarboxylate exchanger indirectly coupled to the Na<sup>+</sup> gradient. *Am J Physiol Renal Physiol* **284**(4):F763-769.
- Sweet DH, Wolff NA and Pritchard JB (1997) Expression cloning and characterization of ROAT1. The basolateral organic anion transporter in rat kidney. *J Biol Chem* **272**(48):30088-30095.
- Tahara H, Shono M, Kusuhara H, Kinoshita H, Fuse E, Takadate A, Otagiri M and Sugiyama Y (2005) Molecular cloning and functional analyses of OAT1 and OAT3 from cynomolgus monkey kidney. *Pharm Res* **22**(4):647-660.
- Takeda M, Khamdang S, Narikawa S, Kimura H, Hosoyamada M, Cha SH, Sekine T and Endou H (2002) Characterization of methotrexate transport and its drug interactions with human organic anion transporters. *J Pharmacol Exp Ther* **302**(2):666-671.
- Takeda M, Narikawa S, Hosoyamada M, Cha SH, Sekine T and Endou H (2001) Characterization of organic anion transport inhibitors using cells stably expressing human organic anion transporters. *Eur J Pharmacol* **419**(2-3):113-120.
- Takeda M, Sekine T and Endou H (2000) Regulation by protein kinase C of organic anion transport driven by rat organic anion transporter 3 (rOAT3). *Life Sci* **67**(9):1087-1093.
- Tanaka K, Xu W, Zhou F and You G (2004a) Role of glycosylation in the organic anion transporter OAT1. *J Biol Chem* **279**(15):14961-14966.
- Tanaka K, Zhou F, Kuze K and You G (2004b) Cysteine residues in the organic anion transporter mOAT1. *Biochem J* **380**(Pt 1):283-287.
- Tune BM (1997) Nephrotoxicity of beta-lactam antibiotics: mechanisms and strategies for prevention. *Pediatr Nephrol* **11**(6):768-772.
- Ullrich KJ (1997) Renal transporters for organic anions and organic cations. Structural requirements for substrates. *J Membr Biol* **158**(2):95-107.
- Uwai Y, Okuda M, Takami K, Hashimoto Y and Inui K (1998) Functional characterization of the rat multispecific organic anion transporter OAT1 mediating basolateral uptake of anionic drugs in the kidney. *FEBS Lett* **438**(3):321-324.
- Uwai Y, Taniguchi R, Motohashi H, Saito H, Okuda M and Inui K (2004) Methotrexate-loxoprofen interaction: involvement of human organic anion transporters hOAT1 and hOAT3. *Drug Metab Pharmacokinet* **19**(5):369-374.

- van Montfoort JE, Hagenbuch B, Groothuis GM, Koepsell H, Meier PJ and Meijer DK (2003) Drug uptake systems in liver and kidney. *Curr Drug Metab* **4**(3):185-211.
- Villar SR, Brandoni A, Anzai N, Endou H and Torres AM (2005) Altered expression of rat renal cortical OAT1 and OAT3 in response to bilateral ureteral obstruction. *Kidney Int* **68**(6):2704-2713.
- Wolff NA, Grunwald B, Friedrich B, Lang F, Godehardt S and Burckhardt G (2001) Cationic amino acids involved in dicarboxylate binding of the flounder renal organic anion transporter. *J Am Soc Nephrol* **12**(10):2012-2018.
- Wolff NA, Thies K, Kuhnke N, Reid G, Friedrich B, Lang F and Burckhardt G (2003) Protein kinase C activation downregulates human organic anion transporter 1-mediated transport through carrier internalization. *J Am Soc Nephrol* **14**(8):1959-1968.
- Wolff NA, Werner A, Burkhardt S and Burckhardt G (1997) Expression cloning and characterization of a renal organic anion transporter from winter flounder. *FEBS Lett* **417**(3):287-291.
- Xu G, Bhatnagar V, Wen G, Hamilton BA, Eraly SA and Nigam SK (2005) Analyses of coding region polymorphisms in apical and basolateral human organic anion transporter (OAT) genes [OAT1 (NKT), OAT2, OAT3, OAT4, URAT (RST)]. *Kidney Int* **68**(4):1491-1499.
- Xu W, Tanaka K, Sun AQ and You G (2006a) Functional role of the C terminus of human organic anion transporter hOAT1. *J Biol Chem* **281**(42):31178-31183.
- Xu W, Tanaka K, Sun AQ and You G (2006b) Functional Role of the C Terminus of Human Organic Anion Transporter hOAT1. *J Biol Chem* **281**(42):31178-31183.
- Yarchoan R, Mitsuya H, Myers CE and Broder S (1989) Clinical pharmacology of 3'-azido-2',3'-dideoxythymidine (zidovudine) and related dideoxynucleosides. *N Engl J Med* **321**(11):726-738.
- You G, Kuze K, Kohanski RA, Amsler K and Henderson S (2000) Regulation of mOAT-mediated organic anion transport by okadaic acid and protein kinase C in LLC-PK(1) cells. *J Biol Chem* **275**(14):10278-10284.
- Zalups RK and Ahmad S (2005) Transport of N-acetylcysteine s-conjugates of methylmercury in Madin-Darby canine kidney cells stably transfected with human isoform of organic anion transporter 1. *J Pharmacol Exp Ther* **314**(3):1158-1168.
- Zalups RK, Aslamkhan AG and Ahmad S (2004) Human organic anion transporter 1 mediates cellular uptake of cysteine-S conjugates of inorganic mercury. *Kidney Int* **66**(1):251-261.
- Zhou F, Illsley NP and You G (2006) Functional characterization of a human organic anion transporter hOAT4 in placental BeWo cells. *Eur J Pharm Sci* **27**(5):518-523.



Zhou F, Xu W, Hong M, Pan Z, Sinko PJ, Ma J and You G (2005) The role of N-linked glycosylation in protein folding, membrane targeting, and substrate binding of human organic anion transporter hOAT4. *Mol Pharmacol* **67**(3):868-876.

**ACKNOWLEDGEMENTS**

It is a pleasure to thank the many people who made this thesis possible. It is difficult to overstate my gratitude to my Ph.D. supervisor, Prof. Dr. Gerhard Burckhardt for his encouragement, sound advice, excellent teaching, company, and lots of great ideas. I would like to thank Dr. Wolfgang Krick, my co-supervisor for always making time for my questions. I wish to thank Professors R. Hardeland and D. Doenecke for overseeing my thesis from time to time.

I really enjoyed the companionship and guidance of postdocs and friends Dr. Yohannes Hagos and Dr. Andrew Bahn, especially towards increasing my 'level of significance' and frequent discussions. I would like to thank Prof. Dr. Brigetta Burckhardt for her help and for teaching me how to work with oocytes.

I appreciate all the useful tips and pointers I got from Gesche Dallmayer and Sören Petzke, on how to work in the lab. I would like to thank my fellow PhD students Nicole Nogoy, Vladimir Shnizar, Yeruva Sunil, Goutham Ganjam, and friends- Fahad Haroon, Shaida Andrabi, Agnieszka, Sadanad Gaikwad, Ashraf Mannan, Tabrez Siddiqui, and Mohiuddin Ahmed for a great time in Göttingen.

My father and mother were most supportive when I decided to pursue a PhD and their pride in my work was a constant source of motivation for me. My elder brother and role model, Sami is the reason for my achievements. I wish to thank him and his wife Zehra for their love support and advice. Little Meraj (their son), who is so fond of reading, will receive a copy of this thesis to color!

My charming wife Noushine, I thank for her patience and love. The last year with her, in this beautiful country has been amazing and we will cherish it forever.

## PUBLICATIONS

## Articles in peer-reviewed journals

- 2006 1. **The chloride dependence of the human organic anion transporter 1 (hOAT1) is blunted by mutation of a single amino acid.**  
Rizwan AN<sup>1</sup>, Krick W and Burckhardt G. (Manuscript under revision at the Journal of Biological Chemistry).
2. **Organic anion transporters of the SLC22 family: Biopharmaceutical, Physiological, and pathological roles.**  
Rizwan AN<sup>1</sup> and Burckhardt G. Journal: Pharmaceutical Research, 2006. Review (*In press*).
3. **Functional roles of cationic amino acid residues in the sodium-dicarboxylate cotransporter 3 (NaDC-3) from winter flounder.**  
Hagos Y, Steffgen J, Rizwan AN<sup>1</sup>, Langheit D, Knoll A, Burckhardt G, Burckhardt BC. Am J Physiol Renal Physiol. 2006 May 30; F1224-F1231.
- 2004 4. **The effect of a combination of sertraline with anticonvulsants on picrotoxin-induced convulsion and lipid peroxidation.** (Research letter)  
Rizwan AN<sup>2</sup>, A. Ali, K. K. Pillai, S. N. Pal. Indian Journal of Pharmacology. 2004 February 36 (1): 42.
- 2003 5. **Effects of gabapentin and antidepressant drug combinations on convulsions and memory in mice.**  
Rizwan AN<sup>2</sup>, Ali A, Dua Y, Pal SN, Pillai KK. Pol J Pharmacol. 2003 Nov-Dec;55(6):965-71.

## Abstracts

- 2006 **Arginine 466 in human Organic Anion Transporter 1 confers chloride sensitivity.** Rizwan AN<sup>1</sup>, Krick W and Burckhardt G. 2006 Experimental Biology meeting abstracts. The FASEB Journal, 20, Abstract #758.13.
- 2005 **The influence of dicarboxylates and pH on transport by the human Organic Anion Transporter 1 (hOAT1).** Rizwan AN<sup>1</sup>, Krick W and Burckhardt G. The 84th annual meeting of the DPG (German Physiological Society of) 2005 in Göttingen. (Abstract: European Journal of Physiology, Vol 449, Supplement 1, March 2005)

<sup>1</sup> Department of Vegetative Physiology and Pathophysiology, Center for Physiology and Pathophysiology, Georg-August-University Goettingen, Germany.

<sup>2</sup> Department of Pharmacology, Faculty of Pharmacy. Hamdard University, New Delhi, India.

**CONFERENCES**

<b>Conference</b>	<b>Organization</b>	<b>Location</b>	<b>Date</b>	<b>Contribution</b>
EMBO Conference on Structures in Biology	EMBO (European Molecular Biology Organisation)	Heidelberg, Germany	November 10-13, 2004	-
84th Congress of the DPG	(DPG) Deutsche Physiologische Gesellschaft	Goettingen, Germany	March 6-9, 2005	poster presentation and volunteer
Conference of the German Society of Biochemistry and Molecular Biology	Study Group Biomembranes and the German Society of Experimental and Clinical Pharmacology and Toxicology	Castle Rauschholzhausen, Marburg, Germany	May 20-21, 2005	poster presentation
BioMedical Transporters 2005: Membrane Transporters: Bridging Basic and Applied Sciences	Harvard Medical School Boston, MA, USA.	St. Gallen , Switzerland	August 14 - 18, 2005	-
Göttinger Transporttage	Centre for Physiology and Pathophysiology: Georg-August University	Göttingen, Germany	December 3-4, 2005	talk
85th Congress of the DPG	(DPG) Deutsche Physiologische Gesellschaft	Munich, Germany	March 26 - 29, 2006	poster presentation
Experimental Biology 2006	FASEB (Federation of the American Societies for Experimental Biology)	San Francisco (CA), USA.	April 1-5, 2006	poster presentation
Göttinger Transporttage	Centre for Physiology and Pathophysiology: Georg-August University	Göttingen, Germany	November 4-5, 2006	talk

**BIOGRAPHY**

- Name: Ahsan Naqi Rizwan
- Date of birth: 15.07.1977
- Place of Birth: Lucknow (U.P), India
- Citizenship: Indian
- 1983 - 1993: Primary and High school, Scholars Home, Dehradun, U.P, India
- 1993 - 1995: Senior secondary school (science stream), AMU, Aligarh (U.P), India
- 1996 - 2000: B.Pharm, Hamdard University, New Delhi, India
- 2000 - 2002: M.Pharm (Pharmacology), Hamdard University, New Delhi, India.
- Thesis title: A study of the effects of some select anticonvulsant and antidepressant drug combinations on convulsions and memory.
- Aug 2002-Feb 2004: Research Associate, Medical Affairs and Clinical Research, Ranbaxy Research Laboratories, new Delhi, India.
- Mar 2004-Mar2007: Ph D at the Georg-August-Universität, Göttingen, Germany. Member of the DFG-funded Graduiertenkolleg 335, entitled: "Clinical and cellular and molecular biology of the internal organs" Thesis title: Importance of charged amino acids in the human organic anion transporter 1 (hOAT1).